SIMULATION OF WIND RESPONSE OF TALL BUILDINGS USING COMPUTATIONAL FLUID DYNAMICS – A CASE STUDY

K.D.Y.E.SIRIWARDANA

(168929B)

Master of Science Degree in Structural Engineering

Department of Civil Engineering

University of Moratuwa
Sri Lanka

APRIL 2021

SIMULATION OF WIND RESPONSE OF TALL BUILDINGS USING COMPUTATIONAL FLUID DYNAMICS – A CASE STUDY

K.D.Y.E.SIRIWARDANA

(168929B)

Thesis submitted in partial fulfilment of the requirements for the degree of Master of Science

Department of Civil Engineering

University of Moratuwa

Sri Lanka

APRIL 2021

"I declare that this is my own work and this thesis does not incorporate without acknowledgement any material previously submitted for a Degree or Diploma in any other University or institute of higher learning and to the best of my knowledge and belief it does not contain any material previously published or written by another person except where the acknowledgement is made in the text.

Also, I hereby grant to University of Moratuwa the non-exclusive right to reproduce and distribute my thesis, in whole or in part in print, electronic or other medium. I retain the right to use this content in whole or part in future works (such as articles or books)."

Signature:………………………… Date:

The above candidate has carried out research for the Masters dissertation under my supervision.

Signature of the supervisor: …………………. Date:

ABSTRACT

High-rise buildings with unique architectural features has become popular in Sri Lanka in last few decades. Interaction of wind with buildings with complex geometry leads to a complex building-wind environment. However, all codes of practice and standards are only applicable for buildings with simple geometry and height limitations. Moreover, all wind codes mainly present static based calculation. Generally, the static analysis is suitable only for structures less than 50 m height. Therefore, the actual wind effect is difficult to assess by the wind loading codes, hence recommend using Computational Fluid Dynamics (CFD) models.

In this research, wind loads and its effects are calculated on a 31-storey high rise building utilizing three different international wind loading codes/standards, namely CP3 CHAPTER V-2:1972, BSEN 1991-4:2005 with SLS EN 1991-1-4:2019, AS/NZ 1170.2:2011 by encountering different factors and methods specified. The estimated forces are compared with each other since the different codes introduced different factors to estimate wind turbulent characteristics. Numerical Simulation has been carried out for the same building using RANS approach (Spalart-Allmaras). Comparison is carried out between the results obtained from simulation and code based calculations. This study has been used to evaluate the applicability / limitations of codes of practice via numerical simulation and identify the more suitable wind loading code. AS/NZS 1170.2:2011 is more suitable to evaluate the wind loads and their effects on tall buildings due to its advanced flow parameters. In addition, S-A turbulent model well performed in evaluating the complex building – wind environment accurately and different flow features such as vortices, wake formations etc. are clearly observed. The advantages of commercially available CFD software on complex fluid -structure problems has been discussed in terms of time, cost and accuracy of results opposed to other methods such as codes of practice and wind tunnel testing.

Specially dedicated to my beloved sister…..

Acknowledgements

First of all, I would like to express gratitude to my supervisor, Dr. H.M.Y.C. Mallikarachchi for his valuable advices and guidance during this research study. Moreover, I would like to express my gratitude to Dr. C. S Lewangamage and Dr. C. Ranasingha for their valuable advices. I would also like to express my sincere appreciation to staff members of Civil Engineering Department of University of Moratuwa for their kind assistances. Furthermore, I would like to express my gratitude to staff members of Central Engineering Consultancy Bureau.

I wish to acknowledge my friends and colleagues for their support and encouragement.

Last but not least, my most heartfelt appreciation goes to my family who give me invaluable support as always.

Finally I am grateful to everyone who helped me in various ways to complete this research.

Table of Contents

List of Figures

List of Tables

List of Abbreviations

Abbreviation	Description
q_b	Basic velocity pressure (BSEN 1991-1-4:2005)
q_p	Peak velocity pressure (BSEN 1991-1-4:2005)
$\tilde{\upsilon}$	Spalart–Allmaras variable
Re_L	Reynolds Number based on your problem's characteristic length scale
$V_{des,\theta}$	Building orthogonal design wind speed (AS/NZS 1170.2:2011)
$V_{sit,\beta}$	Site Design wind speed (AS/NZS 1170.2:2011)
δ_{ij}	Kronecker delta
Δt	Small time step
Δy	distance of the first node from the wall
A	Altitude (BSEN 1991-1-4:2005)
A_{ref}	Reference area of individual surface (BSEN 1991-1-4:2005)
b	Width of the structure (BSEN 1991-1-4:2005)
B_s	Background factor (AS/NZS 1170.2:2011)
B_{sh}	Average breadth of the structure heights s and h (AS/NZS 1170.2:2011)
C_{alt}	Altitude correction factor (BSEN 1991-1-4:2005)
c_d	dilatational wave speed
C_{dir}	Directional factor (BSEN 1991-1-4:2005)
C_{dyn}	Dynamic response factor (AS/NZS 1170.2:2011)
C_e	Exposure factor (BSEN 1991-1-4:2005)
$C_{e,T}$	Exposure Correction factor (BSEN 1991-1-4:2005)
C_{fig}	Aerodynamic shape factor (AS/NZS 1170.2:2011)
$C_o(z)$	Orography factor (BSEN 1991-1-4:2005)
C_p	Pressure coefficient
$C_r(z)$	Roughness factor (BSEN 1991-1-4:2005)

$C_{r,T}(z)$	Roughness correction factor (BSEN 1991-1-4:2005)
C_sC_d	Structural factor (BSEN 1991-1-4:2005)
C_{season}	Seasonal factor (BSEN 1991-1-4:2005)
d	Distance from the closest surface
E	Young's modulus
E	Effective height 10 m above Y (CP3 Chapter V-2:1972)
E_t	(π/4) times the spectrum of turbulence (AS/NZS 1170.2:2011)
G	Gust Effect Factor
GLF	Gust Loading Factor
G_q	Gust Factor for wind Load Effect
g_R	Peak factor for the resonant response (AS/NZS 1170.2:2011)
g_v	Peak factor for the upwind velocity fluctuations(AS/NZS 1170.2:2011)
h	Height to top of the tower (AS/NZS 1170.2:2011)
H	Building height
h_{mk}	distance between m-th and k-th cells that lie near the fluid-structure interface
H_s	Height factor for the resonant response (AS/NZS 1170.2:2011)
I_h	Turbulent Intensity (AS/NZS 1170.2:2011)
K_a	Area reduction factor (AS/NZS 1170.2:2011)
$K_{c,e}$	Combination factor (AS/NZS 1170.2:2011)
K_l	Local pressure factor (AS/NZS 1170.2:2011)
K_p	Peak factor for the upwind velocity (BSEN 1991-1-4:2005)
K_p	Porous cladding reduction factor (AS/NZS 1170.2:2011)
k_r	terrain factor depending on the roughness length
L	flow characteristic length scale
L_h	A measure of the integral turbulence length scale
L_{min}	Smallest element dimension in the FEA mesh
M_d	Wind directional multiplier (AS/NZS 1170.2:2011)
M_s	Shielding Multiplier (AS/NZS 1170.2:2011)
M_t	Topographical Multiplier (AS/NZS 1170.2:2011)

$M_{z, cat}$	Terrain height Multiplier (AS/NZS 1170.2:2011)
N	Reduced frequency (non- dimensional) (AS/NZS 1170.2:2011)
n_a	First mode natural frequency of vibration of a structure in the along-wind direction in hertz. (AS/NZS 1170.2:2011)
P	Pressure
q	Dynamic pressure (CP3 Chapter V-2:1972)
R^2	Resonance Response Part (BSEN 1991-1-4:2005)
R_e	Reynold's number
R_h , R_b	Aerodynamic admittance (BSEN 1991-1-4:2005)
s	Height of the level which wind action effects are calculated (AS/NZS 1170.2:2011)
S	Size reduction factor (AS/NZS 1170.2:2011)
S_1	Topography factor CP3 Chapter V-2:1972)
S_2	Ground roughness, building size & height above ground factor (CP3 Chapter V-2:1972)
S_3	Statistical based factor (CP3 Chapter V-2:1972)
S_4	Directional factor (CP3 Chapter V-2:1972)
S_{ij}	Mean rate of strain tensor
U^*	Frictional velocity
V	Average wind speed
V	Basic wind speed
V'	Fluctuation wind speed
$V_{10, 3}$	3 *s* speed at 10 m height in open terrain category (CP3 Chapter V-2:1972)
$V_{10, 3}$	3 *s* speed at 10 m height in open terrain category (CP3 Chapter V-2:1972)
V_b	Basic wind velocity (BSEN 1991-1-4:2005)
$V_{b, map}$	Characteristic 10 minutes mean wind velocity before altitude correction (BSEN 1991-1-4:2005)
$V_{b,0}$	Fundamental value of basic wind speed (BSEN 1991-1-4:2005)
V_H	Wind speed at 'H' height (AS/NZS 1170.2:2011)
V_{Ht}	t *s* speed at height H in appropriate category (CP3 Chapter V-2:1972)

V_m	Mean wind velocity (BSEN 1991-1-4:2005)
V_{mk}	velocity of the fluid between those cells
V_R	Regional 3 s gust wind speed (AS/NZS 1170.2:2011)
V_s	Design wind speed
V_t	Wind velocity at any given instantaneous time't'
v_t	Turbulent Eddy viscosity
W_e	Wind pressure on surface (BSEN 1991-1-4:2005)
Y	level corresponding to general roof top level or obstruction level(CP3 Chapter V-2:1972)
Y^+	non-dimensional distance between from the wall to first mesh node
$z0$	Roughness length.
z_{max}	maximum height taken as 200 m
z_{min}	minimum height defined (BSEN 1991-1-4:2005)
α	Power law exponent (CP3 Chapter V-2:1972)
α	Lame constant
κ	Von Karman's constant
λ	Lame constant
ξ	Ratio of structural damping (AS/NZS 1170.2:2011)
S	Rotational tensor
ρ	Density of fluid

List of Appendices

1. INTRODUCTION

In last few decades, number of high-rise structures are rapidly increasing in all over the world as a result of fast construction techniques, development of finite element analysis software, high strength materials as well as the horizontal and vertical transportation modes in the building such as speed lift systems, travellators, escalators etc. Consequently, high-rise buildings with unique architectural features became popular in Sri Lanka. Altair Tower, Twin Towers, Lotus Tower are few examples to be mentioned.

"Skyscraper" as a concept, was initially used to define 42 m height building constructed in Chicago in 1885. However, in earlier times, all tall structures in the world were built for religious purpose namely, Ulm Minster (161 m), a church in Germany; the Great Pyramid of Giza (145 m) in Egypt (Bendini, 2019). However, constructing tall structures for living purpose of human (apartment concept) is a huge transfer for Architects and Engineers from the 20th Century due to its construction complexity. In addition, creating a comfortable and safe environment for people both inside and outside is a big challenge for Structural Engineers.

As a result of American Industrial Revolution, construction industry was confronted for the major change. The structures rise higher therefore, the vocabulary had to adjust accordingly. Currently, a building having 40+ floors or above 150 m height is termed as "skyscraper". Furthermore, buildings of 300 m high or greater are called as "Super tall" and if the top of the building hit beyond 600 m is categorized as "Mega tall". Those definitions was specified by the Council on Tall Buildings and Urban Habitat (CTBUH) in America and most of the countries follow the same definitions though the terms do not have internationally agreed explanations (Bendini, 2019).

The most conspicuous tall buildings in most of the countries are denominated as 'High-Rise Buildings' whilst UK and some of the European countries use the term of 'Tower Blocks' (Hall , 2005). Therefore, "High-rise building" definition can vary with the country or region. In general consensus, structures taller than 35 m or more than 9 stories fall into the above category. In Structural Engineers' viewpoint, if natural period of vibration of a building is greater than 1 *s (*T > 1*s*) consider as high-rise building. However, as per the building categorization by Society of Structural Engineers in Sri Lanka (SSESL), structure having 20+ floors are termed as "High-rise building".

1.1 Wind Loading and its Effects on Tall Buildings

In case of designing tall buildings, Engineers do not only have to deal with the gravitational loads but also lateral loads such as wind loads and earthquake loads. Lateral loads become more influential since tall building behave as a freestanding cantilever. When the wind flows over and around building creates pressure differential zones identified as calm and eddies (circular movement of wind). Positive pressure can be observed on the windward face of the building due to aggregation of air. Therefore, velocity of wind flow slows down until it finds a new path free from disturbances. However, wind flow velocity increases than that of the initial value at the location where the new path is found. Additionally, negative pressure is formed on the leeward and side faces of the building due to the lower air density, therefore, wakes formation can be observed at those locations as shown in Figures 1.1 and 1.2 (Moghaddam, et al., 2011)

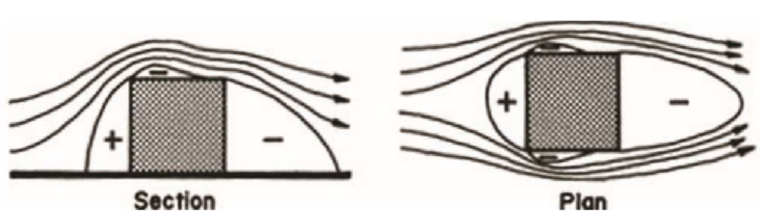

Figure 1.1 Wind flow movement over a structure

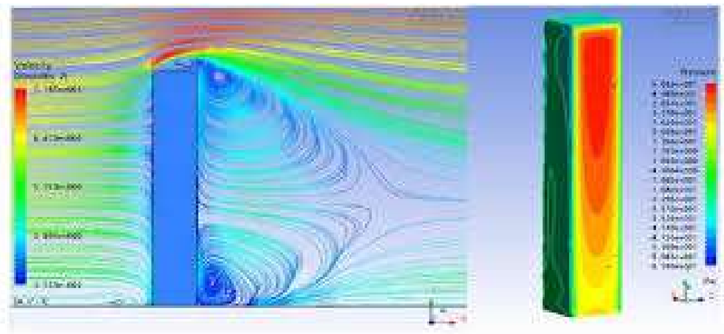

Figure 1.2 Stream lines of a flow over a building model (Mendis, et al., 2007)

With the increment of the wind velocity, wind pressure on the building increases proportionally with the square of the mean wind velocity ($P \propto V^2$). However, the pressure varies dynamically with respect to the degree of shielding provided by other buildings and topographical features (Taranath, 2005). Interaction of wind with tall building creates the complex building-wind environment when the building is subjected to wind loads both along and crosswind direction as shown in Figure1.3. The maximum wind load and deflection are generally reported in the along wind direction and the maximum acceleration of a building can be observed in crosswind direction (Taranath, 1998).

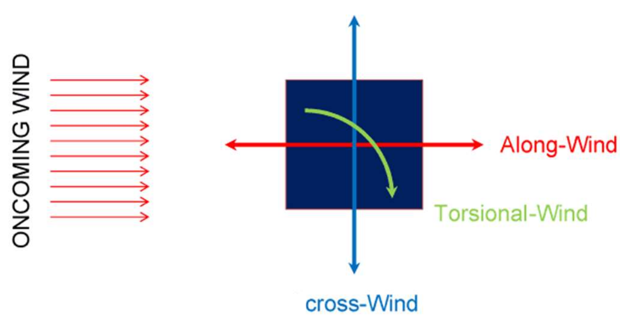

Figure 1.3 Component of tall building response to wind excitation (Gerges & Benuska, 2013)

In addition, vortex shedding can be observed due to the crosswind effect when the natural frequency of the building nearly equal to the wind frequency. Hence, vortex-shedding effect should be considered as a dominant factor in case of designing tall buildings (Alaghmandan & Elnimeiri, 2013). Besides, buffeting and galloping can be occurred as a result of crosswind effect (Bwail, 2019).

Therefore, Structural Engineers have to pay much more attention to the "Wind Engineering" field due to the complexity of wind behaviour when it interacts with the structure.

1.2 International Codes of Practice for Wind Loading

A number of advanced wind loading codes came into the industrial platform in last two decades to estimate the wind loading and their effects on and around structures. This reflects the rapid development in the field of "Wind Engineering". All experimental results, field investigation data as well as the Computational Fluid Dynamics (CFD) research findings have been used to develop empirical equations to evaluate complex building – wind environment accurately. Furthermore, most of the researchers/ engineers endeavoured to develop the National Annexures or wind loading code for their countries. As a result of it, number of wind loading codes are now available in the industry such as CP 3 Chapter V–Part 2:1972, BS-EN1991-1-4:2005, AS/NZS 1170.2:2011, ASCE /SEI 7-10; 2010AIJ 2015 (Japan) etc. However, this research, mainly focus on three different codes of practice, namely CP3 Chapter V-2:1972 & BS-EN1991-1-4:2005 with NA (National Annex) to SLSEN 1991-1- 4:2016 and AS/NZS 1170.2:2011 (details are given in Section 2.2.4).

Wind induced effects on a structure can be mainly categorized in to three different types, which are static, dynamic and aerodynamic (Alaghmandan & Elnimeiri, 2013). More details are contained within Section 2.2.4.1.

1.3 CFD in Wind Engineering

International wind loading codes have been developed using fundamental fluid laws and structural dynamics. However, all codes of practice and standards are applicable only for buildings less than 200 m height with simple geometry (square or rectangular shape). As stated by CP 3 Chapter V–Part 2:1972, wind loads can be estimated for the buildings both a length to width ratio less than four ($l/w < 4$) and a height to width ratio less than six ($h/w < 6$). In BS-EN1991-1-4:2005, external pressure coefficients are recommended only up to the height to width ratio of five ($h/d \leq 5$). Then the code recommends to multiply the resulting force by 1 for the structures which are beyond that ratio due to the lack of correlation. Besides, AS/NZS 1170.2:2011 code can be applied for the buildings with aspect ratio less than 6 (Mohotti, et al., 2013) . Therefore, the actual wind effect on the high-rise buildings with complex geometry cannot be assessed by those wind loading codes.

The application of CFD in wind Engineering named as Computational Wind Engineering (CWE), which is widely spreading since last two decades (Franke, et al., 2014). For the reason that, complex numerical simulations can be processed within a realistic time due to high-speed super computers. In CFD, fluid flow problems can be solved and analyzed by numerical methods and algorithms. Therefore, modelling the interaction between fluid and the surfaces specifying the boundary conditions is mainly required to execute the calculations in computers (Mohotti, et al., 2013). Moreover, simulating wind flow in different domains is an added advantage of CFD.

The main approach of the computations of turbulent flow is Averaged Navier–Stokes equations (RANS), which specifies the relation of the velocity, pressure, temperature, and density in a moving fluid (Rouse, 2014).The RANS equations are averaged in a time period for all the turbulent scales to reach a statically steady solution of flow variables. The main purpose of having turbulent model is to define the turbulent fluxes or ‘Reynolds Stresses’ as a function of mean flow variables. Therefore, two different methods are used. One method is based on eddy viscosity assumptions, which "Reynolds stress" is equalizing to the molecular stresses to set it as the function of mean velocity. The Second method is to use an additional transportation equation to solve the "Reynolds stress" component (Franke, et al., 2014).

Different types of turbulent models have been developed to predict the different flow conditions named Spalart– Allmaras (S-A), k-ε, k-ω. S-A turbulent model used for this second method to solve the "Reynolds Stress" component described in the previous paragraph (Spalart & Allmaras, 1992).

Various type of commercially available CFD software are available in nowadays such as ABAQUS, ANSYS Fluent, DIANA, and Auto Desk Simulation. However, among all these, Simulia ABAQUS is selected to perform the wind simulation for this research due to its well performance for the complex fluid dynamic problems due to its powerful backing of pre-processing and post processing. Furthermore, Abaqus/CFD leads to get accurate results by solving the fluid–structure interaction (FSI) problems with the support of co-simulation (ABAQUS 6.14 User Documentation, 2014).

If the structure height and the geometry are exciting, CFD analysis would be helpful to estimate the wind loads and their effect accurately on and around the structure.

1.4 Problem Definition

Interaction of wind with tall building creates the complex building-wind environment when the building is subjected to wind loads for both along and crosswind direction as described in Section 1.1.Crosswind effect may cause vortex shedding, galloping and buffeting characteristics of fluid as well as the acceleration of the building. However, all codes of practice and standards are only applicable for the buildings less than 200 m height with simple geometry (square or rectangular shape) and aspect ratio less than 6 (stated in Australian wind code). Therefore, the actual wind effect on tall buildings with complex geometry is difficult to assess by those wind loading codes. Hence, CFD can be used to solve the complex fluid-structure interaction problems and observe the flow characteristics such as pressure variation, flow separation, vortex shedding, channeling effect along with the structure behavior.

Buildings in Sri Lanka that are approved or proposed and are planned to rise at least 100 m at the Colombo city area (List of tallest structures in Sri Lanka, 2020). Among those, most of them are proposed for residential purposes. Therefore, design and construction of 100 m tall building will become common in future. Estimating wind loads and their effects for 100 m tall building with complex geometry is the dominant part in the design process. Generally, code based calculation are being used to estimate the wind loads and their effects in such situations (structures which are not categorized in to 'Mega tall' or 'Super tall'). Therefore, it is required to understand the limitations and applicability of codes of practice via numerical simulation. Furthermore, it is prominent that limited research have been conducted on CFD analysis for the structures with different geometries. Besides, a handful research on CFD were carried out for the structures in Sri Lanka.

1.5 Objective

The objective of the research is to simulate the wind response of tall buildings with complex geometry using Computational Fluid Dynamics (CFD) and study the applicability and limitations of codes of practice via numerical simulation. A 102 m high apartment complex at Colombo suburban region is selected as a case study.

1.6 Scope of Work and Expected Outcome

The Scope of this research is to

1. Estimate static based wind pressure acting on the tall building for two orthogonal directions based on CP3 Chapter V-2:1972, BSEN 1991-1-4:2005 with National Annex , AS/NZS1170.2:2011 and compare with each other.
2. Analyze the effect of the different factors introduced by different codes of practice to estimate wind pressure on the structure.
3. Carry out the numerical simulation for the same building under similar wind flow directions using Spalart - Allmaras (S-A) turbulent model available in ABAQUS software.
4. Compare the results obtained from numerical simulation with the code based calculations and evaluate the applicability / limitations of codes of practice via numerical simulation.

Main outcome of this study is to comprehend the effect of the different factors introduced by different codes of practice to estimate the wind loads on structures. As well, the results conclude the more suitable wind code by evaluating the applicability / limitations of codes of practice via numerical simulation. Moreover, advantages and the importance of CFD to solve complex fluid flow problems will be highlighted.

1.7 Chapter Organization

Following Introduction, Chapter 2 presents literature reviews and discuss the applicability of the codes of practice on estimating wind loads and their effects for complex building geometries and the effectiveness and practicality of using commercially available CFD software in such situations. Chapter 3 presents the analysis of different factors and equations used to estimate the wind loads and their effects on selected case study (102 m tall building containing two towers) pertaining to three different wind-loading codes (CP3 Chapter V-2:1972, BSEN 1991-1-4:2005 with NA, AS/NZS1170.2:2011). Chapter 4 presents the details of CFD analysis on the same case. Finally, Chapter 5 evaluates the applicability / limitations of codes of practice via numerical simulation and the suitable wind loading code to assess complex –building wind environment. Moreover, it presents the advantages of CFD analysis opposed with manual calculation in terms of accuracy of results, time, and cost.

2. LITERATURE REVIEW ON PREVIOUSE STUDIES AND FLUID FLOW AROUND BUILDINGS

First half of this Chapter describes various studies carried out to estimate the wind loads and their effects on tall buildings by conventional methods using codes of practice and wind tunnel testing. Furthermore, the different research on fluid – structure interaction problems and their findings using CFD are presented. Second half of the Chapter comprises the types of fluid flow, different flow patterns around the tall building, applicability and limitations of codes of practice when assessing wind loads on tall building as well the practicality and the advantages of using CFD in such situations.

2.1 Previous Studies

Wind plays a vital role when designing tall buildings having unique architectural features. All codes of practice and standards are only applicable for buildings with simple geometry. Further, they are mainly static based calculation, while providing some design guidance for dynamic analysis for tall, slender and wind sensitive structures. However, static analysis is suitable only for structures less than 50 m height, therefore, existing codes are incapable of evaluating the wind loads and their effects on tall, irregular shaped buildings. (Mendis, et al., 2007)

Australian Standard clearly specify its limitations such as structure height shall be less than 200 m and the first-mode fundamental frequency shall be larger than 0.2 Hz (AS/NZS1170.2, 2011). Therefore, the code recommends performing wind tunnel tests in advance for the buildings, which are outside the above limitations. Since, wind tunnel testing is an expensive and time-consuming, Finite Element Analysis (FEM) is preferred by many designers.

CFD is one of the famous tool among engineers to study the wind response of tall building through fluid-structure interaction. For the reason that, complex numerical simulations can be processed within a realistic time period due to high speed super computers. Moreover, designers can easily modify the inflow parameters and model geometry and observe various flow parameters and their effects. It saves the time, cost and ultimately conciliates accurate result compared to experimental works. Hence, numerous research studies have looked in to the CFD analysis.

Comparison of Five Major Wind Codes namely, CP3 Chapter V– Part2:1972, BS 6399.2:1997, AS 1170.2:1989, AS/NZS 1170.2:2002 and EN 1991-1-4:2005 was carried out by Wijesooriya, Lewangamage & Jayasinghe (2010) to check their suitability with Sri Lankan context. All codes of practice provide fundamental basic wind speed with respect to different averaging times. Yet, engineers have only 3 *s* gust wind speed data, the authors stated two methods to convert 3 *s* gust wind speed into characteristic 10 minutes mean wind speed. According to their study, the 3 *s* gust wind speed can be converted to 10 minute mean wind speed by combination of two methods suggested by Cook (1999) and IECUK. Meanwhile, they suggested to uses higher regional wind speed for ULS calculations as per Australian code of practice in order to eliminate the safety factors. 183 m tall building was analysed for wind loadings obtained by all five wind loading codes in order to get reactions, forces in structural elements in the building. The analysis has been carried out for all three wind zones in Sri Lanka at ultimate limit state. Maximum base moment, base shear, shear wall stresses and column and beam forces (BM, SF, and AF) were observed in zone1, for AS 1170.2:1989. Computed results are nearly double the values obtained from CP3 Chapter V-2:1989. In addition, computed results obtained from Euro code for zone 2 and zone 3 showed higher values compared to other wind loading codes. Also, the researchers highlighted the incapability of Sri Lankan Design manual and CP3 Chapter V-2: 1972 in order to assess the wind loadings for tall buildings. Ultimately, the Study concludes that the AS/NZS 1170.2:2002 is expedient to use for the Sri Lankan context until the country produce its own wind loading standard.

Revuz, Hargreaves & Owen (2010) presented the CFD modelling of a tall building (H=180 m, L=10 m and B= 20 m) by ANSYS Fluent software to study the impact of the domain size pertaining to pressure distribution on the building. The recommendation follows inlet, lateral, top and outlet boundary should be located consecutively 5H, 5H, 5H and 15H away from the building (H= building height) and the blockage ratio should not be exceed 3%. Four different domains (small, medium, medium 2 and large) are created and analysed using RNG k-ε turbulent model. The velocity profiles in upstream and downstream showed good agreement in all four models by showing similar wake pattern. Computed results exhibited the setting of the lateral boundaries in 13B distance is fair enough. The researchers found that the 20B distance for the upstream is sufficiently enough for undisturbed upwind flow by comparing the results in large domain and the medium 2 domain. According to their study, the top boundary should be at least positioned in 5H distance in order to have lesser suction on top of the building. Finally, they concluded that the minimum length of the downstream should be 30B for undisturbed wakes formations.

Kumar & Reddy (2016) presented the numerical simulation of wind for a square shaped tall building (aspect ratio of 1:1:7) in an urban area. The analysis has been carried out for two orthogonal directions under unsteady flow condition by Realizable k-ε turbulence model and DES turbulence model with Realizable k-ε in ABAQUS software. In addition, drag and lift force co-efficient are evaluated. Moreover, wind loads are manually calculated based on gust factor approach in IS 875 Part 3: 1987. For both directions, computed results of mean force showed its highest value at mid height of the. Computed results of 0^0 direction for all levels are increased by 0.3 ratio compared to the manual calculation due to the buffeting characteristics of fluid flow. However, computed results in 90^0 direction for all the levels are decreased by 0.2 ratio compared to code calculations. Standard deviation of force coefficients decreased with the height due to reduction of turbulence intensity with height.

Kwon & Kareem (2013) carried out a comparative study of major international wind codes and standards to obtain the wind effects on tall buildings. ASCE 2010 (USA), AS/NZ 2011 (Australia and New Zealand), AIJ 2004 (Japan), CNS 2012 (China), NBCC 2010 (Canada), Euro code 2010 (Europe), ISO 2009 and IWC 2012 (India) are selected for their study. The main objective has been to identify the differences and similarities in the estimated wind loads and the forces and reactions in the structure such as base shear, base moment and torsional effect etc. Most of the codes followed general concepts to model the dynamic load effects. At the time being, researchers tried to identify the importance of various parameters which directly affect to the analyses. Therefore, basic equations are re written in a general format for the easiness of the comparison. An averaging time period, exposure categories, power law co-efficient, friction velocities and roughness length, turbulent length scale and intensity etc. are few of main parameters which have been used for comparison including the survivability design and serviceability requirements in the along wind and crosswind directions. Gust loading factor is used in order to calculate the along wind load effects. The overall wind loads showed consistency in the along wind response. However, significant discrepancy is exhibited in the crosswind response. The study revealed that the wind induced forces are greatly influenced by some of flow parameters such as velocity profile, averaging time, turbulence profile etc. Therefore, some modifications are proposed to reduce the discrepancy among the codes/standards such as assure consistent velocity pressure at the reference height for all the codes. Similarly, the researchers suggested to reduce the differences of loads by reducing the discrepancies of other parameters like peak factors, turbulence intensity, energy factors, etc. as well. Finally, they revealed that the effects by the wake formation in the torsional and crosswind directions are more dominant than the buffeting characteristics of the fluid flow along wind direction. NALD has been proposed a design procedure for assessing such loading effects accurately. Similarly, ASCE 7 also provided guidelines in their additional design documents related to the standard.

Vafaeihosseini, Sagheb & Kumar (2012) presented the application of the computational fluid dynamics (CFD) tool through wind analysis. Wind analysis has been carried out for 38 storey high rise building under four different wind directions by ANSYS software in order to obtain the most cost effective structural arrangement adhering to codes. Furthermore, structural analysis has been carried out using SAP2000 by importing the structure model and wind forces from ANSYS CFX-Post. 90^0 building placement with respect to the wind flow direction exhibited the maximum pressure in front face of the structure. 60^0 angle of the building configuration exhibited the higher wind pressure on the front face compared to 0^0 and 30^0 angles due to greater exposure area to the wind flow. Average base shear increased with the increase of rotation of the structure with respect to the wind flow angles. Hence, the study concludes symmetric, rectangular shaped building with 0^0 orientation to the wind direction is the most economical shape and the alignment. Moreover, the smaller side of the building should be aligned with the wind flow direction in order to minimize the building materials.

Li, Liu, Luo & Man (2015) evaluated the performance of various RANS models of CFD to find out the most accurate model which will predict the building-wind environment. 105 mm height 23 rectangular blocks are arranged in to an unequal staggered layout for wind tunnel testing. 11 number of turbulence models including S-A, k-ε, k-ω and their combinations of different correction methods are used for testing to compare and validate the turbulence models by evaluating the building-wind environment. Similarly, a numerical wind tunnel simulation has been carried out. Non-slip wall boundary condition is applied for all walls. The study concludes that the group of RNG k- ε model showed the most prominent and the longest wake flow area. Realizable k-ε model exhibited the lowest velocity value in wake flows area. RNG k-ε models with different viscosity modifications (DVM) are suggested as more suitable for estimating the plan view contours of velocity and drag force co-efficient by observing surface pressure measurements. The group of the standard k-ε and low Re k-ω model overestimated the performance of drag co-efficient. Conversely, standard k-ε and k-ω models with modifications underestimated it. In addition, Spalart-Allmaras model showed more accurate results for the drag force co-efficient based on surface pressure measurements. However, the researchers are still in doubt for the accuracy of turbulence length scale estimation in S-A model. Therefore, the reliability of S-A model which predicts the buildings wind environment is still doubtful. Hence, the researchers emphasized the further studies for both flow field and drag force evaluation.

Elshaer, Aboshosha, Bitsuamlak, Damatty & Dagnew (2016) investigated the aerodynamic response of CAARC building using LES turbulent model. The Consistent Discrete Random Flow Generation (CDRFG) technique is used to generate the inlet boundary condition which represents the turbulence field and coherency accurately. Analysis has been carried out for two configurations (an isolated building and a building with surrounded buildings) to study the aerodynamic behaviour of this tall building. Test results have been plotted and compared with the results obtained from a previous boundary layer wind tunnel (BLWT) test and literature reviews. Computed results for pressure and wind-induced responses, such as top displacement, top acceleration and base moments well agreed with BLWT results. The average difference between LES and wind tunnel results for the pressures and dynamic responses is found to be 4% and 6% respectively. However, significant differences are observed between the isolated and the surrounded configuration in order to pressures and dynamic responses. Surrounded configuration showed 50% lower mean pressure values and 40% higher rms (root mean square) value than the isolated configuration. The along-wind and torsional responses of the surrounded configuration exhibited 30% lower than the isolated structure. Conversely, the cross-wind responses of the surrounded configuration showed 15% higher than the isolated structure evidently displaying the surrounding structures' effect. Finally, the study concludes that the LES model with CDRFG technique is useful to simulate the inflow boundary condition on a high-rise building model accurately.

Aksenov, Dyadkin, Luniewski & Pokhilko (2004) studied the Fluid Structure Interaction (FSI) analysis using Abaqus and Flow Vision. Coupling between the finite-element code Abaqus and finite-volume code Flow Vision is used to simulate the Fluid Structure Interaction. Sub- Grid Resolution Method (SGRM) is a unique mesh generation method which use in Flow Vision. The SGRM is capable of linking FE and CFD meshes without introducing any structure in-between them Furthermore, SGRM can transfer data between structure and fluid domains by connecting different type of grids having different resolutions while ensuring the zero data loss. In addition, analysis has been carried out for a flexible cylindrical tank with sloshing water to simulate the fluid structure interaction (FSI).

Franke, Hirsch, Jensen, Krus, Schatzmann, Wesetbury, Miles, Wisse & Wright (2004) formed a set of guidelines/recommendations related to the Computational Fluid Dynamics (CFD) by published computed results related to pedestrian wind in urban areas. The researchers emphasized the importance of accuracy level in physical and numerical input parameters, which are directly influencing to the results. Literature review related to RANS simulations are used to produce the guild lines. The study conclude the following important facts. The authors suggested to perform either non-linear eddy viscosity model or advanced linear eddy viscosity model such as RNG k-ε, realizable k-ε in order to account the anisotropy of the "Reynolds stresses". The inlet, lateral, top and outlet boundaries should be positioned in the order of 5H, 5H, 5H and 15H away from the building as per the guideline of Hall. The blockage ratio should be less than 3% in front area of the domain. Furthermore, they suggested to carry out the simulation for an empty domain with the same grid and applying same boundary conditions in order to verify the equilibrium boundary layer assumption. First order numerical approximation should be avoided and the minimum residuals should be at least in five order concerning the termination criteria. As well, for the iteration convergence, the recommendation emphasized to use the 10-12 double precision machine accuracy to avoid the iterative error completely. The initial minimum grid resolution should be 10 cells per cube root of a building and 10 cells per building separations. Hexahedra or prism cells should be preferred especially in wall areas for better iteration convergence. Finally, they expressed the importance of validating the recommendations/guidelines refer to the wind tunnel test data.

Irwin (2009) presented the new challenges in Wind Engineering related to super tall buildings. Wind is governing lateral load relative to service requirements in super tall building. The study revealed the impotency of taking velocity measurements at upper level wind flows such as 600 m due to the inadequacy of 10 m wind speed data in order to obtain the wind statistics at the top level of tall building. According to the study, response of super-tall building against the wind flow depends on several key factors as shape of the building, damping, distribution of stiffness, distribution of mass etc. Balloon measurements taken from great heights as well as the software models for weather forecasting have been used over the traditional models developed in 1960s to predict to boundary layer. Also the author suggested various methods as softening corners by chamfering, avoid square and rectangular shapes by rounding or stepping the structure, tapering or changing cross section of the structure, adding spoilers, introducing openings and porous sections etc. to reduce the influence of vortex shedding. Additionally, he proposed to increase the stiffness of the building, increase the building mass, employing additional damping system to reduce it further. The paper described the different wind tunnel test methods including different techniques such as aero elastic modelling, Frequency Force Balance method etc. Frequency Force balance (HFBB) tool is used to estimate the design loads at the building base in early stage. Moreover, HFFB can be applied in the time domain analysis especially for a building with additional damping system. High Frequency Pressure Integration (HFPI) method is more appropriate for the irregular shapes buildings to obtain time histories of complete modal loads related to the each vibration mode. HFPI technique was fairly useful to optimize Burj Dubai Tower as aerodynamic favourable shape. Therefore, necessity of additional damping system will not be required further. Finally, the paper concluded that aero elastic model test leads to better results compared to other techniques. In addition, it is a challengeable work for designing terrace and balconies at upper levels while minimizing the wind impact on people in there.

Zhang, Dou, & Li (2013) studied the wind pressure distribution in 303 m height square shaped building in China. Selected wind tunnel test results are compared with the numerical simulation carried out using Standard k-ε turbulence model in FLUENT software. The wind tunnel test has been conducted representing the urban terrain condition under different wind angles. Mean wind speed and turbulence intensity are measured at different heights of the building model. Results are converted in to the mean wind pressure coefficient by MATLAB. Additionally, FEM analysis (dynamic time history response of the wind load) has been carried out opposed with wind tunnel test to evaluate the displacement of the building. The analysis results concluded that streamline around complex high-rise building and average wind pressure distribution of the surface are well predicted by the numerical simulation. Simulation results showed good agreement with the wind tunnel test results for overall. Highest value of wind- induced vibration of the building increased with the increase of wind vibration coefficient. Therefore, author suggested to use the simplified wind vibration coefficient for resistance designing. Moreover, he suggested to use the wind vibration coefficient and shape coefficient obtained from wind tunnel test when calculating building face wind pressure.

Mendis, Ngo, Haritos, Hira, Samali & Cheung (2007) studied the key factors for designing tall buildings for wind loadings. An engineering wind model developed by Deaves and Harris (1978) has been used in Australian wind Designs. Also, various important factors such as area reduction factor, local pressure factor and multiplying factors like terrain, directional, height etc. has been introduced in AS/NZS1170.2:2002 code. Authors suggested to consider three basic wind effects namely, surrounding wind effect, wind loads on façade and wind loads on structure when designing wind sensitive buildings. Furthermore, they emphasized to consider the overall design requirement in terms of structural strength and serviceability requirement if the structure is experiencing dynamic loadings. In addition, occupant comfort level should be kept within allowable limit opposed to the structure vibration. Hence, they proposed various damping systems such as active, semi-active and passive in order to reduce the vibration. Wind tunnel test can be performed to simulate the wind response of structure related to the wind direction, topographical condition as well as surrounding buildings. Similarly, numerical simulation can be carried out, where codes of practice cannot be applied directly.

Mohotti, Mendis & Ngo (2013) discussed the application of computational fluid dynamics (CFD) for evaluating the wind effects on tall buildings. A rectangular shaped building (dimension of 100 m (B) x 150 m (L) x 600 m (H)) in an open terrain has been selected for their case study. Numerical simulation has been carried out by ANSYS FLUENT software for six different configurations under two different flow fields. A uniform velocity profile with a constant speed and ABL based wind profile developed by Deaves and Harris (D&H model, 1978) with k-ε turbulent model have been used for the analysis. The results obtained from the simulation of isolated building with a constant velocity profile exhibited considerable difference with the D & H model results. In addition, the velocity increment of the streamline has been observed at the sharp edges near corners of the building. This results showed good agreement with the results published by Baetke et al (1990). Also results obtained from the two different elevations of the building in D&H model showed the significant difference between the development of flows separation and the outflow velocity due to the variant of incoming wind velocity. In addition, the pressure distribution on surface disclosed a considerable discrepancy with the procedure of the code of practice. Moreover, the analysis has been carried out for the two adjacent buildings of same heights both in upwind and downwind directions to investigate the pressure distribution and flow pattern. The results concluded that the shielding effect from the other structure helps to reduce the vulnerability of the principal building. In such case, the pedestrian comfort should be additionally cared in the area of between the buildings due to turbulence occurring. Therefore, the researchers proposed to have vegetation or landscape in such areas to improve the comfort level of the pedestrians. The aforementioned analysis has been repeated with the replacement of the adjacent building with half of the prior height. In case of the smaller building located in the windward direction, the significant reduction of mean pressure has been observed in the principle building compared to isolated building model due to shielding effect. Also, the pressure contours movement has been observed towards the building top compared with the isolated building model. However, in the case of locating the adjacent building in the leeward direction, the results showed the considerable reduction of the pressure in the back face and no considerable pressure reduction in the front face. Finally, the paper revealed the power of CFD tool which can be used more for the future development of the wind engineering field.

Yoshikawa & Tamura (2013) investigated the effect to the high-rise building by windward building using LES model. A rectangular prismatic shaped building (dimension of 50 m (B) x 50 m (L) x 200 m (H)) has been selected as the principal building under the wind speed of 49.1 ms^{-1} at top of the building. The analysis has been carried out for two type of surrounding structure configurations called Case A (same size of the main building) and Case B (1.5 H of main building). Unstructured grid system was generated for the whole domain. Simulation results have been plotted and compared with wind tunnel test results by Terazaki and Nakamura (2009, 2010). The shape of contours of mean pressure co-efficient (C_{p-m}) and fluctuating pressure co-efficient (C_{p-s}) obtained by Case A simulation showed good agreement with the experimental results. In Case A, C_{p-m} and C_{p-s} results in front wall and side wall of principal building increased by 10% and 20% compared to the experimental results. The computed results of pressure co-efficient highly correlated with the experimental results in both Case A & B. In addition, the simulation revealed that the mean, maximum and minimum pressure coefficients for the adjacent building with 1.5H height are expansive in low range compared to Case A. In both cases, the horizontal distributions of pressure coefficients of computed results well agreed with experimental results and the highest negative peaks pressure showed at height of

0.975H. Moreover, the negative pressure coefficients value was locally increased on the side surface of main building at a height of 0.525H in Case B. Finally, the paper concluded that the LES results can be used to show the complicated flow mechanisms such as the shear layer separation between buildings and which is well suited to predict the complex building-wind environment induced by adjacent structure.

Yoshikawa & Tamura (2012) studied the Large Eddy Simulation Turbulent model (LES) for evaluating the wind loads using unstructured grid system. A square cylinder shaped building (dimension of 30 m (B) x 30 m (L) x 90 m (H)) has been selected for the analysis under two different wind angles. Wind tunnel experiment has been carried out for the 1/300 scaled model. In addition, numerical simulation has been performed opposed to the wind tunnel test to compare the results.Unstructured tetrahedral prismatic grid system has been created for the whole domain. The mean pressure co-efficient Cp-m and fluctuating pressure co-efficient Cps are presented graphically for 0^0 and 15^0 wind directions. In case of 15^0 wind angle, surface pressure co-efficient showed symmetrical distribution. The computed results of Cp-m well agreed with the experimental results for both cases. The computed results of maximum, fluctuating and minimum pressure co-efficient highly correlated with the experimental results. However, they showed comparatively dispersed distribution with mean pressure co efficient. The computed results for mean pressure co-efficient well agreed with the wind tunnel test results. Also, the computed value for peak pressure co efficient showed slightly overestimation than the experimental results. Finally, paper concluded that the LES turbulent model with unstructured grid system is more appropriate for assessing the fluctuating pressure component of the wind flow.

Olenkov & Puzyrev (2017) studied the wind effect on a unique building of “Church of the Intercession of the Holy Virgin” in the Russia. The selected building is mainly a brick one-dome temple consisting different geometrical parts such as an octagonal drum at temple top, a rectangular refectory with aisles, a three-tier bell towers etc. In such case, the guidelines of building regulations/guidelines of “Load and effect”

(Moscow) cannot be followed for calculating the wind loads. Therefore, the numerical simulation has been performed by ANSYS. The inlet, lateral, top and outlet boundaries of the fluid domain were set to 6-8 H (H - building height) distance away from the building. Fine mesh was used in near wall region in order to properly simulate the near-wall flow. A computing algorithm was developed to represent the static component of the wind flow. The analysis has been carried out under 8 different wind angles. Non-shear flow boundary condition was applied on the building walls. The results were used to study the various important fluid characteristics such as surface pressure on the building, wind velocity field, aerodynamic coefficients, draughty regions, wind stagnation regions, turbulence kinetic energy, loads on base etc. Ultimately, the paper revealed that existing codes and guidelines fail to predict the wind effects on unique buildings like this case study. Furthermore, the researchers recommended to carry out the unsteady numerical simulation using DES or URANS turbulence models and verify with the actual field measurements. Also, they emphasized the importance of "preliminary" numerical simulation in in terms of critical wind directions, needful of wind tunnel test, flow parameters refinement by simulation and compare with test results when evaluating the wind effects for theses sort of buildings.

Antipin, Alekhin, Gorodilov, Khramtsov & Noskov (2014) studied the wind effects on high-rise building. Numerical analysis has been carried out for the wind flow around the 8 mm diameter cylindrical object to study the wind characteristics. Analysis has been performed by ANSYS software under three different fluid flow conditions, namely, laminar, SST turbulent and k-ε turbulent. Tetrahedral finite element mesh was used for the domain. Simulation was performed using four different grid sizes in order to find the optimal grid size. In addition, experiment was conducted opposed with the simulation in order to estimate the accuracy of results. The results of wind velocity of STT turbulent model showed good agreement with experimental data. In addition, a cylindrical shaped 209 m height Iset Tower has been selected as their case study. The inlet, lateral, top and outlet boundaries of the fluid domain were set in sequence of 10H, 10H, 5H and 10H (H - Building height) distances. Tetrahedral prismatic cells were used for the domain. The wind pressure results were compared with the results of wind tunnel test carried out by the German company "WACKER INGENIEURE". Results concluded that the maximum wind loads obtained by analysis showed in good agreement with experimental results. Thus, the researchers recommended to perform the both aerodynamic test and numerical analysis when designing the high-rise, unique buildings.

Sadh & Pal (2018) studied literature on wind analysis for high rise building. Few important research papers have been selected for their literature survey to understand the behaviour of the wind forces. Vyavahare, Godbole & Nikose (2012) studied the response of the tall slender building in order to wind excitation for along wind and crosswind. However, the Indian code (code IS-875 Part-3 1987) didn't provide the calculation procedure for the crosswind response. Therefore, the recommendations /guidelines have been set by IIT Kanpur to evaluate the crosswind response of tall buildings following the same procedure of AS/NZS 1170-2:2002. In this paper revealed that the Artificial Neural Network (ANN) can be used to obtain the above process by limited available data. Muffassir & Kalurkar (2016) carried out the comparative study on the wind effect between the multi-storey RCC building and composite building. Fifteen different building configurations including various heights such as 20 m, 50 m, 80 m etc. have been considered for their analysis. The wind analysis was performed by ETABS 2015 software. The study concluded that the composite structure is more suitable for high rise building compared to the RCC since the composite structure showed highly elastic behaviour under wind loads. Also researchers observed the structure response such as time period for vibration modes, story displacement, base reaction etc. under the wind effect in order to find out the most effective shape for the high rise building structure. Lakshmanan, Gomathinayagam, Harikrishna, Abraham & Ganapathi (2009) evaluated the design wind speed for each site in India for a return period of 50 years. Hourly wind speed data from 70 meteorological centres have been used for their analysis. Finally, researchers proposed some changes in to the wind zone map in India for designing the structures. Gunawardena, Fernando, Mendis, Waduge, & Hettiarachchi (2017) discussed the challenges and the engineering solutions for a successful design of a tall building in terms of stable, strength, safe and also well-performing under wind effect. Arya, Hussain & Khan (2014) investigate the result of wind speed and structural response of building on sloping ground. The wind analysis was performed by STAAD-Pro software. Analysis has been carried out for 60 different cases under different building configurations, different sloping grounds and different wind zones. Structural member forces such as moment, shear force, deflection and storey drift were observed with respect to the various ground slopes. Reddy (2015) studied the vibration of tall reinforced concrete chimneys under along wind effect according to the three different wind codes , namely India (IS 4998 (part 1)), America (ACI 307) and Australia (AS/NZS 1170.2:2002).Furthermore, the calculation procedure from Indian, American and Australian codes were studied and discussed including the assumptions which were used to simplify the procedure. The study concluded that the code methods of a long-wind analysis is inadequate to estimation the deflection of the chimney accurately. Ultimately, performed literature survey concluded that the code guidelines are inadequate to understand the behaviour of the wind. Therefore, various types of wind analysis has been performed to find out the key parameters of the fluid.

2.1.1 Summary

- Various studies have been carried out to estimate the wind loads and their effects on tall buildings by Codes of practice. Furthermore, similarities and differences have been identified between different wind loading codes.
- Numerous researches have been conducted to assess the complex building-wind environment using CFD technique. Moreover, some researchers tried to develop the CFD guidelines , which helps for modelling the fluid - structure interaction problems.(Ex: size of the fluid domain, mesh type)
- Some of the researches have been conducted to observe the suitability of different types of turbulent models relate with their applications.

- Number of experiments have been carried out to observe the wind interaction with tall building and compared with the numerical simulation results.
- Most of the researchers highlighted the advantage of CFD tool when assessing the complex fluid flow problems. Also, indicate the incapability of providing adequate guidelines/recommendation of existing codes of practice to assess such kind of environments accurately.

2.2 Analysis and Modelling of Fluid Flow around Buildings – Theoretical Framework

This section describes the types of fluid flow, different flow patterns around the tall building and building performance under the wind action. Moreover, this chapter discusses the applicability and limitations of codes of practice when assessing wind loads on tall building as well the practicality and the advantages of using CFD in such situations.

A fluid flow has different characteristics as steady or unsteady, compressible or incompressible, rotational or irrotational, viscous or non-viscous Newtonian or Non-Newtonian and laminar or turbulent. Some of the above features signify the properties of the fluid and some represent the flow characteristics. As well, fluid flow is very complex when it becomes turbulent.

Fluid dynamics can be applied to solve various type of real life problems as calculating aerodynamic forces on aircraft wing, measuring blood flow rates in arteries, predicting weather patterns, simulating wind forces and their effects on high-rise buildings and modelling fission weapon detonation etc. The main focus on all the above applications is to find the changes of the fluid properties such as velocity, pressure, density, and temperature w.r.t space and time using empirical and semi empirical equations (Anon., 2020). Mainly fluid flow can be categorized in to two, namely, laminar and turbulent.

Laminar flow

Laminar flow is described by fluid particles following smooth paths in parallel layers, with little or no mixing with adjacent layers. The viscous forces are dominant to keep all the fluid particles in a line. (Reynolds, 1895)

$$R_e = \frac{Inertia\ Force}{Viscous\ Force}$$

Generally, at low velocities, the fluid have a tendency to flow without mixing with adjacent layer .Therefore, the chance to occur eddies is zero or less. In laminar flow, if the particles are moving close to the solid surface, which would be likely to move as an orderly parallel layers. High momentum diffusion and as well as the low momentum convection are the main physiognomies of Laminar flow. Moreover, shear stress in laminar flow depends only the viscosity of the fluid.

Turbulent flow

Converse to laminar flow, turbulent flow is described by the fluid particles experiencing irregular fluctuations and mixing with adjacent layers (Reynolds, 1895). Therefore, the velocity of a fluid particle in a turbulent flow is changing with the time resulting the corresponding pressure changes. Hence, when the inertia force is dominant over viscous force, laminar flow can be transferred in to a turbulent flow. Most of the events in real life such as wind flow around structures and aircrafts, eddies or swirls, ocean waves, blood flow in arteries etc. fall in to the category of "turbulent flow".

Reynolds number for flow around the building can be found using the below expression (Reynolds number, 2020).

$$R_e = \frac{\rho u L}{\mu} = \frac{uL}{\vartheta}$$

ρ = density of the fluid (SI units: kg/m^3)

u = flow speed (m/s)

L = characteristic linear dimension (m)

μ = dynamic viscosity of the fluid (Pa·s or N·s/m^2 or kg/ (m·s))

ϑ = kinematic viscosity of the fluid (m^2/s).

2.2.1 Wind loading on tall buildings

Interaction of wind with tall building creates complex building-wind environment when the building is subjected to wind loads both along and crosswind direction as described in Chapter 1.1. As a result of it, one or few of the below characteristics can be observed: flow separations, wake formations, buffeting, vortex shedding, galloping (transverse oscillation of the structures due to the development of aerodynamic strengths), flutter motion (unsteady oscillation of the building due to coupling between elastic deformations of the structure and aerodynamic forces). (Effect of Wind Design of High Rise Buildings, 2019) Therefore, it is important to understand the different wind flow patterns around the tall building, which may cause for the building performance.

Interaction of wind with a building depends on several factors: structure geometry, free-stream turbulence, approaching boundary layer flow etc. Therefore, various researches have been conducted to study the wind flow patterns around an isolated building. Wind flow was categorized in to five main regions: incident turbulent flow, near wake flow, turbulence wake, horse-vortex system and reattachment of the flow in the building faces. (Hulle, 2012) & (Becker, et al., 2002).

As shown in Figure 2.1, when the wind runs into the building, it gradually diverts in to different paths. Maximum pressure occurs in the region of 60-70% of the building height (stagnation point) at the windward face. At that point, the flow is guided to the lower pressure zones of sideward and leeward. Part of the wind is directed over the building. (Streamline 1-3, Figure 2.1) and another part is diverted around the vertical edges (Streamline 2and 4, Figure 2.1).The upward and sideward flows detach at the edges of the windward face of the building consequently, forms a separation bubble (recirculation zone), where velocity of the wind is low and the turbulence intensity is high. However, separated flow can reattach at the side face and roof but it depends on the size of the building and the turbulence intensity of the approaching flow (Figure 2.2).

Considerable amount of wind is guided to the downward from the stagnation point and creates a vortex at ground level (standing vortex or horseshoe vortex) (Streamline 6, Figure 2.1). Then it sweeps around the corners (Stream line 8, Figure 2.1) and reconnect to the overall flow around the building at the ground level (Stream line 9, Figure 2.1). Therefore, velocity of corner streams is high. Part of the standing vortex at ground level is reversed to the direction of the incident flow. This interaction between the approach flow and reverse flow creates a region with low wind speed at ground level (Region 7, Figure 2.1).

In general, complex and powerful transient wind flow patterns occur at the leeside of the building. Those are having less velocity values. (Streamline 10–16, Fig 2.1). At the leeward side of the building, an under pressure zone exists. As a result of the low pressure region at the downstream, reverse flow or recirculation flow occurs in a cavity zone that consists of vortices (near wake). The cavity reattachment line at the leeside of the building as shown in Figure 2.2. However, the wind moves its normal direction beyond the reattachment line. Nevertheless, wind velocity is low for a considerable distance behind the structure (far wake). Nevertheless, the flow patterns will be more complex for a building with adjacent structures (Bernek & Koten, 1979).

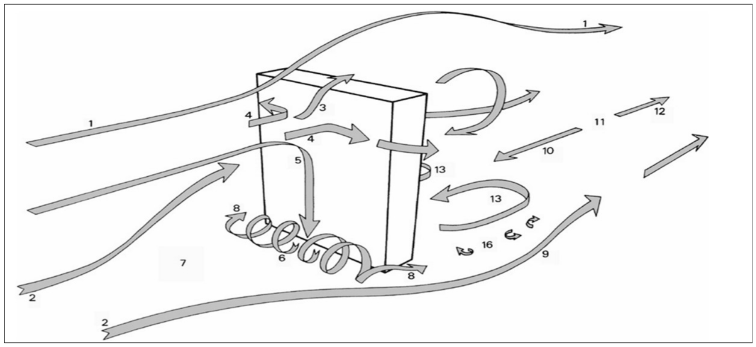

Figure 2.1 Schematic representation of wind flow pattern around the high-rise building (Bernek & Koten, 1979)

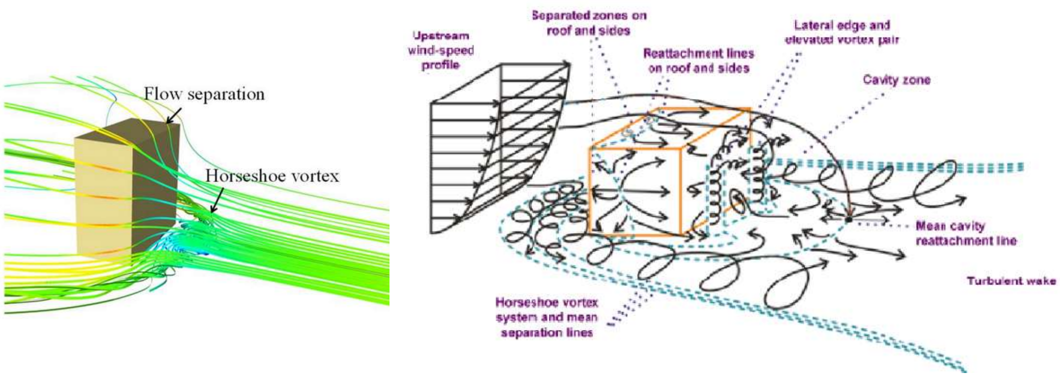

Figure 2.2 Schematic representation of the mean atmospheric boundary layer flow around an isolated sharp-edged building (Blocken, et al., 2011)

2.2.2 Velocity components of a wind flow

Wind flow carries number of eddies along with the general stream having different sizes and different rotational characteristics. These eddies cause to have the gustiness or turbulence in the wind flow. Therefore, in case of a fluid flow, velocity component consists of two parts, namely 'mean part' and 'fluctuating (turbulent) part. As described in Chapter 1.1, with the increment of the wind velocity, wind pressure on the building increases proportionally with the square of the mean wind velocity. Conversely, the gustiness decreases with the height and it remains constant after gradient height. (Mendis, et al., 2007). In general, peak gust tends to occur over a time period of 3.5 to 15 seconds. However, impact of the gust depends on the dimension of the building, for example, large structures are effected more gustiness (Effect of Wind Design of High Rise Buildings, 2019). The relationship between the mean and the fluctuating components is shown in the following expression (Scruton & Rogers, 1971).

$$V_{(z,t)} = V_t + {V^i}_{(z,t)}$$

where,

$V_{(z,t)}$ = wind velocity at any given instantaneous time 't'

V_t = average wind speed

${V^i}_{(z,t)}$ = fluctuation wind speed

Therefore, the additional set of equations are needed to calculate the fluctuating flow variables.

Wind speed increases with the height due to various reasons. One of them is high surface friction near the ground level due to obstructions such as trees, buildings and the effect of the friction is negligible at the great heights above the surface. In addition, density of air decreases with the height resulting the air movement with higher speed at higher levels. Other reason is the pressure gradient between the warm air and the cold air increases with height due to thermodynamic consequences (solar heating of the earth) resulting the strong wind at upper levels. Wind speed at upper level is called as gradient wind velocity (Haby, 2020).

The Australian/New Zealand wind code (AS/NZS 1170.2:2011) and Euro code (EN 1991-1-4:2005) categorized terrain condition according to their roughness lengths (z_o).

Figure 2.3 illustrates the mean wind profile for different terrain categories specified in AS/NZS 1170.2:2011.

Due to the friction at the ground level, wind velocity becomes zero and then varies to the gradient wind thickness within the boundary layer. Depending on the terrain category, the boundary layer thickness may vary from 500-3000 m, for example, gradient height of the Suburbs –Woodland is higher than the open sea area. (Mendis, et al., 2007)

Reference wind speed specified in a different way in different codes of practice, for instance, AS/NZS 1170.2:2011 code defines 3-second gust wind speed at a height of 10 m above the ground relates to the terrain category 2.

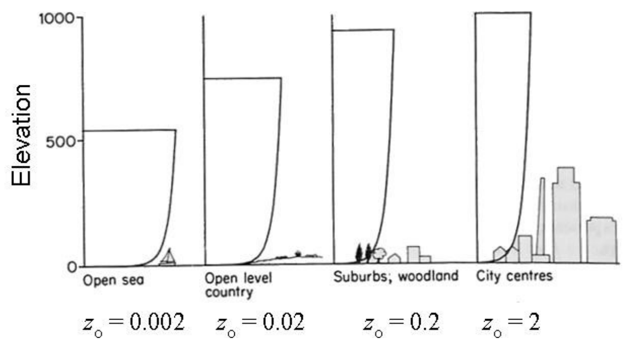

Figure 2.3 Mean wind profile for four different terrain categories (Mendis, et al., 2007)

In general, two different wind profile laws are derived to explain the vertical distribution of the wind speed (u_z) in horizontal direction.

Power Low wind profile is given by

$$U(z) = U(zA) \; (\frac{Z}{Z_A})^{\alpha}$$

where,

$U(z)$ = Wind speed at height Z

$U(zA)$ = Wind speed at reference height Z_A

α = Hellmann exponent

(Emeis & Turk, 2007)

Logarithmic Law is given by

$$V_z = \frac{U^*}{\mathcal{K}} \left(\ln\left(\frac{z}{z_0}\right) - \varphi\left(\frac{z}{L_*}\right)\right.$$

where,

V_z = Wind speed at height z

U^* = Frictional velocity

K = Von Karman's constant = 0.4

Z_0 = Roughness length

L_* = Monin-Obukhov length

φ = Stability Correction

However, under natural stability condition, φ drops out and the equation is simplified as below. (Emeis & Turk, 2007)

$$V_z = \frac{U^*}{\mathcal{K}} \left(\ln\left(\frac{z}{z_0}\right)\right)$$

Prediction of mean wind speed by log wind profile considers as more realistic compared to power law profile between the 10 -20 m heights in atmospheric boundary layer. However, both profiles generate reliable values between 20-100 m in natural atmospheric condition. Then, mean wind speed values from power law are more realistic from 100 m to the top of the Atmospheric boundary. Moreover, power law profile is typically used for the wind energy purposes due to its mathematical simplicity (Log wind profile, 2018).

Further, the Atmospheric Boundary Layer (ABL) is the lowest part of the atmosphere, which is effected due to the interaction with the planetary surface. Physical properties of this layer as temperature, flow velocity and moisture fluctuate rapidly with strong vertical mixing (Planetary boundary layer, 2020).

2.2.3 Building performances and the optimal structure design under the wind action

Basically, wind load can be divided in to two: Static and Dynamic. For short time period wind load can be considered as dynamic .Conversely, it can be seen as static for long time period. A consequences of turbulence may cause to have dynamic loadings (Effect of Wind Design of High Rise Buildings, 2019). Furthermore, the wind load varies dynamically with respect to the degree of shielding provided by other buildings and topographical features etc. (Taranath, 2005). As a result of dynamic loading, tall or slender building tends to vibrate in a sinusoidal manner or narrow band random manner for both along and crosswind direction. Displacement of the structure depends on several factors: mass, stiffness, shape of the building as well as the velocity distribution (Effect of Wind Design of High Rise Buildings, 2019).

As described in Sections 1.1 & 2.2.1, tall or slender structure tends to have dynamic response due to several different phenomena. A consequence of turbulent buffeting in along wind direction may cause to structure vibration. Also, structures are more sensitive to crosswind response due to vortex shedding, galloping as well as excitation by turbulent buffeting. Flutter is unsteady oscillation of the structure due to combination of bending and torsion. However, galloping and flutter are not serious issues for the design (Mendis, et al., 2007). Hence, all the above conditions should be carefully considered and analysed to get the optimum design.

In case of optimal design, placing smaller side (width) of the building aligned with the wind flow may cause to have lower pressure as lateral loads on the building. Therefore, it is not required to provide more building materials such as reinforce steel to prevent overturning due to huge lateral force (Vafaeihosseini, et al., 2012). Furthermore, aforementioned researchers studied the most cost effective building configuration with the wind direction along with the reduction of the materials quantities. Hence, the results showed the 43% increment of the required concrete quantity for the building under 90^0 wind direction compared to 0^0 wind direction. Similarly, required steel quantity showed 21% increment building under 90^0 wind direction compared to 0^0 wind direction (Vafaeihosseini, et al., 2012). Therefore, building placement against the wind load is more important to have economical design.

2.2.4 Estimating wind loads using codes of practice

A number of advanced wind loading codes have been developed for estimating the wind loading and their effects on and around the structures as described in Section 1.2. The min available design manual for "Wind Engineering'' in Sri Lankan is "Design Building for High Winds – Sri Lanka", which is prepared based on CP 3 Chapter V – Part 2:1972. However, it can be used only for estimating wind loads and their effects on low-rise buildings by its simple techniques. Therefore, among all these codes of practice, CP 3 Chapter V– Part 2:1972 is the most common practice amongst Sri Lankan Engineers since last few decade (Weerasuriya, et al., 2010). Nowadays, Structural Design Engineers prefer to follow more advanced wind loading codes such as BS-EN1991-1-4:2005 with National Annex SLS EN 1991-1-4 :2019 & AS/NZS 1170.2:2011 due to the inadequate provisions in CP 3 Chapter V – Part 2:1972 for designing tall buildings against the wind loadings.

2.2.4.1 Static and dynamic analysis

Wind induced effects on a structure can be mainly categorized in to three different types, which are static, dynamic, and aerodynamic (Alaghmandan & Elnimeiri, 2013). The analysis procedure in all the codes of practice is parted in two: Static Analysis and

Dynamic Analysis. However, all the wind codes mainly approach the static method while providing some design guidance for dynamic analysis, which is for tall, slender, wind sensitive buildings. In addition, all wind codes emphasis that dynamic analysis must be carried out for the structures with both a height to breadth ratio greater than five and a first natural frequency less than 1 Hz (Mendis, et al., 2007).

The static analysis is built on an assumption (quasi-steady) that the structure is a fixed rigid body for the period of the wind flow. However, in general, the static analysis can be suitable only for structures less than 50 m height. (Mendis, et al., 2007)

All the codes of practice assume that wind forces are relatively constant with time (Mendis, et al., 2007). But in reality, wind velocity consists static component as well as a fluctuating (dynamic) component. Gusty or turbulence effect may occurs due to set of eddies with different size and different rotational speeds. The magnitude of the fluctuations depends on many factors associated with turbulence or local gustiness caused by structure and the surrounding environment.Therefore, wind loading codes use different approaches to evaluate the turbulent characteristics of flow field when flow goes around the structure and end up in a single equivalent static wind pressure value. The static pressure value signifies the maximum peak pressure on the structure. (Mendis, et al., 2007). Therefore, use of these standards/codes without clearly understanding the basis and flow parameters, leads to problems (Weerasuriya, et al., 2010). Hence, it is necessary to have a thorough understanding of the basic commonalities and differences among major international wind codes/standards.

2.2.4.2 CP3 Chapter V-2:1972

In Sri Lanka, CP3 Chapter V–Part 2:1972 is the most common practice for assessing the wind loads on the buildings due to its simplicity and the familiarity. In CP3 Chapter V-Part2:1972, quasi-static method is used to calculate the wind loadings on a building (Weerasuriya, et al., 2010). In quasi-static approach, which considers an additional static force to calculate the dynamic phenomenon. However, the value of the additional force, which is fair enough to represent the dynamic condition and get accurate result, is a thoughtful question.

In CP3 chapter V-2:1972 considers the 3*s* gust wind speed at 10 m height in open terrain with no obstructions as the fundamental basic wind speed. CP3 CHAPTER V-2:1972 uses power law expression to describe the vertical distribution of the horizontal mean wind speed.The code considers only few factors such as topography factor, ground roughness, building size & height above ground factor, statistical based factor and directional factor for calculating the dynamic wind force on the structure. However, the factors such as wind adjustment for seasonal variation, altitude correction, aerodynamic shape, turbulent intensity, turbulent length scale, resonant response etc. are not accounted in CP3 CHAPTER V-2:1978 compared to other international wind loading codes.

Apart from the codes, "Design Buildings for High Winds – Sri Lanka" is the only available design manual to evaluate the wind loads on structures. However, this design document is prepared based on the CP3 Chapter V – Part 2:1972, this can be more suitable for designing low – rise buildings. (Weerasuriya, et al., 2010) Therefore, most of the Sri Lankan Designers are now following the advanced international wind loading codes/standards such as BSEN 1991-1-4:2005 with National Annex (SLSEN 1991-1-4:2019) & AS/NZ 2011:2002 since the CP3 Chapter V – Part 2:1972 code provisions are inadequate for evaluating the wind loads on medium & high-rise buildings.

2.2.4.3 Euro Code – BSEN 1991-1-4:2005 and NA SLS EN 1991-1-4:2019

BS-EN1991-1-4:2005 has been prepared based on the European Standard**;** Euro code 1: Actions on structures – Part 1– 4: General actions – wind actions. (EN 1991-1-4:2005). Unlike the Euro code, BS-EN1991-1-4:2005 is much simple and easy to follow when calculating the wind loads on structures. Furthermore, dynamic behavior of the structure when it subjected to wind loading can be assessed.

SLS EN 1991-1-4:2019

Apart from the code, our own National Annex (SLS EN 1991-1-4:2019) has been prepared considering the Sri Lankan context and which is already published in 2019. National Annex (SLS EN 1991-1-4:2019) manly follows the BS-EN1991-1-4:2005. Besides, nationally determined parameters are recommended considering the country context such as fundamental value of basic wind speed ($V_{b,0}$), orography factor (c_0 – SLS EN 1991—1:2019 A.3) , background permeability etc. Furthermore, SLS EN 1991-1-4:2019 provides nationally determined parameters for estimating the wind loads on bridges such as Angle of wind direction to the deck axis in vertical and horizontal planes , Dynamic response procedure for bridges, Force coefficients for parapets and gantries on bridges etc . Therefore, this is more helpful for the Wind Engineering field in Sri Lanka.

In BS-EN1991-1-4:2005 and the National Annex (SLS EN 1991-1-4:2019), gust effect factor method is used to evaluate both fluctuating wind speeds and dynamic behavior of the structure. Gust effect factor is represented by the "Structural factor" (C_sC_d). Gust effect factor can be expressed in following expression (Kwon & Kareem, 2013).

$$Gust\ Effec\ \ Factor\ (G) = \frac{Gust\ Loading\ Factor\ (GLF)}{Gust\ factor\ for\ the\ wind\ load\ Effect\ (G_q)}$$

However, both CP3 chapter V-2:1972 & AS/NZS 1170.2:2011 specify the 3s gust wind speed as the fundamental basic wind speed, BS-EN1991-1-4:2005 considers characteristic 10 minutes mean wind velocity as their fundamental basic wind speed. Yet, we have only 3s gust wind speed data, which should be converted in to characteristic 10 minutes mean wind speed data for the reference. In 1999, Cook introduced a method for converting 3 s gust wind speed to mean hourly wind speed.

Then ICEUK proposed 1.06 conversion factor to convert mean hourly wind speed in to 10 minute mean speed (Weerasuriya, et al., 2010). BS-EN1991-1-4:2005 specifies the wind profile using natural logarithmic expression.

BS-EN1991-1-4:2005 considers so many factors such as topography factor, ground roughness, topography factor, wind directional factor, roughness factor, and exposure factor when calculating the wind loadings on the structure. Apart from those factors, some special factors are introduced in BS-EN1991-1-4:2005 compared to other two wind loading codes such as altitude correction factor, seasonal correction factor for wind. Altitude correction factor is particularly useful when calculating the wind loads for the buildings locate in hill country. SLS EN 1991-1-4:2019 recommended nationally determined parameters and procedures to calculate some of the above factors considering the country context.

In BS-EN1991-1-4:2005 and the SLS EN 1991-1-4:2019, the velocity profile should be divided into few parts to make the calculation process easy. First, from the ground to the height equal to the width of the building (b= width of the building face which perpendicular to wind direction) is considered as the “lower portion”. Similarly, b width is measured from the top of the structure and takes it as the “upper portion”. In the middle portion is divided in to several horizontal strips according to the designer’s requirement. Correspondingly, the pressure profile is developed with the height of the building (Weerasuriya, et al., 2010).

2.2.4.4 Australian Code – AS/NZS 1170.2:2011

AS/NZS 1170.2:2011 is an Australian wind code, which is now becoming a common practice amongst Sri Lankan Engineers/Designers. AS/NZS 1170.2:2011 is more advanced wind loading code, which is more capable for predicting the complex building- wind environment.

Similar to BS-EN1991-1-4:2005, gust effect factor approach is used in the AS/NZS 1170.2:2011 code as well. In AS/NZS 1170.2:2011, gust effect factor is represented by the "dynamic response factor" (C_{dyn}) which is a combination of several other factors such as turbulent Intensity, peak factor for the upwind velocity fluctuations, background factor, peak factor for the resonant response etc. (Kwon & Kareem, 2013). Apart from those factors, AS/NZS 1170.2:2011 considers similar factors defined in CP3 Chapter V-2:1972 and BS- EN1991-1-4:2005 such as topography factor, roughness length, wind directional factor etc. to calculate the wind loadings on the structure.

AS/NZS 1170.2:2011 also considers the 3*s* gust wind speed at 10m height in terrain category 2 as the fundamental basic wind speed. Moreover, it specifies the wind profile using natural logarithmic expression.

One of the key difference between the AS/NZS 1170.2:2011 with the other two codes is that the code presents the different regional wind velocities with respect to the different average recurrence intervals such as V_{50}, V_{100} etc. Generally, other two codes use the safety factors (1.4, 1.2) for Ultimate Limit State calculations. However, AS/NZS 1170.2:2011 prefers to use the higher regional wind speed for ULS calculations omitting the safety factors (Weerasuriya, et al., 2010).

2.2.5 CFD in wind engineering

The application of CFD in "Wind Engineering" field becomes more popular in last few years due to the burgeoning of high rise buildings with unique architectural features. Wind load effects on those type of buildings are quite significant. In such cases, evaluating the wind loads and their effects on the building is a challenge. Therefore, it is essential to perform the wind flow simulation using CFD tool.

Computational fluid dynamics (CFD) is one of the key tools, which can be used to assess the complex building-wind environment and aerodynamic effects on the building accurately. CFD tool is strengthened by various solution approaches such as RANS and LES etc. More details are contained in Chapter 1.3.

2.2.5.1 Averaged Navier Stoke's equations (RANS)

Reynolds Averaged Navier-Stokes (RANS) equations are mainly used to find the flow variables in a turbulent flow. RANS is one of the main approach of computing the turbulent flow, which was initially suggested by Osborne Reynolds in 1895. RANS equation is mainly applicable for an incompressible Newtonian fluid. As described in Section 2.2.2, flow variables such as velocity and pressure can be parted into mean and fluctuating components by the concept of "Reynolds's decomposition". Consequently, RANS equations are derived from the instantaneous Navier–Stokes equations by introducing the new term "Reynolds Stress". The term of "Reynolds stress is defined with the intention of setting the fluctuating component as a function of the mean flow variable. Hence, the "turbulence model" is defined by setting the "Reynolds stresses" term and this is called as the "closure problem". RANS equations should be averaged over a sufficiently large time in order to obtain the statically steady solution of the flow variables (Reynolds, 1895). Moreover, two different approaches for representing the 'Reynolds Stresses' as a function of mean flow variables are discussed in Chapter 1.3.

In addition, RANS equation can be written using Einstein notation in Cartesian co-ordinates as well. The general expression of RANS is shown in below ((Reynolds, 1895).

$$\rho\bar{u}_j \frac{\partial \bar{u}_i}{\partial x_j} = \rho\bar{f}_i + \partial/_{\partial x_i}\left[-\left(\bar{P}\,\delta_{ij}\right) + \mu\left(\frac{\partial \bar{u}_i}{\partial x_j} + \frac{\partial \bar{u}_j}{\partial x_i}\right) - \rho\overline{u'_i u'_j}\right] \quad (1)$$

ρ = Density of fluid

$\rho\bar{u}_j \frac{\partial \bar{u}_i}{\partial x_j}$ = Change in mean momentum of fluid element due to the unsteadiness in the mean flow and the convection by the mean flow

$\rho\overline{f_i}$ = Mean body force the isotropic stress due to the mean pressure field

$\overline{P}\,\delta_{ij}$ = The isotropic stress due to the mean pressure field

$\mu\left(\frac{\partial\overline{u}_i}{\partial x_j}+\frac{\partial\overline{u}_j}{\partial x_i}\right)$ = The viscous stresses

$\frac{1}{2}*\left(\frac{\partial\overline{u}_i}{\partial x_j}+\frac{\partial\overline{u}_j}{\partial x_i}\right)$ $= S_{ij}$ - The mean rate of strain tensor.

$\rho\overline{u'_i u'_j}$ = Reynolds stress due to the fluctuating velocity field

2.2.5.2 Turbulence models

As described in Section 2.2.5.1, turbulence model is introduced in order to define the fluctuating component of the flow variable as a function of mean flow variable. Turbulent model is a mathematical model containing set of equations. These equations can only be used to solve the simple turbulent flow problems. However, most of real life problems cannot be solved by the equations due to their complexity. Therefore, researchers did not show much more interest on this topic in past decades. However, the rapid development of Computational Fluid Dynamics (CFD) technique corresponding to computer configurations in recent past years helps to get much more attention from researchers and structural design engineers to solve real life turbulent flow problems.

The relationship between the turbulence stresses to mean rate of deformation was proposed by introducing the new term “turbulence eddy viscosity” (υ_t) (Boussinesq, 1877). This can also be used to close the aforementioned system of equations. These type of models are called as eddy viscosity models or EVM's. However, this model was not validated yet.

$$-\overline{u_i' u_j'} = \upsilon_t \left(\frac{\partial \bar{u}_i}{\partial x_j} + \frac{\partial \bar{u}_j}{\partial x_i} \right) - 2\, k \delta_{ij} \qquad (2)$$

Sij = Mean rate of strain tensor

υ_t = Turbulent Eddy viscosity

k = $\frac{1}{2}\ (u_i' u_j')$

δ_{ij} = Kronecker delta

Different types of turbulence models such as Spalart– Allmaras, 2-equation (k-ε), 2-equation (k-ω) are used with RANS.

The LES approach is mainly developed to reduce the computational cost compared to DNS (Direct Numerical Simulation) approach. Therefore, smallest length scales are disregarded when performing LES model due to its higher computational cost. Generally, LES approach generally fits for the situations such as combustion, acoustics, simulations of the atmospheric boundary layer etc. However, the Designers and the Research students are still faltering to use this model owing to the higher computational cost. For that reason, performing of LES model in engineering applications becomes an impractical solution (Smagorinsky, 1963).

Therefore, in this case study S-A turbulent model was performed in order to compare the results with codes of practice.

However, selection of more suitable approach for the particular fluid flow problem depends on the several facts such as type of the problem, level of accuracy in results, computational cost, time etc.

2.2.5.3 Spalart –Allmaras (S-A) turbulence model

Spalart –Allmaras is one equation model, which contains an additional transport equation to find the modified eddy viscosity (υ_t).The Boussinesq hypothesis is used to model the Spalart – Allmaras (S–A) model as described in Section 2.2.5.2. Eddy viscosity is a flow property which is obtained from the assumption of an equilibrium boundary layer concept. Therefore, the eddy viscosity ratio is defined as the ratio of molecular viscosity over to kinematic eddy viscosity. The main advantage of using the eddy viscosity ratio is that which gives the impression of how strong the influence of the turbulent viscosity over to the molecular viscosity. Therefore, the eddy viscosity ratio is especially convenient to use in low-turbulence cases when it is difficult to estimate the characteristic turbulent length scale. In addition, S-A is a low cost model compared to other models. This model can be well suited for the situations, where the wall-bounded turbulent flow exists like flow around cars, buildings, aircrafts etc. (Schmitt, (2007). Generally, the model shows good results when boundary layers are subjected to adverse pressure gradients.

The following set of equations can be used to calculate the kinematic eddy viscosity (Spalart & Allmaras, 1992).

$$\upsilon_t = \tilde{\upsilon} f_{v1} \tag{3}$$

$\tilde{\upsilon}$ - Spalart–Allmaras variable

$$f_{v1} = \frac{\mathcal{X}^3}{\mathcal{X}^3 + C_{v1}^3} \quad ; \quad \mathcal{X} = \frac{\tilde{\upsilon}}{\upsilon} \tag{4}$$

$$\frac{\partial \tilde{\upsilon}}{\partial t} + u_j \frac{\partial \tilde{\upsilon}}{\partial x_j} = C_b \left[1 - f_{t2} \right] \tilde{S}\, \tilde{\upsilon} + \frac{1}{\sigma} \{ \nabla . \left[\left(\upsilon + \tilde{\upsilon} \right) \nabla \tilde{\upsilon} \right] + C_{b2} |\nabla \tilde{\upsilon}|^2$$

$$- \left[C_{w1} f_w - \left(C_{b1}/_{\kappa^2} \right) f_{t2} \right] \left(\tilde{\upsilon}/_{d} \right)^2 + f_{t1}\, \Delta U^2 \tag{5}$$

$$\tilde{S} = S + \frac{\tilde{\upsilon}}{\kappa^2 d^2} f_{v2} \quad ; \quad f_{v2} = 1 - \frac{\chi}{(1 + \mathcal{X} f_{v1})} \tag{6}$$

$$f_w = [\frac{1 + C_{w3}^6}{g^6 + C_{w3}^6}]^{(1/6)} \quad ; \quad g = r + c_{w2}(r^6 - r) \quad ; r \equiv \frac{\tilde{\upsilon}}{\tilde{S}\kappa^2 d^2} \tag{7}$$

$$f_{t1} = C_{t1} g_t \exp[-C_{t2} \frac{\omega_t^2}{\Delta U^2} (d^2 + g_t^2 d_t^2)] \tag{8}$$

$$C_{t3} = \exp(-C_{t4}\,\chi^2) \tag{9}$$

$$S = \sqrt{(2\Omega_{ij}\Omega_{ij}} \quad - rotational\ tensor \quad ; \quad \Omega_{ij} = \frac{1}{2}\left(\frac{\partial u_i}{\partial x_j} - \frac{\partial u_i}{\partial x_i}\right) \tag{10}$$

d - Distance from the closest surface and

ΔU^2 - The norm of the difference between the velocity at the trip (usually zero) and that at the field point which we are considering.

The values of the following constants are, (Spalart & Allmaras, 1992).

$\sigma = 2/3$, $C_{b1} = 0.1355$, $C_{b2} = 0.622$,
$\kappa = 0.41$ –Von Karman's constant (Gaudio, et al., 2010).

$$C_{w1} = {C_{b1}}/{\kappa^2} + {(1 + C_{b2})}/{\sigma} \tag{11}$$

$C_{w2} = 0.3$, $C_{w3} = 2$, $C_{v1} = 7.1$, $C_{t1} = 1$, $C_{t2} = 2$, $C_{t3} = 1.1$, $C_{t4} = 2$

SIMULIA.ABAQUS 6.14 software offers three packages Abaqus/CFD, Abaqus/Standard and Explicit and Abaqus/Electromagnetic. Among these, Abaqus/CFD is well-performing for the non-linear fluid dynamic problems as well as the large scale linear dynamic problems with the powerful backing of pre-processing and post processing. Abaqus/CFD leads to get accurate results by solving the fluid – structure interaction (FSI) problems with the support of co-simulation. Therefore, which is more popular among in the professionals as well as the research students.

Capable of using various linear and non-linear material models, facilitate to introduce the new materials, customize of settings are added advantages in this software. In addition, Abaqus/CFD is capable of solving various types of fluid flow problems such as fluid -thermal problems, deforming-mesh ALE problems (Arbitrary Lagrangian Eulerian problems) etc. (ABAQUS 6.14 User Documentation, 2014).

2.2.6 FSI – Coupling type – fluid and solid

The deformation of tress and the motion of the sand dunes under wind action are some of the examples for fluid- structure interaction, which can be observed in nature. Similarly, wind can interact with the buildings and other structure. The interaction problems can be solved by laws and equations from different physical disciplines. Hence, these are called as multiphysics problems.

Flow around a body makes strong effect on the structure and the structure also makes the significant influence on the flow. Fluid dynamics and structural dynamics are two different disciplines relate with these kind of multiphysics problems.

In FSI simulation, solution approaches are mainly divided in to two, namely monolithic and partitioned. Partitioned method can be further divided in to two as one-way coupling and two-way coupling. The information exchanged between the fluid solver and the structure solver mainly depends on the coupling method. One-way coupling strategy means only the fluid pressure acting on the structure is transferred to the structural solver.Two-way coupling means the fluid pressure acting on the structure is transferred to the structure solver and the structure displacement is also transferred to the fluid solver. This can be further divided in to two namely, strongly coupled and weakly coupled (Benra, et al., 2011).

In two-way coupling method, the deformation of the fluid – solid boundary effects to deform the fluid mesh. Therefore, displacement diffusion algorithms is used to calculate the deformation.

Calculations of the fluid side are manly based on the continuity equations and Navier-Stokes equations. The following continuity equation contains three set of terms, consequently, change in the mass in the control volume, mass flux through control volume boundary and change of the control volume throughout the mesh deformation (Benra, et al., 2011).

$$\frac{d}{dt}\int_{V} \rho \,.\, dv \;+\; \int \rho \,.\; U_j \,.\, dn_j + \;\int_{S} \rho \,.\; W_j \,.\, dn_j \;\; = 0 \qquad (12)$$

In the structure side, impulse conservation (equation 13) is solved using a finite element approach (Benra, et al., 2011). The dynamic response of the structure is shown in the below generalized form.

$$M.\ddot{\vec{u}} \;+\; C.\dot{\vec{u}} \;+ K\,.\vec{u} \;\;=\;\; \vec{F}. \qquad (13)$$

M = Mass

$\ddot{\vec{u}}$ = Acceleration , $\dot{\vec{u}}$ = Velocity , $\vec{u}$ = Displacement

C = Damping

K = Stiffness

$\vec{F}$ = Force

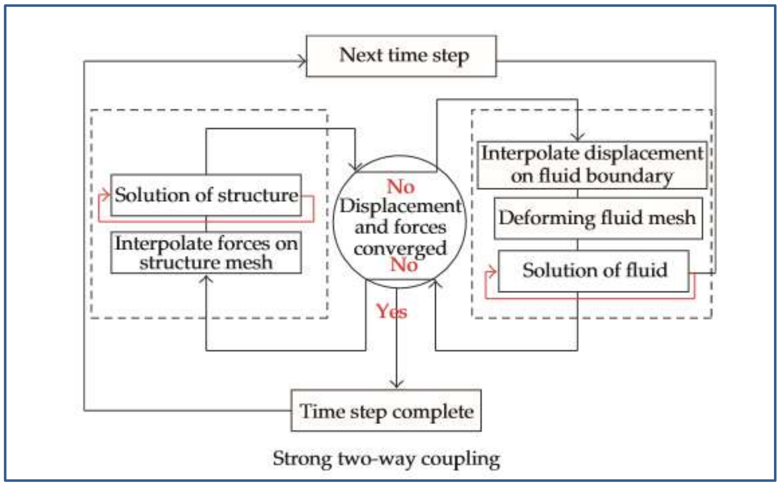

Figure 2.4 Solution algorithm for strong two-way coupling (Benra, et al., 2011)

The flow chart of the process of the strong two-way coupling method is shown in Figure 2.4. Generally, two-way coupling method is more accurate in case of larger deformations when the fluid field is strongly affected by the structure deformation.

According to this case study, fluid–structure interaction (FSI) is defined as the interaction between the deformable high-rise buildings with the surrounding wind flow. Moreover, two –way coupling method is used for the data exchange method.

2.2.7 Summary of analysis and modelling

- A number of advanced wind loading codes have been developed for estimating the wind loading and their effects on and around the structures. Different codes of practice used different parameters and equations to estimate the turbulent characteristics.
- In general, structure with unusual shape and more than 50 m height required dynamic analysis.

- CFD software offers different approaches to evaluate the complex building – wind environment.
- Spalart – Allmaras is one equation model, which contains an additional transport equation to solve the "Reynolds stress" component.
- Hence, S-A can be used to evaluate the wind loads and effects on the complex geometries precisely whilst saving time and cost.
- Different coupling methods can be used for FSI simulations.

3. ESTIMATION OF STATIC BASED WIND FORCES

This chapter describes the different factors and the different equations use to estimate the static based wind forces on 102 m tall building using three different wind loading codes.

In this research, three codes of practice namely, CP3 Chapter V–2:1972, BSEN 1991-1-4:2005 with National Annex SLS EN 1991-1-4:2019 and AS/NZS 1170.2:2011 have been selected to conduct the comparative study. Among these, CP 3 Chapter V–Part 2:1972 is the most common practice for assessing the wind loads on the buildings due to its simplicity and the familiarity. Apart from the code, "Design building for high winds – Sri Lanka" is the only design manual, which can be used to evaluate the wind loads on structures. However, at present, most of the Sri Lankan Designers are following the advanced international wind codes/standards such as BSEN 1991-4:2005 with NA SLS EN 1991-1-4 :2019 & AS/NZS 1170.2:2011 .

One of the objective of this research is to select the most suitable wind code/ codes by evaluating the applicability / limitations of codes of practice via numerical simulation. Therefore, estimation of wind loads and their effects on tall building has been carried out utilizing three major international wind codes/standards. Comparative study has been conducted by some of the Sri Lankan researchers utilizing some of international wind codes/standard. However, it is essential to study the updated versions of these codes/standards since most of the wind codes/standards have been updated in the last few years.

Thirty-one storey building (containing two Towers) having rare architectural form was selected as the case study. The selected building details are described in Section 3.1.

3.1 Case Study - 31 Storey Apartment Building Located in Colombo Suburb

A 102 m high building locates in suburban area (near to Colombo city) is selected as the case study to assess the wind loads and its effects on the structure.

Selected building is a 31-storey apartment building with strong architectural signature. This building comprises of 4-storey Vehicle Park, entertaining area, community hall and apartments. The plan dimensions of the building up to 21 m height from the ground level are approximately having a shape of pentagon as shown in Figure 3.1 (a). From 0 m -21 m, each floor level contains 5840 m^2 floor area. The first four floors (ground to 3rd floor) comprise for parking with 472 stalls. The 4th floor contains a large public amenity space including entertaining area, community hall, children play area and an indoor garden. The transfer floor exists on the sixth floor. At the 21m height from ground level, structure is parted in to two towers as shown in Figure 3.1 (b).The shape of the tower is rectangular. Each tower contains 25 floors and each floor space in tower 1 and tower 2 cover 1298 m^2 and 1127m^2 area respectively. In addition, each floor level of a tower contains 6 apartments including 2 bed rooms, 2 bathrooms, living room, dining room and a kitchen for each apartment. Tower 1 and Tower 2 are not inter-connected as shown in Figure 3.3. The roof of the 31 floors tower rises to a height of 102 m. Floor to floor height up to 21m level from the ground is 3 m and from 21m to roof level is 3m.The building is typical column - beam frame structures with service core of shear walls.

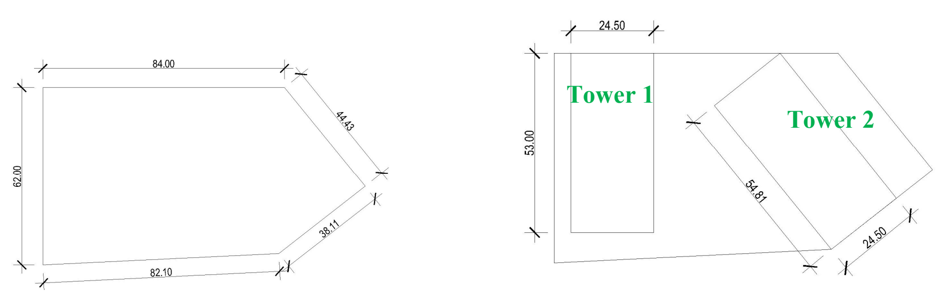

(a) (b)

Figure 3.1 Plan view of the building (a) from ground to 6th floor (b) 6th - 30th floor)

- Lower part - (62 m x 84 m x 46 m x 46 m x 84 m) - Ground level to 21 m
- Tower 1 - (53 m x 24.5 m) Tower 2 (46 m x 24.5 m) - 21 m to 102 m
- Terrain category - 3

Wind forces are calculated utilizing three different international wind loading codes/standards of CP3 CHAPTER V-2:1972, BSEN 1991-4:2005 with SLS EN 1991-1-4: 2019, AS/NZS 1170.2:2011 by encountering different factors and methods. Floor levels which have been considered to calculate the wind loads in Tower 1 and 2 are shown in Figure 3.2.The calculation is performed for two orthogonal directions (0^0 and 90^0) (Figure 3.3(a) and(b)).Wind Calculation procedure for above three codes are described in Sections 3.3.1, 3.3.2 and 3.3.3 respectively.

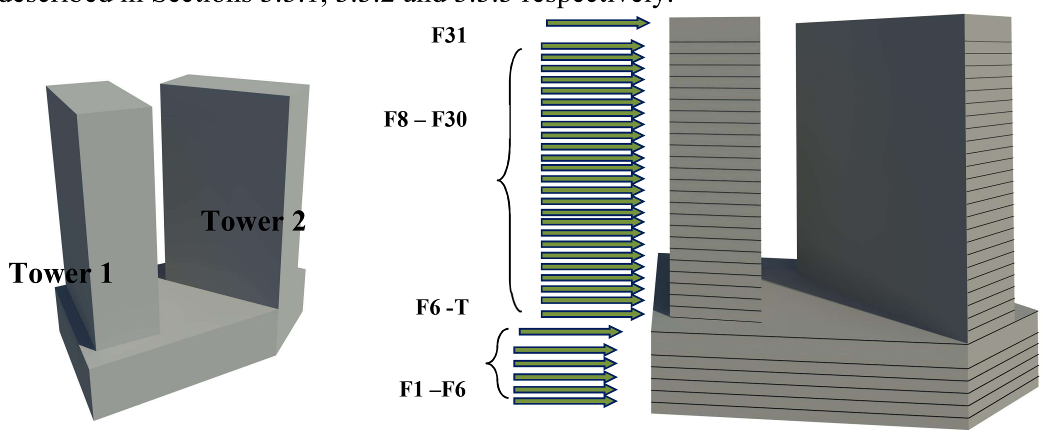

(a) (b)

Figure 3.2 (a) 3-D view (b) floor levels of the building (wind force calculated)

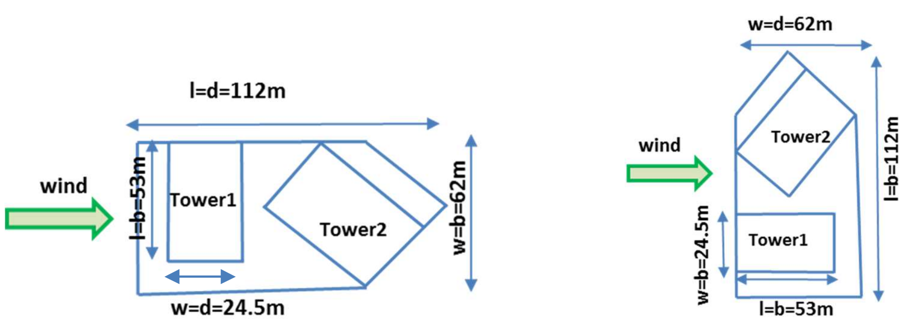

(a) (b)

Figure 3.3 (a) 0^0 wind direction and (b) 90^0 wind direction to the structure

3.2 Wind Zones in Sri Lanka

Sri Lanka is divided in to three wind zones as shown in Figure 3.4. Moreover, building is divided in to two categories by considering the safety level of the structure when it is facing to the natural disaster. Therefore, two types of wind speeds are defined per each zone, which can be named normal structure wind speed and post disaster structure wind speed. For Sri Lankan context, available wind speed data is only the 3-second gust wind speed at 10 m height in open terrain with no obstructions in 50 years return period. However, BS EN 1991-1-4:2005 with NA SLS EN 1991-1- 4 :2019 consider characteristic 10 minutes mean wind velocity for their design. Therefore, the 3s gust wind speed can be converted to 10 minute mean wind speed by combination of two methods suggested by Cook (1999) and IECUK.

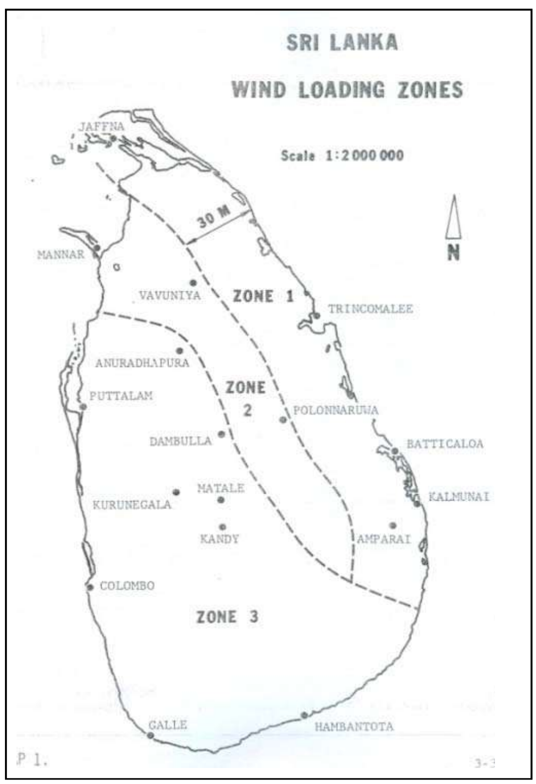

Figure 3.4 Wind zone map in Sri Lanka (Design Manual "Design building for high winds", 1978)

3.3 Estimation of Wind Forces for Tall Building by Codes of Practice

3.3.1 Estimation of wind forces for tall building by CP3: Chapter V-2:1972

Following chart (Figure 3.5) shows the steps of estimating the static based wind force using CP3: Chapter V-2:1972

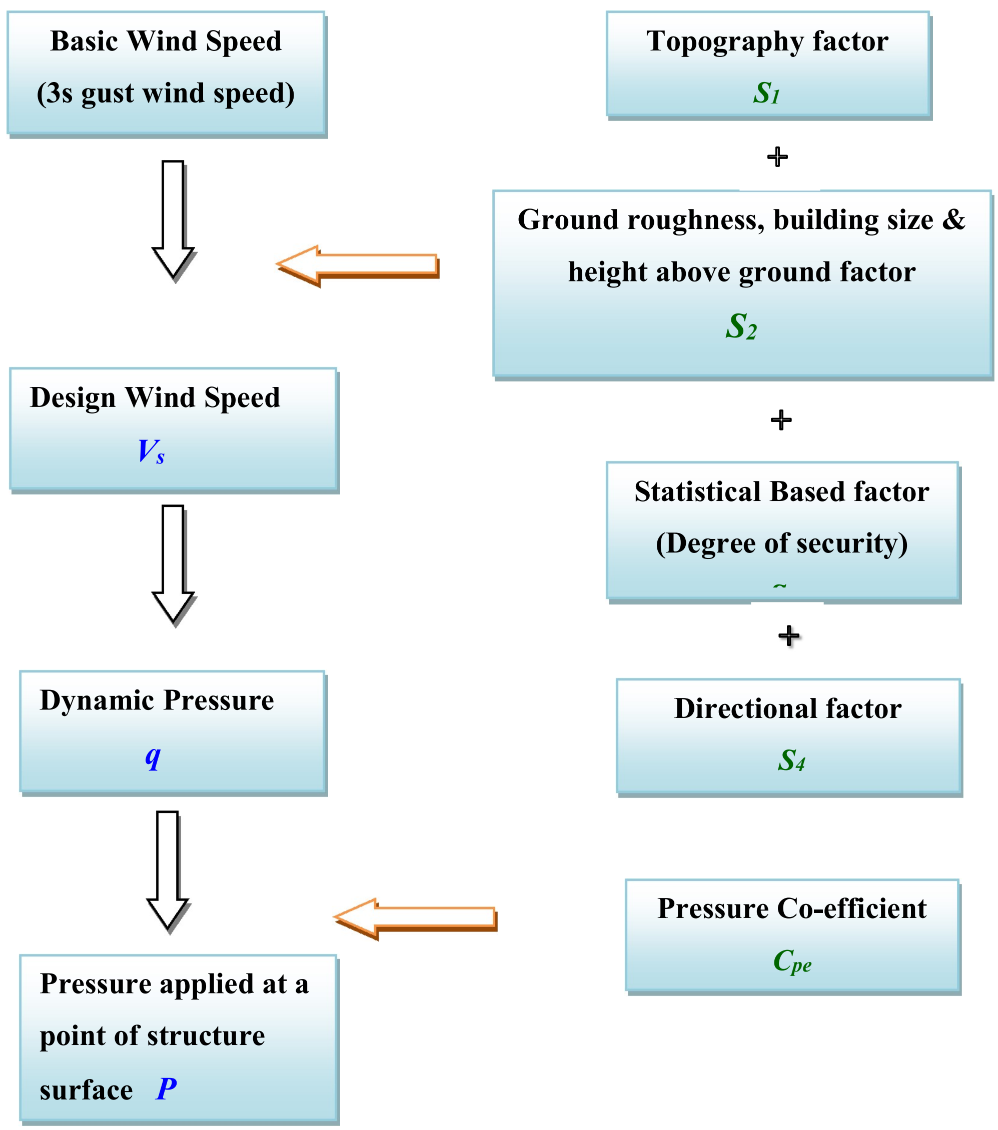

Figure 3.5 Steps of wind force calculation for CP3: Chapter V-2:1972

Following equations are to be used to estimate the static based wind force using CP3: Chapter V-2:1972

3.3.1.1 Design wind speed

Design wind speed should be calculated by Clause. 4.3 (2) of CP3: Chapter v-2:1972

$$V_s = V\ S_1 S_2 S_3\ S_4 \quad (1)$$

V – The basic wind speed should be according to the Clause 5.2.1 of CP3: Chapter V-2:1972.As described in Clause 5.2.1 , V is the 3second gust speed at 10m (33ft) above ground in an open terrain which is likely to be exceeded on the average only once in 50 years.

S_1 – Topography factor – Should be calculated as per Clause 5.4 of CP3: Chapter V-2:1972 & method of calculating should be included in Appendix D of CP3: chapter v-2:1972

S_2 – Ground roughness, building size & height above ground factor – Should be calculated as per Clause 5.5.1& 5.5.2 of CP3: Chapter V-2:1972. Ground roughness should be classified in to four categories (1 to 4) and the building size should be classified in to three categories (Class A, B &C) as shown in Table 3.1. Table 3 of CP3: Chapter V-2:1972 should be used to find the S_2 factor.

Table 3.1 Ground roughness, building size and height above ground, factor S_2

	(1) Open country with no obstructions			(2) Open country with scattered windbreaks			(3) Country with many windbreaks; small towns; outskirts of large cities			(4) Surface with large and frequent obstructions, e.g. city centres		
	Class			Class			Class			Class		
H	A	B	C	A	B	C	A	B	C	A	B	C
m												
3 or less	0.83	0.78	0.73	0.72	0.67	0.63	0.64	0.60	0.55	0.56	0.52	0.47
5	0.88	0.83	0.78	0.79	0.74	0.70	0.70	0.65	0.60	0.60	0.55	0.50
10	1.00	0.95	0.90	0.93	0.88	0.83	0.78	0.74	0.69	0.67	0.62	0.58
15	1.03	0.99	0.94	1.00	0.95	0.91	0.88	0.83	0.78	0.74	0.69	0.64
20	1.06	1.01	0.96	1.03	0.98	0.94	0.95	0.90	0.85	0.79	0.75	0.70
30	1.09	1.05	1.00	1.07	1.03	0.98	1.01	0.97	0.92	0.90	0.85	0.79
40	1.12	1.08	1.03	1.10	1.06	1.01	1.05	1.01	0.96	0.97	0.93	0.89
50	1.14	1.10	1.06	1.12	1.08	1.04	1.08	1.04	1.00	1.02	0.98	0.94
60	1.15	1.12	1.08	1.14	1.10	1.06	1.10	1.06	1.02	1.05	1.02	0.98
80	1.18	1.15	1.11	1.17	1.13	1.09	1.13	1.10	1.06	1.10	1.07	1.03
100	1.20	1.17	1.13	1.19	1.16	1.12	1.16	1.12	1.09	1.13	1.10	1.07
120	1.22	1.19	1.15	1.21	1.18	1.14	1.18	1.15	1.11	1.15	1.13	1.10
140	1.24	1.20	1.17	1.22	1.19	1.16	1.20	1.17	1.13	1.17	1.15	1.12
160	1.25	1.22	1.19	1.24	1.21	1.18	1.21	1.18	1.15	1.19	1.17	1.14
180	1.26	1.23	1.20	1.25	1.22	1.19	1.23	1.20	1.17	1.20	1.19	1.16
200	1.27	1.24	1.21	1.26	1.24	1.21	1.24	1.21	1.18	1.22	1.21	1.18

S_3 – Statistical Based Factor - Should be calculated based on statistical concept which accounting the degree of security required & the period of years during the structure will be exposure to wind by Clause 5.6 & Appendix C of CP3: Chapter V-2:1972.

S_4 – Directional Factor to wind by Appendix L of CP3: Chapter V- 2:1972.

3.3.1.2 Dynamic pressure (q)

The Design wind speed should be converted to the dynamic pressure according to the Clause 4.3(3) & Clause 6 of CP3: Chapter V-2:1972.

$$q = kV_s^2 \tag{2}$$

k – 0.613 in SI unit (N/m^2 & m/s)

The effect of wind on the structure as a whole is determined by the combined action of external and internal pressures acting upon it. However, only the external pressure induced by the wind should be considered for this comparative study.

Pressure applied at any point of the surface of the structure should be calculated as per Clause 4.3(4) & Clause 7 of CP3: Chapter V-2:1972. In all cases, the calculated wind loads act normal to the surface to which they apply.

$$p = C_p\, q \tag{3}$$

C_p – Pressure coefficient

Values of external pressure co-efficient (C_{pe}) for walls should be taken from Table 7 of CP3: Chapter V-2:1972.

Table 3.2 External pressure co-efficient for vertical walls of rectangular plan building

Building height ratio	Building plan ratio	Elevation	Plan	Wind angle α	C_{pe} for surface A	B	C	D	Local C_p
				degrees					
$\frac{h}{w} \leq \frac{1}{2}$	$1 < \frac{l}{w} \leq \frac{3}{2}$	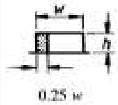	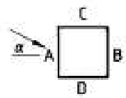	0	+0.7	−0.2	−0.5	−0.5	−0.8
				90	−0.5	−0.5	+0.7	−0.2	
	$\frac{3}{2} < \frac{l}{w} < 4$		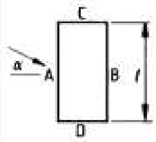	0	+0.7	−0.25	−0.6	−0.6	−1.0
				90	−0.5	−0.5	+0.7	−0.1	
$\frac{1}{2} < \frac{h}{w} \leq \frac{3}{2}$	$1 < \frac{l}{w} \leq \frac{3}{2}$	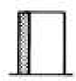	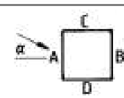	0	+0.7	−0.25	−0.6	−0.6	−1.1
				90	−0.6	−0.6	+0.7	−0.25	
	$\frac{3}{2} < \frac{l}{w} < 4$	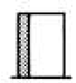	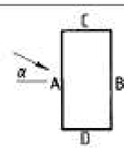	0	+0.7	−0.3	−0.7	−0.7	−1.1
				90	−0.5	−0.5	+0.7	−0.1	
$\frac{3}{2} < \frac{h}{w} < 6$	$1 < \frac{l}{w} \leq \frac{3}{2}$	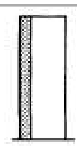	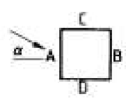	0	+0.8	−0.25	−0.8	−0.8	−1.2
				90	−0.8	−0.8	+0.8	−0.25	
	$\frac{3}{2} < \frac{l}{w} < 4$	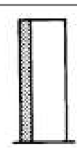	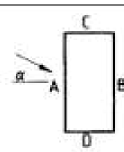	0	+0.7	−0.4	−0.7	−0.7	−1.2
				90	−0.5	−0.5	+0.8	−0.1	

NOTE h is the height to eaves or parapet, l is the greater horizontal dimension of a building and w is the lesser horizontal dimension of a building.

External Pressure co-efficient for windward, leeward and side faces should be considered as shown in Table 3.2.

Calculation of the static based wind force for apartment building (Tower 1) utilizing CP3: Chapter V-2: 1972 is attached in Appendix A.

3.3.2 Estimation of wind forces for tall building by BS-EN1991-1-4:2005

Figure 3.6 shows the steps of estimating the static based wind force using BS-EN1991-1-4:2005 with NA SLS EN 1991-1-4:2019.

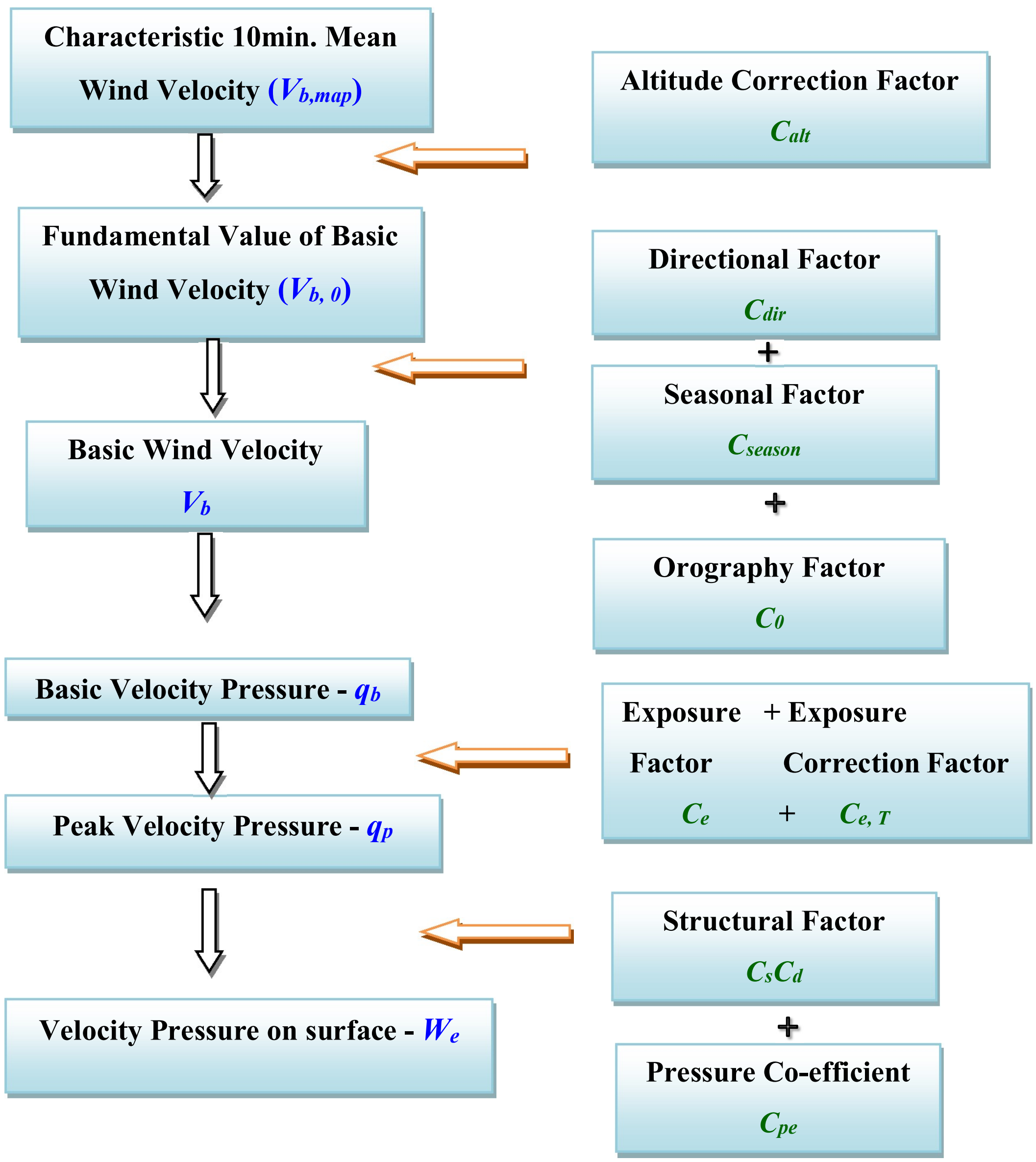

Figure 3.6 Steps of wind force calculation for BS-EN1991-1-4:2005 with SLS EN 1991-1-4:2019

Following equations are to be used to estimate the static based wind force using BS-EN1991-1-4:2005.According to the code velocity & velocity pressure are composed of a mean & fluctuating components.

3.3.2.1 Fundamental value of basic wind velocity

The fundamental value of basic wind velocity should be calculated according to the with respect to the wind direction & time of year by SLSEN 4.2(1) P Note2 & SLSEN 4.2(2) P Note 1. (National Annex to BS-EN1991-1-4:2005)

$$V_{b,0} = V_{b,map} c_{alt} \; ; \; c_{alt} \leq 1.5 \; (maximum) \quad (4)$$

$$c_{alt} = 1 + 0.01A \quad (5)$$

$V_{b,\ map}$ – characteristic 10 minutes mean wind velocity before altitude correction applied. The value should be taken from Table1: SLSEN 4.2(1) P Note 2

C_{alt} – Altitude correction factor

A – Altitude

The basic wind velocity should be calculated according to the Clause 4.2 of BS-EN1991-1-4:2005

$$V_b = C_{dir} C_{season} V_{b,0} \quad (6)$$

$V_{b,0}$ – Fundamental value of basic wind speed should be as per 1(P) of BS-EN1991-1-4:2005, v is the characteristic 10 minutes mean wind velocity at 10 m (33ft) above ground in an open terrain .

C_{dir} – Directional factor – Should be taken as per Note2 of Clause 4.2 of BS-EN1991-Recommanded value is 1.0.

C_{season} – Seasonal factor –Should be taken as per Note3 of Clause 4.2 of BS-EN1991-Recommanded value is 1.0.

Terrain orography is neglected.

$C_o(z)$ – Orography factor –Should be calculated as per Clause 4.3.3 of BS-EN1991- Recommanded value is 1.0.

Terrain Category

Five terrain categories as shown in Figure 3.7 are illustrated in Appendix A in BS-EN1991- 1-4:2005 such as 0, I, II, III, and IV.

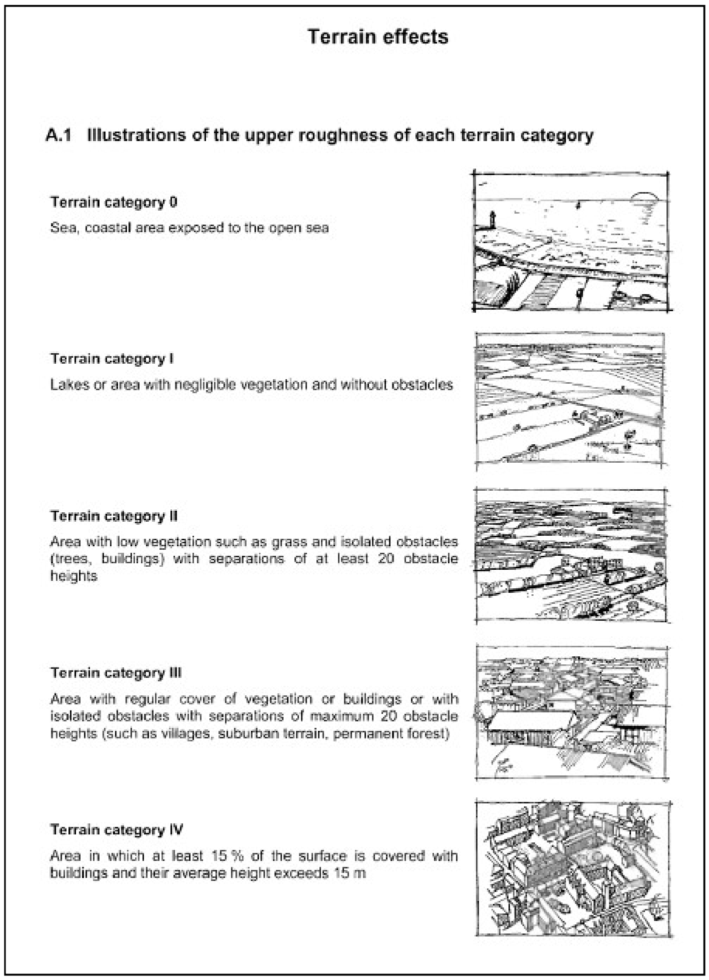

Terrain effects

A.1 Illustrations of the upper roughness of each terrain category

Terrain category 0
Sea, coastal area exposed to the open sea

Terrain category I
Lakes or area with negligible vegetation and without obstacles

Terrain category II
Area with low vegetation such as grass and isolated obstacles (trees, buildings) with separations of at least 20 obstacle heights

Terrain category III
Area with regular cover of vegetation or buildings or with isolated obstacles with separations of maximum 20 obstacle heights (such as villages, suburban terrain, permanent forest)

Terrain category IV
Area in which at least 15 % of the surface is covered with buildings and their average height exceeds 15 m

Figure 3.7 Terrain Categories

Neighboring Structures

Effect of neighboring structures should be taken in to account as per Appendix A (A.4 & A.5) of BS-EN1991- 1-4:2005.The affected area, which should be considered for the calculation as shown in Figure 3.8 and 3.9.

(1) If a building is more than twice as high as the average height h_{ave} of the neighbouring structures then, as a first approximation, the design of any of those nearby structures may be based on the peak velocity pressure at height z_n ($z_e = z_n$) above ground (Expression A.14), see Figure A.4.

$x \leq r$: $\quad z_n = \frac{1}{2} \cdot r$

$r < x < 2 \cdot r$: $\quad z_n = \frac{1}{2}\left(r - (1 - \frac{2 \cdot h_{low}}{r}) \cdot (x - r) \right) \qquad$ (A.14)

$x \geq 2 \cdot r$: $\quad z_n = h_{low}$

in which the radius r is:

$r = h_{high}$ if $h_{high} \leq 2 \cdot d_{large}$

$r = 2 \cdot d_{large}$ if $h_{high} > 2 \cdot d_{large}$

The structural height h_{low}, the radius r, the distance x and the dimensions d_{small} and d_{large} are illustrated in Figure A.4 Increased wind velocities can be disregarded when h_{low} is more than half the height h_{high} of the high building, i.e. $z_n = h_{low}$.

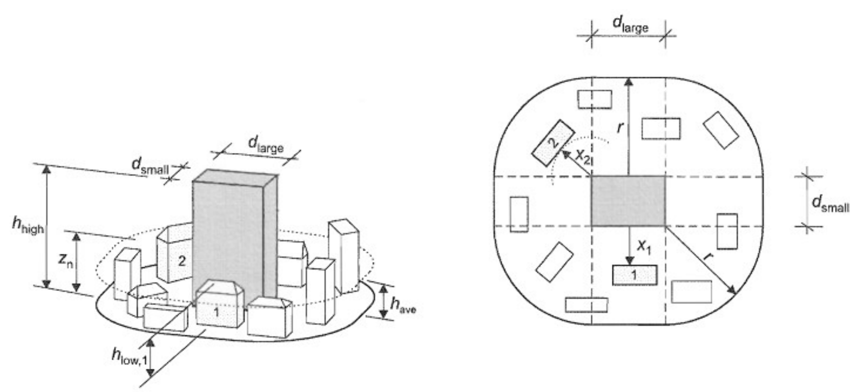

Figure 3.8 Influence of high-rise building by neighbouring structures

Obstruction height & upwind spacing

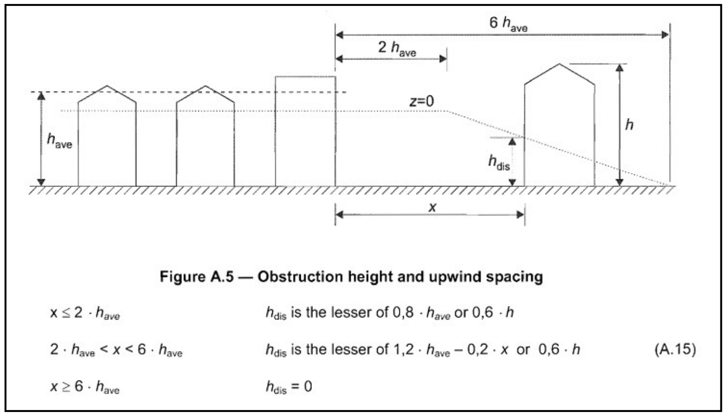

Figure 3.9 Obstruction height and upwind spacing

3.3.2.2 Basic velocity pressure and peak velocity pressure

The basic velocity pressure should be calculated by the expression of 4.10 of BS-EN1991-1-4:2005

$$q_b = \frac{1}{2}\rho V_m^2 \quad , \ \rho \text{ – Density of air} \tag{7}$$

Peak velocity pressure at height (z) is composed of a mean & short term fluctuating components. It should be calculated according to the Clause 4.5 of BS-EN1991-1-4:2005 and the National Annex to BS-EN1991-1-4:2005

$$q_p = C_e(z) C_{e,T} q_b \tag{8}$$

C_e– Exposure factor – The factor should be taken from graph developed for Sri Lankan context (Figure NA.5 of NA to BS- EN1991-1-4:2005)

$C_{e,T}$ – Exposure Correction factor – The factor should be taken from graph developed for Sri Lankan context. (Figure NA.8 of NA to BS- EN1991-1-4:2005).

Shape of velocity pressure profile (Figure 3.10) should be determined according to the Clause7.2.2 & Figure7.4 of .BS-EN1991-1-4:2005.

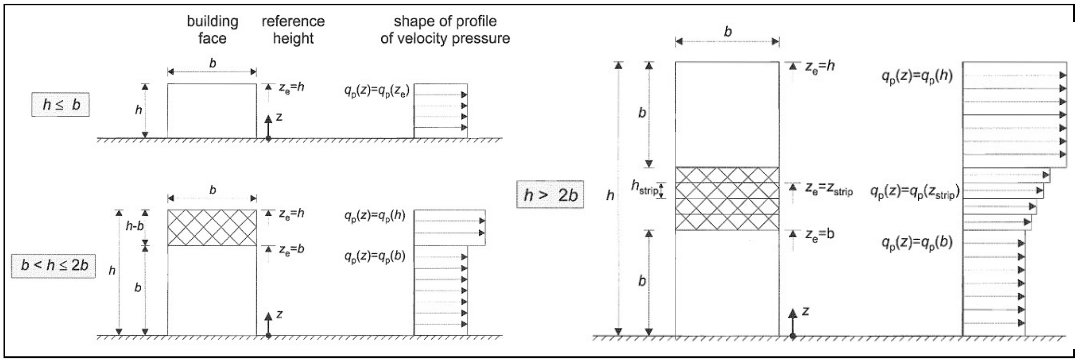

Figure 3.10 Shape of velocity profile

The effect of wind on the structure as a whole is determined by the combined action of external and internal pressures acting upon it. However, only the external pressure induced by the wind should be considered for this comparative study. Wind pressure on surfaces should be calculated according to the Clause5.2 of BS-EN1991-1-4:2005.

$$W_e = q_p(z_e)C_{p,e} \tag{9}$$

$C_{p,e}$ – Pressure co-efficient – The values shown in Table 3.3 should be in accordance with Clause 7.2.1, Clause 7.2.2(3),Figure7.5 & Table 7.1 of NA to BSEN1991-1-4:2005

Table 3.3 External pressure co-efficient for vertical walls of rectangular building

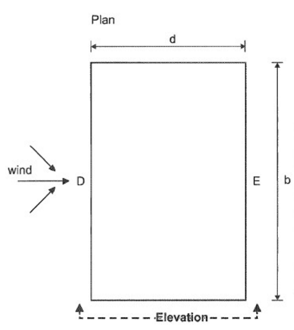

Zone	A		B		C		D		E	
h/d	$c_{pe,10}$	$c_{pe,1}$	$c_{pe,10}$	$c_{pe,1}$	$c_{pe,10}$	$c_{pe,1}$	$c_{pe,10}$	$c_{pe,1}$	$c_{pe,10}$	$c_{pe,1}$
5	-1,2	-1,4	-0,8	-1,1	-0,5		+0,8	+1,0	-0,7	
1	-1,2	-1,4	-0,8	-1,1	-0,5		+0,8	+1,0	-0,5	
≤ 0,25	-1,2	-1,4	-0,8	-1,1	-0,5		+0,7	+1,0	-0,3	

Wind force acting on a structure or structural element should be calculated according to the Clause5.3 (3) & Appendix D (Figure D.2) of BS-EN1991-1-4:2005.

External forces;

$$F_{w,e} = C_s C_d \sum_{surfaces} W_e \ A_{ref} \tag{10}$$

C_sC_d – Structural factor – Factor should be designed according to Clause 6.2, 6.3 & Annex D of BS-EN1991-1-4:2005.

A_{ref} – Reference area of individual surface

Calculation of the static based wind force for apartment building (Tower 1) utilizing BS-EN1991-1-4:2005 is attached in Appendix B.

3.3.3 Estimation of wind forces for tall building by AS/NZS 1170.2:2011

Figure 3.11 illustrates the steps of estimating the static based wind force AS/NZS 1170.2:2011.

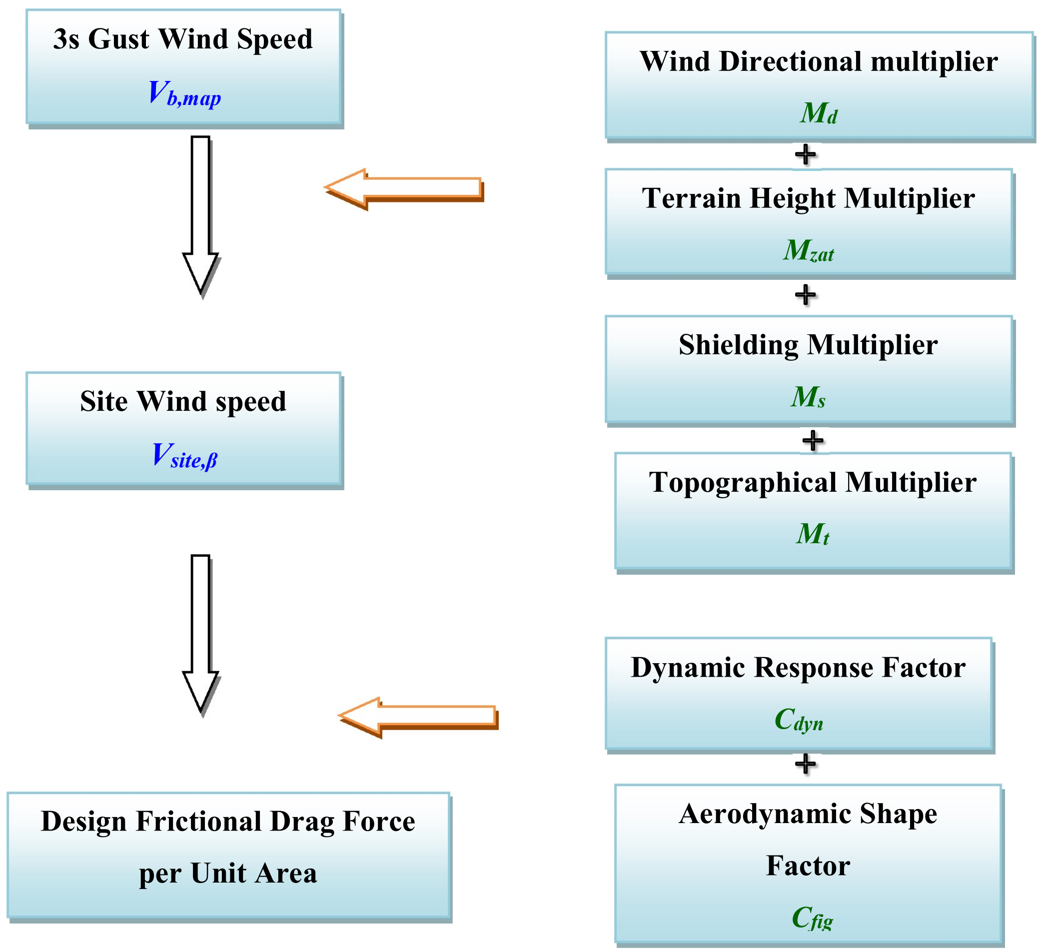

Figure 3.11 Steps of wind force calculation for AS/NZS 1170.2:2011

Following equations are to be used to estimate the static based wind force using AS/NZS 1170.2:2011.

3.3.3.1 Site wind speed

The site design wind speed should be calculated with respect to the cardinal wind directions, reference height (z) above ground level by the Clause of 2.2 of AS/NZS 1170.2:2011.

$$V_{sit,\beta} = V_R M_d \left(M_{z,cat} M_s M_t\right) \tag{11}$$

V_R– Regional 3s gust wind speed, (m/s), for annual probability of exceedance of 1/R- The values should be taken from Table 3.1 of AS/NZS 1170.2:2011.The wind speed values are shown in Table 3.4.

Table 3.4 Regional wind speed related with Return period

Regional wind speed (m/s)	Region				
	Non-cyclonic			Cyclonic	
	A (1 to 7)	W	B	C	D
V_1	30	34	26	$23\times F_C$	$23\times F_D$
V_5	32	39	28	$33\times F_C$	$35\times F_D$
V_{10}	34	41	33	$39\times F_C$	$43\times F_D$
V_{20}	37	43	38	$45\times F_C$	$51\times F_D$
V_{25}	37	43	39	$47\times F_C$	$53\times F_D$
V_{50}	39	45	44	$52 \times F_C$	$60 \times F_D$
V_{100}	41	47	48	$56 \times F_C$	$66 \times F_D$
V_{200}	43	49	52	$61 \times F_C$	$72 \times F_D$
V_{250}	43	49	53	$62 \times F_C$	$74 \times F_D$
V_{500}	45	51	57	$66 \times F_C$	$80 \times F_D$
V_{1000}	46	53	60	$70 \times F_C$	$85 \times F_D$
V_{2000}	48	54	63	$73 \times F_C$	$90 \times F_D$
V_{2500}	48	55	64	$74 \times F_C$	$91 \times F_D$
V_{5000}	50	56	67	$78 \times F_C$	$95 \times F_D$
V_{10000}	51	58	69	$81 \times F_C$	$99 \times F_D$
V_R ($R \geq 5$ years)	$67-41R^{-0.1}$	$104-70R^{-0.045}$	$106-92R^{-0.1}$	$F_C\,(122-104R^{-0.1})$	$F_D\,(156-142R^{-0.1})$

M_d – Wind directional multiplier for the 8 cardinal directions (β) –M_d should be calculated according to the Clause of 3.3.2 of AS/NZS 1170.2:2011. For Sri Lankan Context, the recommended value is 1.0

$M_{z,\,cat}$ – Terrain height Multiplier – $M_{z,\,cat}$ should be calculated according to the Clause of 4.2.2 of AS/NZS 1170.2:2011. The values for serviceability limit state

(Table 3.5) should be taken from Table 4.1(A) of AS/NZS 1170.2:2011.

Table 3.5 Terrain height multiplier –SLS Design- Region A1-A7,W &B

Height (z) m	Terrain/height multiplier ($M_{z,cat}$)			
	Terrain category 1	Terrain category 2	Terrain category 3	Terrain category 4
≤3	0.99	0.91	0.83	0.75
5	1.05	0.91	0.83	0.75
10	1.12	1.00	0.83	0.75
15	1.16	1.05	0.89	0.75
20	1.19	1.08	0.94	0.75
30	1.22	1.12	1.00	0.80
40	1.24	1.16	1.04	0.85
50	1.25	1.18	1.07	0.90
75	1.27	1.22	1.12	0.98
100	1.29	1.24	1.16	1.03
150	1.31	1.27	1.21	1.11
200	1.32	1.29	1.24	1.16

NOTE: For intermediate values of height z and terrain category, use linear interpolation.

M_s – Shielding Multiplier – M_s should be calculated according to the Clause of 4.3.1 & the Table 4.3 of AS/NZS 1170.2:2011.The Recommended value should be 1.0 if the shielding is not effected.

M_t – Topographical Multiplier – M_t should be calculated according to the Clause of 4.4 of AS/NZS 1170.2:2011. The Recommended value should be 1.0 if the topography is not significant.

<u>Terrain Categories</u>

Four terrain categories shown in Figure 3.12 are illustrated in Clause 4.2 of AS/NZS 1170.2:2011 such as Category 1, 2, 3 &4

(a) *Category 1*—Exposed open terrain with few or no obstructions and water surfaces at serviceability wind speeds.

(b) *Category 2*—Water surfaces, open terrain, grassland with few, well-scattered obstructions having heights generally from 1.5 m to 10 m.

(c) *Category 3*—Terrain with numerous closely spaced obstructions 3 m to 5 m high, such as areas of suburban housing.

(d) *Category 4*—Terrain with numerous large, high (10 m to 30 m high) and closely spaced obstructions, such as large city centres and well-developed industrial complexes.

Figure 3.12 Terrain category definition

3.3.3.2 Design frictional drag force per unit area

Design Frictional Drag Force per Unit Area shall be calculated for structures and parts of structure by Clause of 2.4.2 of AS/NZS 1170.2:2011.

$$f = (0.5\rho_{air})[V_{des,\theta}]^2 C_{fig} C_{dyn} \quad (12)$$

$V_{des,\theta}$ – Building orthogonal design wind speed. Express as a function of height (z) as per Clause 2.3 of AS/NZS 1170.2:2011.

C_{fig} – Aerodynamic shape factor – C_{fig} should be calculated according to the Clause of 5.2 of AS/NZS 1170.2:2011.

C_{dyn} – Dynamic response factor – C_{dyn} should be calculated according to the Clause of Section 6 (Clause 6.1 &6.2) of AS/NZS 1170.2:2011.

Dynamic response factor (C_{dyn}) should be calculated according to the Clause 6.2 of AS/NZS 1170.2:2011.

$$C_{dyn} = \frac{1 + 2I_h\sqrt{g_v^2 B_s + \frac{H_s g_R^2 S E_t}{\xi}}}{1 + 2g_v I_h} \quad (13)$$

s– Height of the level which action effects are calculated as shown in Figure 3.13 for a structure .This is calculated according to the figure 6.1 of AS/NZS 1170.2:2011.

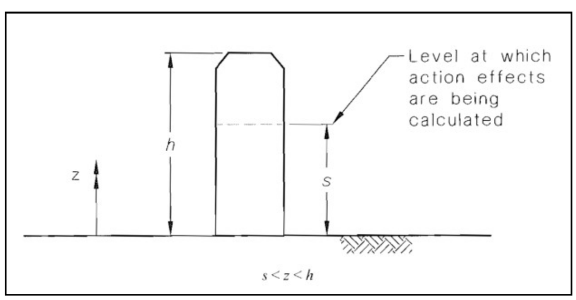

Figure 3.13 Level at which action effects - *s*

h – Height to top of the tower

I_h – Turbulent Intensity –should be obtained from Table 6.1 of AS/NZS 1170.2:2011. by setting z = h. The values are shown in Table 3.6.

Table 3.6 Turbulence Intensity–I_z

Height (z) m	Limit state, region and terrain category			
	Serviceability limit states			
	Terrain category 1, all regions	Terrain category 2, all regions	Terrain category 3, all regions	Terrain category 4, all regions
	Ultimate limit states			
	Terrain category 1, Regions A, W and B	Terrain category 2, Regions A, W and B	Terrain category 3, Regions A, W and B / Terrain categories 1, 2, and 3: Regions C and D	Terrain category 4, all regions
≤3	0.171	0.207	0.271	0.342
5	0.165	0.196	0.271	0.342
10	0.157	0.183	0.239	0.342
15	0.152	0.176	0.225	0.342
20	0.147	0.171	0.215	0.342
30	0.140	0.162	0.203	0.305
40	0.133	0.156	0.195	0.285
50	0.128	0.151	0.188	0.270
75	0.118	0.140	0.176	0.248
100	0.108	0.131	0.166	0.233
150	0.095	0.117	0.150	0.210
200	0.085	0.107	0.139	0.196

NOTE: For intermediate values of height (z) and terrain category, linear interpolation shall be used.

g_v – peak factor for the upwind velocity fluctuations, which will be taken as3.7

B_s – background factor which is measured of the slowly varying background component of the fluctuating response, caused by low-frequency wind speed variation .The values should be calculated according to the expression 6.2(2) of AS/NZS 1170.2:2011.

$$B_s = \frac{1}{1 + \frac{\sqrt{0.26(h-s)^2 + 0.46\ {}_{sh}^{2}}}{L_h}} \tag{14}$$

B_{sh} – average breadth of the structure heights s and h

L_h – a measure of the integral turbulence length scale at height h in meters.

= $85*(h/10)^{0.25}$

H_s – height factor for the resonant response given by: $1+(s/h)^2$

g_R – peak factor for the resonant response (10min.period) given by:

$\sqrt{2log_e(600n_a)}$

S – Size reduction factor

$$= \frac{1}{[1+\frac{3.5n_a\,h\,(1+g_vI_h)}{V_{des,\theta}}][1+\frac{4n_a\,b_{0h}\,(1+g_vI_h)}{V_{des,\theta}}]}$$

E_t – (π/4) times the spectrum of turbulence in the approaching wind stream, given as follows

$$= \frac{\pi N}{(1+70.8N^2)^{5/6}}$$

N – Reduced frequency (non- dimensional)

$$= n_a L_h[1+g_vI_h]/V_{des,\theta}$$

n_a – first mode natural frequency of vibration of a structure in the along-wind direction in hertz.

ξ – Ratio of structural damping to critical damping of a structure. The values can be considered as shown below.

1 For structural damping for *ultimate* limit states, recommended *maximum* values of ζ are as follows:
Steel structures: 0.02 of critical.
Reinforced-concrete structures: 0.03 of critical.

2 For structural damping for *serviceability* limit states, recommended *maximum* values of ζ are as follows:
Steel structures: 0.012 of critical for deflection calculations; 0.01 of critical for calculation of accelerations at the top of tall buildings and towers.
Reinforced-concrete structures: 0.015 of critical for deflection calculations; 0.01 of critical for calculation of accelerations at the top of tall buildings and towers.

3 Users should seek other sources for advice on possible values of structural damping as a function of the type of construction, building dimensions and amplitude of vibration.

Aerodynamic shape factor should be determined according to the Clause of 5.2(a) of AS/NZS 1170.2:2011.

$$C_{fig,e} = C_{p,e}K_aK_{c,e}K_lK_p \quad (15)$$

C_{pe} – External Pressure co-efficient –Should be taken from Table 5.2(A) for windward wall, Table 5.2(B) for Leeward wall & Table 5.2(C) for Side wall of AS/NZS 1170.2:2011.

The effect of wind on the structure as a whole is determined by the combined action of external and internal pressures acting upon it. However, only the external pressure induced by the wind should be considered for this comparative study. The values of external pressure co-efficient for windward, leeward and side wall are shown in Table 3.7, 3.8 and 3.9 respectively.

Table 3.7 C_{pe} for Windward wall

h	External pressure coefficients ($C_{p,e}$)
>25.0 m	0.8 (wind speed varies with height)
≤25.0 m	For buildings on ground— 0.8, when wind speed varies with height; or 0.7, when wind speed is taken for $z = h$
	For elevated buildings— 0.8 (wind speed taken at *h*)

Table 3.8 C_{pe} for Leeward wall

Wind direction θ degrees (see Figure 2.2)	Roof shape	Roof pitch (α), degrees (see Note 1)	*d*/*b* (see Note 1)	External pressure coefficients ($C_{p,e}$)
0	Hip or gable	<10	≤1 2 ≤4	−0.5 −0.3 −0.2
0 0 0	Hip or gable Hip or gable Hip or gable	10 15 20	All values	−0.3 −0.3 −0.4
0	Hip or gable	≥25	≤0.1 ≥0.3	−0.75 −0.5
90	Gable (see Note 2)	All values	≤1 2 ≤4	−0.5 −0.3 −0.2

Table 3.9 C_{pe} for Side wall

WALLS—EXTERNAL PRESSURE COEFFICENTS ($C_{p,e}$) FOR RECTANGULAR ENCLOSED BUILDINGS—SIDE WALLS (S)

Horizontal distance from windward edge	External pressure coefficients ($C_{p,e}$)
0 to 1*h*	−0.65
1*h* to 2*h*	−0.5
2*h* to 3*h*	−0.3
> 3*h*	−0.2

K_a – Area reduction factor should be taken from Table 5.4 of AS/NZS 1170.2:2011 Recommended value should be 1.0.

$K_{c,e}$ – Combination factor applied to external pressure should be taken from Table 5.5 of AS/NZS 1170.2:2011.Table 3.10 shows the values for combination factor.

Table 3.10 Combination factor- $K_{c,e}$

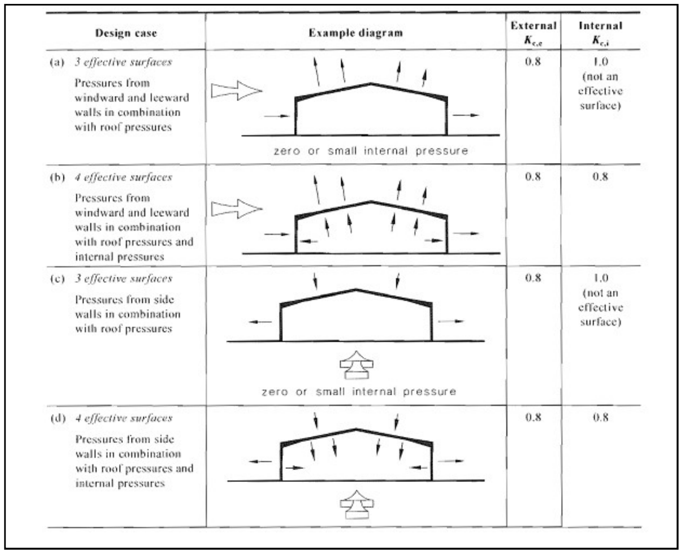

Design case	Example diagram	External $K_{c,e}$	Internal $K_{c,i}$
(a) *3 effective surfaces* Pressures from windward and leeward walls in combination with roof pressures	zero or small internal pressure	0.8	1.0 (not an effective surface)
(b) *4 effective surfaces* Pressures from windward and leeward walls in combination with roof pressures and internal pressures		0.8	0.8
(c) *3 effective surfaces* Pressures from side walls in combination with roof pressures	zero or small internal pressure	0.8	1.0 (not an effective surface)
(d) *4 effective surfaces* Pressures from side walls in combination with roof pressures and internal pressures		0.8	0.8

K_l – Local pressure factor should be taken from Table 5.6 of AS/NZS 1170.2:2011 The Recommended value should be 1.0.

K_p – Porous Cladding reduction factor should be calculated according to the Clause 5.4.5 & Table 5.8 of AS/NZS 1170.2:2011. The Recommended value should be 1.0.

Calculation of the static based wind force for apartment building (Tower 1) utilizing AS/NZS 1170.2:2011 is attached in Appendix C.

3.4 Summary

- Reference wind speed is defined in a three different way in CP3 Chapter V-2:1972, BSEN 1991-1-4:2005 with NA SLS EN 1991-1-4:2019 and AS/NZS1170.2:2011.
- Three Different approaches have been used in three different codes of practices to assess the turbulent characteristics.
- Different factors are introduced by different wind codes to estimate the along wind pressure on the tall building.

4. SIMULATION OF WIND RESPONSE USING COMPUTATIONAL FLUID DYNAMICS (CFD)

This chapter presents the details of numerical modelling of 102 m high building with two towers described in Section 3.1. Further, this describes the properties of the fluid and the building domain, mesh validation, turbulent model used for the analysis.

Use codes of practice is one of the famous conventional method in order to evaluate the wind loadings on high-rise buildings. However, the actual effects of wind on the high-rise building cannot be assessed by those wind loading codes accurately. As described in Section 2.2.5. Computational Fluid Dynamics (CFD) is powerful tool for evaluating the complex building-wind environment and aerodynamic effects on the building accurately. Therefore, CFD tool can be used to simulate the wind response of tall building using different approaches (RANS and LES).

4.1 Testing Against a Known Case Study

Due to the availability of many physical and numerical parameters in CFD approach, user has significant freedom to choose them. Therefore, quantitative as well as sometimes even qualitative predictions of CFD simulations conveyed the lack of confidence of the user. Modeling errors and errors related with numerical approximation are the two different types of errors which may influence to the accuracy of CFD results. Type of turbulent model used, applied boundary condition, size of the fluid domain are examples for modeling errors. Similarly, errors in grid design, truncation error and error from incomplete iterative convergence relate with the numerical approximation errors (Franke, et al., 2014). For that reason, verification and validation of a model is essential to get the accurate and reliable results.

Therefore, a known case study is performed in prior as a verification and validation of the model (102 m height building) used for this research. Accordingly, wind simulation performed for "Commonwealth Advisory Aeronautical Research Council" (CAARC) building by Gangasudan and Mallikarachchi (2018) is selected as the known case study. Thus, wind simulation is carried out for CAARC building through fluid-structure interaction in order to compare the results. Beforehand, numerous researches have been conducted (CFD analysis, wind tunnel experiments) for the same building to observe the building performance under the wind action. In that research, they have compared the numerical simulation with Experimental results (Wind tunnel test) done by Monash, Bristol and City University.

The 183 m tall, CAARC building contains flat-topped prismatic body with 45 m x 30 m rectangular cross section.

Inlet, outlet, lateral and top boundaries of fluid domain are set as 20B, 30B, 13B and 5H consequently as shown in Figures 4.1 and 4.2. (B – Width of the building, H- Height of the building). Furthermore, properties of the materials used for the fluid domain and the structure domain are presented in Table 4.1. 3D - 8 node hexahedral elements (FC3D8) are used for the fluid domain and 3D - 8 node hexahedra elements (C3D8 R) are used for the structure domain.

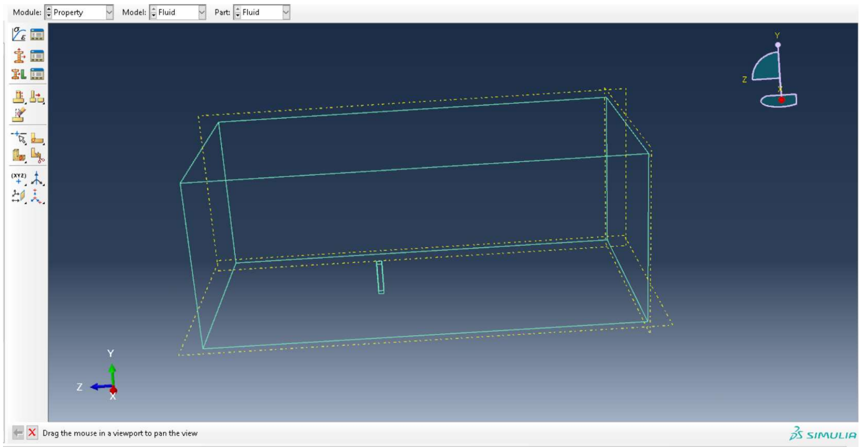

Figure 4.1 Fluid domain

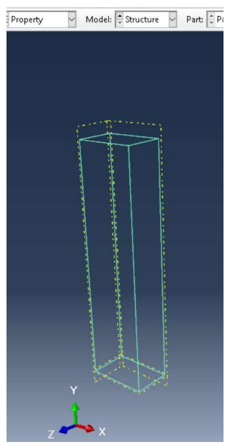

Figure 4.2 Structure domain

Material properties used for fluid domain and structure domain is given in Table 4.1 and Figure 4.3 shows the finite element mesh.

Table 4.1 Properties of fluid domain and structure domain

Structure		Fluid	
Specific mass	160 kg/m^3	Specific mass	1.25 kg/m^3
Young's modulus	2.3×10^8 N/m^2	Viscosity	0.0703 Ns/m^2
Poisson's ratio	0.25		
Critical damping ratio	1%		

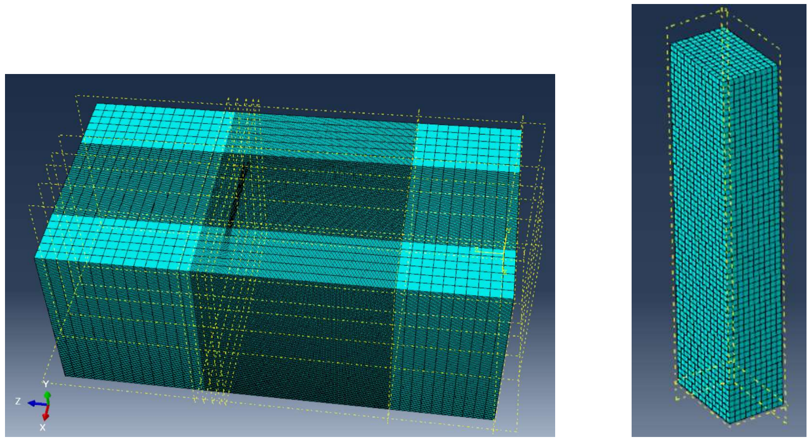

(a) (b)

Figure 4.3(a) Fluid domain 3D - 8 node hexahedral elements, FC3D8 (b) Structure domain 3D - 8 node hexahedra elements -C3D8 R

Power law velocity profile is used as inflow velocity.

V_0 =100 m/s, δ = 180 m, n = 0.19

$$V_1 = V_0(\frac{z}{\delta})^n$$

4.1.1 Results comparison

Comparison has been carried out between the simulation results (wind pressure) with the results of the research conducted by Gangasudan and Mallikarachchi. (2018). First, wind pressure values in the model, which is performed to verify the main model are compared with the results of numerical simulation in the research paper. Results showed averaged 4% lower than the numerical simulation results of the research paper. Differences in mesh size and the number of elements particularly in the fluid domain may cause for that slight deviation from the results in research paper. Then the results of the model, which is performed to verify the main model is compared with the wind tunnel test results and the results are illustrated in Figures 4.4 and 4.5. Maximum pressure of the building is observed at 2/3 of the building height. Therefore, mean pressure co efficient along the building perimeter are considered at that height.

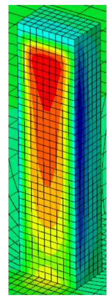

Figure 4.4 Wind pressure on the building

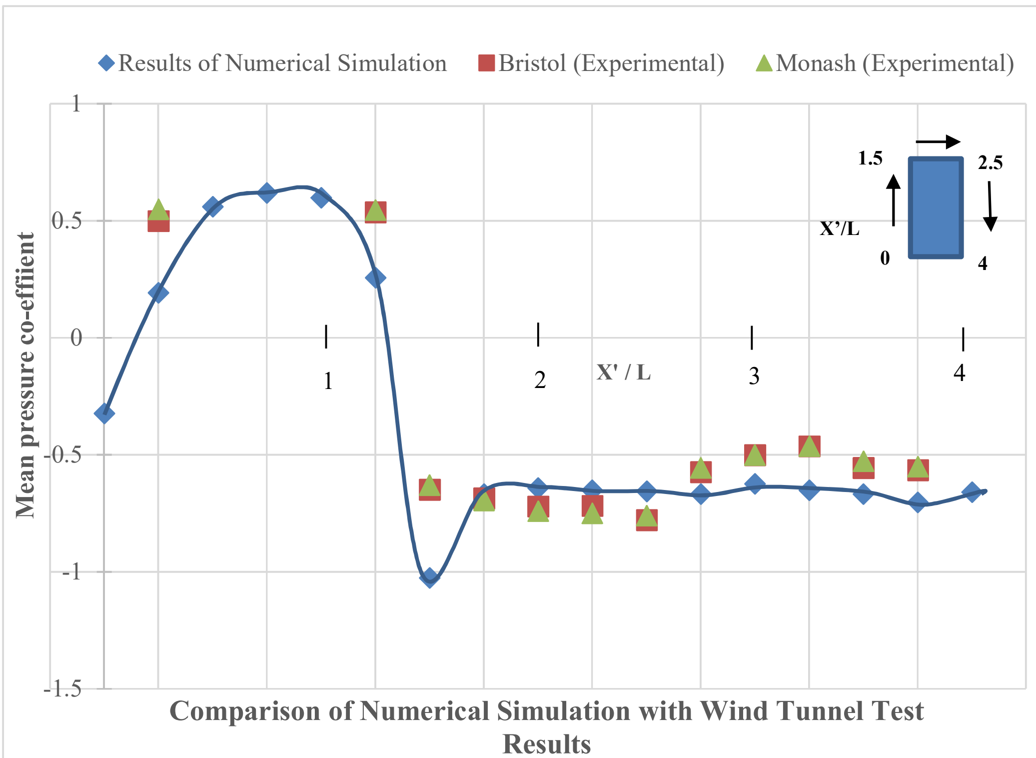

Figure 4.5 Comparison of numerical simulation with Wind Tunnel Test Results

The windward, side and the leeward faces are represented from 0 to 1.5 X' / L, from 1.5 to 2.5 X' / L 2.5 to 4 X' / L respectively. In case of the windward face, results are a little lower than the wind tunnel test results. Simulation results of the side face show good agreement with the wind tunnel test results. Furthermore, leeward face results show a little higher than the experimental values. Differences in mesh size and the number of elements particularly in the fluid domain may cause for that slight deviation from the results in research paper.

4.2 Wind Simulation for 102 m Height Building

Wind flow simulation has been carried out for 31 storey apartment building by commercially available software, SIMULIA.ABAQUS 6.14.2. Numerical simulation has been performed for two orthogonal wind directions (0^0 and 90^0) using Spalart-Allmaras turbulent model available in ABAQUS software.

The input wind profile is specified utilizing same three wind codes CP3 CHAPTER V-2:1972, BS-EN1991-1-4:2005 with National Annex SLS EN 1991-1-4:2019 & AS/NZS 1170.2:2011 with an intention of conducting the comparative study between the simulation results and the code based calculations. Altogether six different configurations have been set for the analysis. The analysis steps and & the important parameters used are described in the following Sections.

31-story apartment building described in Chapter 3.1 is used to assess the wind loads and their effects on the structure. Figures 4.6 (a), (b) and (c) show the plan view of 0-6^{th} floor, 6^{th} to 30^{th} floor and 3D view of the building respectively.

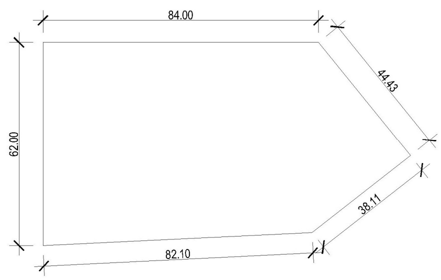

(a)

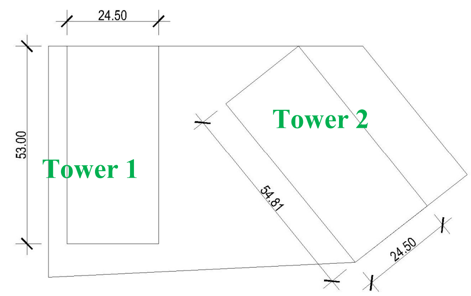

(b)

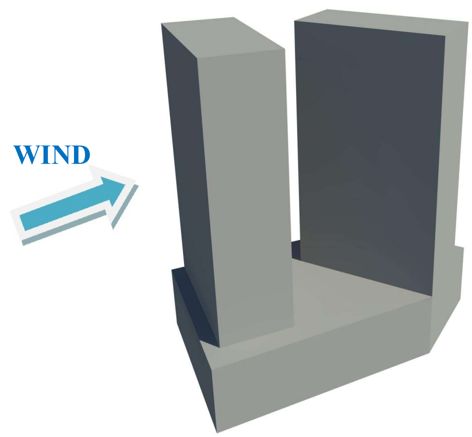

(C)

Figure 4.6(a) Plan view (0- 6th Floor) (b) Plan view (6th -31st Floor) (c) 3-D view

In order to perform the wind simulation, both fluid domain and the structure domain are modeled by ABAQUS. Fluid domain is modeled by ABAQUS/CFD, which represents the fluid flow properties, and the Structure is modeled by ABAQUS/Standard–explicit, which represents the building properties. Ultimately, Fluid- structure Interaction layer is created by defining the co-simulation boundary in both domains in order to couple the fluid dynamic laws and the structural mechanics.

4.3 Selection of Size of Fluid Domain (for undisturbed flow)

Selecting the size of the fluid domain and positioning of the structure in the domain is one of the key step in the simulation. For the reason that, sensitivity of pressure, velocity and turbulence fields around the structure relates with the domain size. Therefore, domain size has to be selected considering the fact that reduction of the computational time without losing the accuracy of results. Hence, CFD guidelines/recommendations and recent researches' outcomes are followed for selecting the domain size. The guidelines & recommendations of Hall R.C. is mainly considered for this case study. Apart from it, publications of Verein Deutscher Ingenieure (VDI) and Beatke & Werner (1990) are considered when deciding the blockage ratio in frontal area. According to the VDI publication, blockage ratio should be less than 3% (ratio of the front area of the building over the inlet area). Similarly Beatke and Werner recommended the limit of the blockage ratio as 3% especially for the building with greater horizontal dimension compared to its vertical dimension (height). By considering all the above facts, the inflow boundary is set in 5H (H = building height) away from the building face allowing undisturbed, fully developed flow when it reached to the building face. The, lateral boundaries are positioned in 5H (H = building height) away from the building. The outflow boundary is positioned in 15H away from the building face in order to have complete flow development & wake formation. Correspondingly, the top boundary is set from 4H away from top of the building to reduce the suction and avoid the artificial acceleration of the fluid flow over the building top. Accordingly, properties of fluid domain are defined in Table 4.2 and the size of the domain is shown in Figures 4.7 and 4.8.

Table 4.2 Properties of fluid domain

Boundary	**Building orientation for 0^0 dir$^{\underline{n}}$ wind**	**Building orientation for 90^0 dir$^{\underline{n}}$ wind**	
Inlet	5H	5H	
Lateral	5H	5H	
Outlet	15H	15H	
Top	5H (from x-y plane = 0)	5H (from x-y plane = 0)	
Blockage Ratio in y-z dir$^{\underline{n}}$		0.096 % < 3%	1.4% < 3%

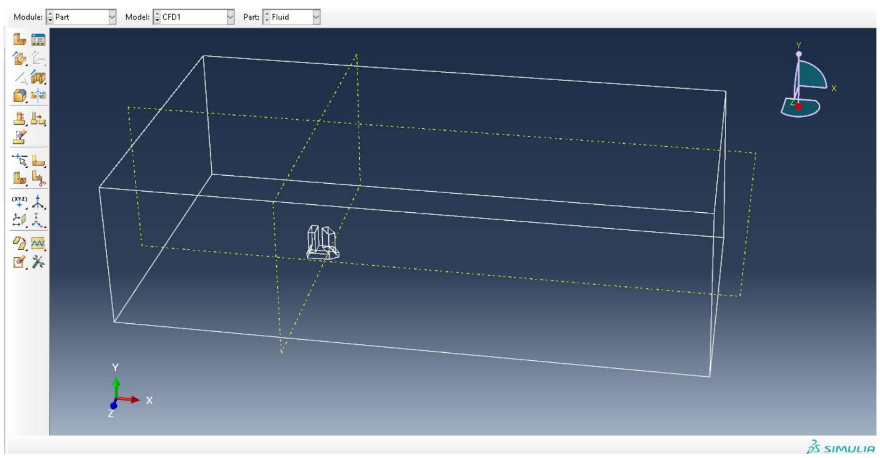

Figure 4.7 Size of the fluid domain

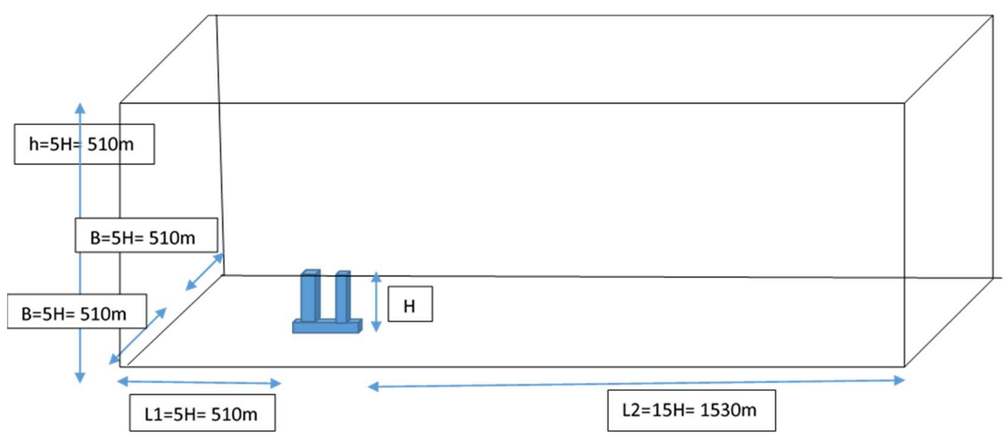

Figure 4.8 ABAQUS /CFD model- Fluid domain

4.4 Material and Section Properties

The structure (consisting 2 Towers) is modelled as a solid concrete member with constant elastic modulus & poisson ratio. Deflection of the building depends on the several factors such as mass, stiffness etc. Therefore, properties of the concrete material are modified in order to have a deformable structure. The elastic modulus of the concrete is modified to corresponding E value to represent the stiffness of the whole structure. In addition, mass and the Poisson ratio values used for the analysis are mentioned below.

However, considering the available data, seismic mass is used as the mass of the structure. Seismic mass is calculated according the code of practice of Earthquake actions in Australia: AS 1170.4-2007. Furthermore, corresponding E value is calculated with the help of a Finite Element Model and all the structural elements were modelled there. Ultimately, E value which correspond to stiffness of the whole structure is calculated.

Seismic mass = Mass of (slab + beam + walls + columns + 0.3* live load) between the mid height of the adjacent stories

= 175 kg/m^3

((Structural Design Actions - Part 4 -Earthquake actions in Australia: AS 1170.4 - 2007, (Amendment No.1 (August 2015)))

Poisson ratio = 0.2 (for dynamic analysis) (Ahmed, 2018)

The material properties used for both fluid and the structure are summarized in Table 4.3

Table 4.3 Material Properties for the fluid domain and the structure

Fluid Properties	Building Properties
Air Density = 1.225 kg/m^3 Dynamic viscosity = 1.7885 E-05	**Concrete** Mass = 175kg/m^3 E = 2.4E +8 N/m^2 υ = 0.2

4.5 Meshing & Element Choices

4.5.1 Fluid

Mesh Type – Hexahedral Mesh = C3D8 R- node linear fluid element

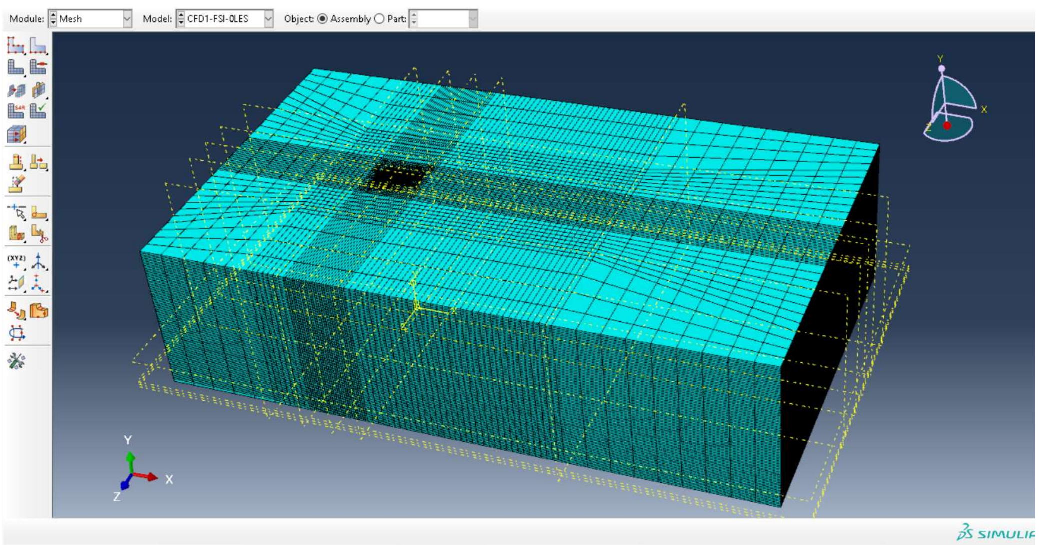

Figure 4.9 ABAQUS /CFD model- Mesh of the fluid domain

In numerical simulations, the accuracy of the results are highly depending on the quality of the grids. Therefore, in this case, hexahedra is chosen over constant strain tetrahedra due its minor truncation error and better iterative convergence (Research gate, 2017). In addition, it is required to control the distortion of the elements if tetrahedral mesh is used for the analysis. Besides, hexahedra cells are considered as more economical in terms of number of cells. Because the degrees of freedom in one hexaedron cell (8 nodes) is equivalence to six tetrahedral cells (ABAQUS 6.14 User Documentation, 2014).

In this case study, both coarse and fine meshes are used for the fluid domain. As well, the grid resolution should be fine enough to capture the important flow features such as flow separation etc. Hence, the coarse elements are locally seeded (edge seeded) further in order to get the good quality mesh in interesting region such as near building region (Figure 4.9).

4.5.2 First grid cell height

The first cell height near the wall should be properly sized in order to get the accurate solution of the flow field. The $\boldsymbol{y}^{+}$value is a non-dimensional distance between from the wall to first mesh node as shown in Figure 4.10.

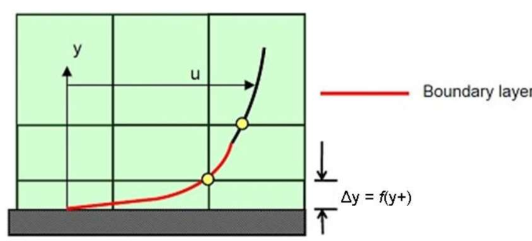

Figure 4.10 y+ definition (Turbulence Part 2 - Wall Functions and y+ Requirements, 2012)

The boundary layer mainly consists four zones: viscous sub layer, buffer layer turbulent layer and outer layer as shown in Figure 4.11.

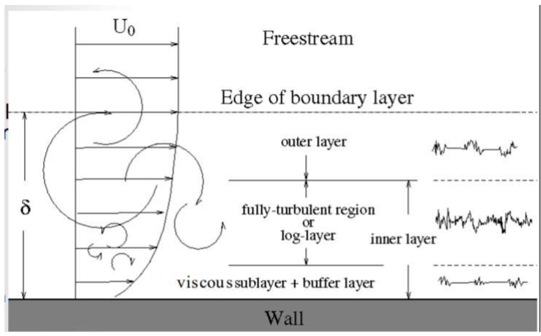

$y^+ > 300$ - outer layer

$31 < y^+ < 300$ - log lower region

$5 < y^+ < 30$ - buffer layer

$y^+ < 5$ - viscous sublayer

Figure 4.11 Turbulent boundary layers (ANSYS-Turbulence Modeling-Introduction to ANSYS Fluent, 2014).

The flows with very high Reynolds number such as flow around aircrafts, ships etc. may experience the turbulent boundary layer, which lengthens to several thousand y^+units. Conversely, low Reynolds number flow problems as turbine blades have an upper limit as 100 y^+units. In general practice, use of wall functions can be avoided for such kind of flow. In addition, it is recommended to position sufficient inflation layer cells within the boundary layer. Furthermore, y^+ value depends on the type of the turbulent model (Turbulence Part 2 - Wall Functions and y+ Requirements, 2012). Distance for the first node form the wall-bounded flow can be defined in the following equation (Turbulence Part 2 - Wall Functions and y+ Requirements, 2012).

$$\Delta y = L\, y^+ \sqrt{74}\, {Re_L}^{-13/14}$$

Δy - distance of the first node from the wall

L - flow characteristic length scale

Re_L - Reynolds Number based on your problem's characteristic length scale

In this research, y^+ is taken as 100. (Y+ range recommendations in documentation, 2020)

Therefore, first mesh cell height is calculated at the common boundary of the fluid domain and the building using above equation. Accordingly, near wall region is meshed with 3.1 m size hexahedra cells in order to get the surface pressure readings accurately. On structure walls, the grid lines are set as perpendicular to the wall satisfying one of main criteria of the grid quality in finite volume method.

4.5.3 Grid discretization

In case of grid discretization, it is recommended to do it in a sensible manner as reduce the computational time without losing the accuracy of the results. Therefore, the fluid domain is mainly divided in to 4 zones as shown in Figure 4.12 and Figure 4.13 to complete the mesh refinement as shown in below table. Region of near the building wall, expansive ratio of two consecutive cells is 2.4 and it is increased with the horizontal distance measured outward from the structure.

Grid discretization has been done by parting the fluid domain in to four zones as shown in Figure 4.13. Properties of grids are given in Table 4.4.

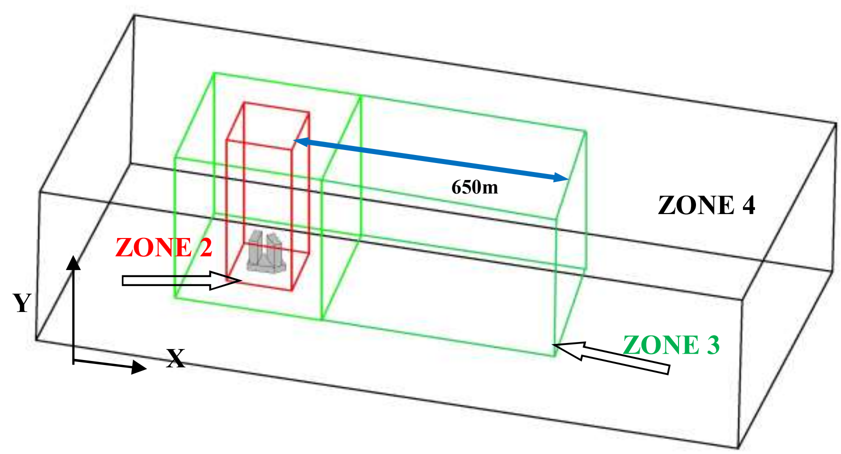

Figure 4.12 Four zone in fluid domain – Grid discretization

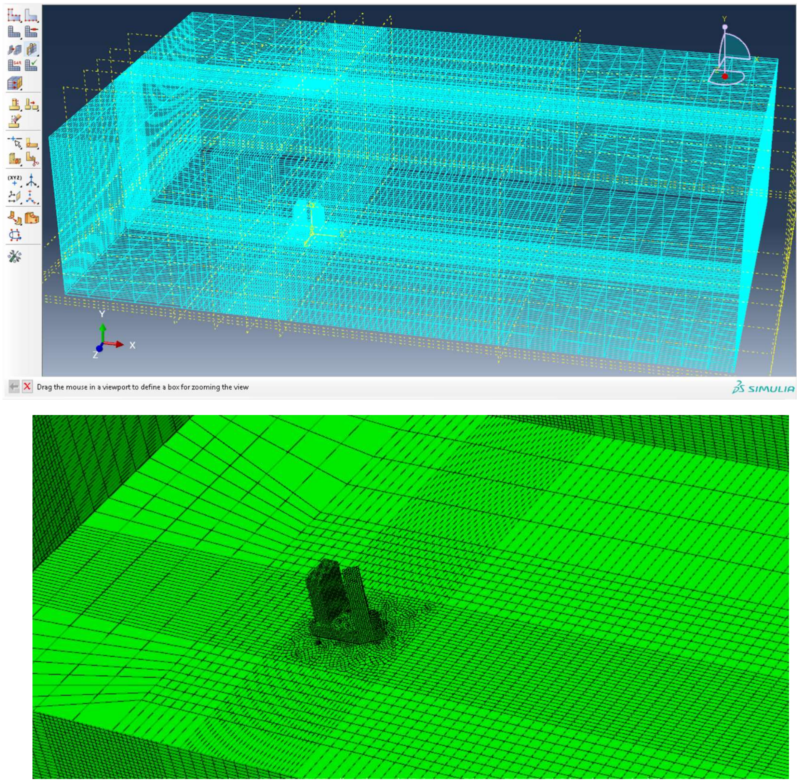

Figure 4.13 Grid discretization of the fluid domain – ABAQUS /CFD

<u>Properties of Grids (Fluid Domain)</u>

Table 4.4 Properties of grids

Distance from wall	Grid Expansion Ratio		
	3.1 < L < 100	100 < L < 225	225 < L< to boundary
Grid size (m) Grid Resolution	$\frac{\Delta Y_k}{\Delta Y_{k+1}}$ $\frac{7.5}{3.1} = 2.4$	$\frac{\Delta Y_k}{\Delta Y_{k+1}}$ $\frac{18.5}{7.5} = 2.5$	$\frac{\Delta Y_{k+1}}{\Delta Y_k}$ $\frac{72}{18.5} = 3.8$
Total Number of Hex Element of fluid domain	455737		

Note: L is measured from the centre of the structure base

The overall cell arrangement resulted in approximately 4348 nodes and 3502 elements in coarse model and 474626 nodes and 455737 elements in refined model.

4.5.4 Mesh validation

Accuracy of the fluid dynamic results mainly depends on the flow solver and the mesh quality (Mohamed, 2013). In addition, it is more difficult to decide the appropriate mesh size and the number for the relevant problem in straight, since two meshes generate different accurate solutions. Therefore, it is required to carry out the few trials to understand the variation of results with the mesh quality.

Chapter 4.5.4 presents the evaluation of the performance of three different meshes and comparative study. The ultimate aim of this work is to find the optimal mesh which helps to reduce the computational time without losing the accuracy of results. Therefore, three different meshes are generated: coarse mesh (239095 elements), medium mesh (455737elements) and fine mesh (602307) in order to evaluate the results (Figure 4.14 (a), (b) & (c)).

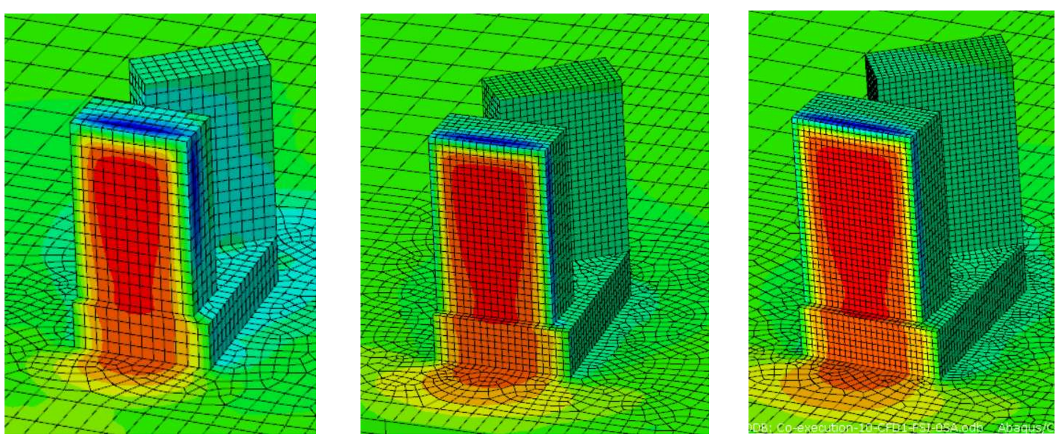

(a) (b) (c)

Figure 4.14 CFD Mesh (a) Coarse -239095 elements (b) Medium -455737 elements (c) Fine - 602307elements

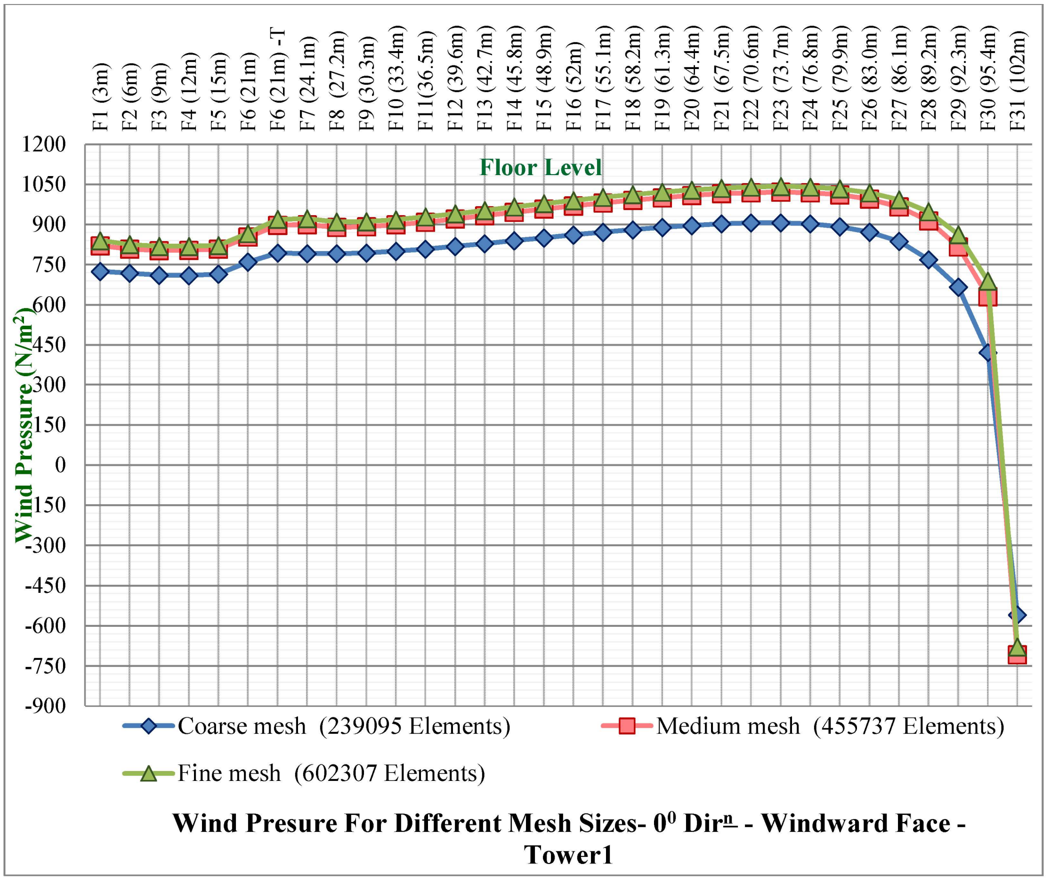

Figure 4.15 Wind pressure variation with the three different mesh qualities

As shown in figure 4.15, medium mesh model (455737 elements) showed averaged 12.8% pressure increment than the results of coarse mesh model (239095 elements). In flow separation area (top of the building), the variation is raised up to 29%. However, fine mesh model (602307 elements) showed averaged 2.2% value increment than the results of medium mesh model. Furthermore, it is observed the 5.6 % pressure increment in fine mesh model in flow separation region.

Therefore, the results clearly show the inadequacy of the coarse mesh model to reach the accurate solution. Furthermore, it is observed the important of the mesh size and number in order to capture the flow features such as flow separation. However, considering both computational time and the accuracy of the results, medium mesh model is selected for this research. More details of the medium mesh model are presented in Sections 4.5.2 and 4.5.3.

4.5.5 Structural model

The solid structure is meshed using the same element type meshed in fluid domain, hexahedral C3D8 R- node linear brick. Even though, tetrahedral elements can be well fitted for complex geometry such as this, the accuracy of results will be lesser in case of integrating the shape functions with Gaussian points. In addition, the quality of the mesh will be evaluated by distortion of the elements. Therefore, multiple partitions are created to prevent the distorted elements forming in case of using the automatic meshing tool in the ABAQUS software. Approximately 3.1 m size cells (same cell size used for the fluid –structure boundary in fluid domain) are used for the structure. The overall structure resulted in approximately 14352 nodes and 11881 elements. The meshed structure is shown in Figure 4.16.

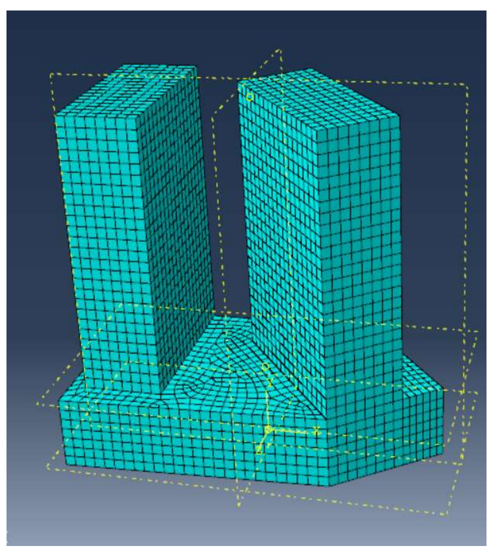

Figure 4.16 Meshed structure – ABAQUS /Standard

4.6 Boundary Conditions

4.6.1 Fluid

Generally, boundary conditions are used to represent the influence of surrounding environment, which have been strike-off by the computational domain. In this case study, four different boundary conditions are set in the CFD solver to run the simulation properly. Accordingly, boundary conditions are prescribed for inlet, top, lateral, bottom wall and outlet in the fluid domain. Inlet velocity profile is defined according to the codes of practices. The expressions of different inlet velocity profiles are defined according to the wind loading codes and which are described in Section 4.7. In the top and lateral boundaries are prescribed in symmetry in order to ensure the parallel wind flow while avoiding the artificial acceleration in the flow. Access of flow cross the boundaries are not permitted. In addition, no slip boundary condition is prescribed for bottom wall. The outlet boundary is set at far away (15H) from the obstacle where all the fluid leaves the domain and flow variable (pressure) is enforced to come to be zero in order to get the converged solution. Therefore, zero static pressure is set for the outlet boundary condition to avoid the reflection pressure wave occurrence (Revuz, et al., 2010).In addition outer boundaries of the fluid domain are prescribed as "pin" (restrict for rotation) condition in the CFD solver in order to run the simulation properly. Boundary conditions applied for the fluid domain are shown in Figure 4.17 and Table 4.5.

Table 4.5 Boundary conditions of fluid domain - ABAQUS/CFD

Inlet	Outlet	Top & two sides	Bottom
V1= V1 (Wind profile)	P = 0	V1	No slip
V2 = 0		V2 = 0	
V3 =0		V3 = 0	

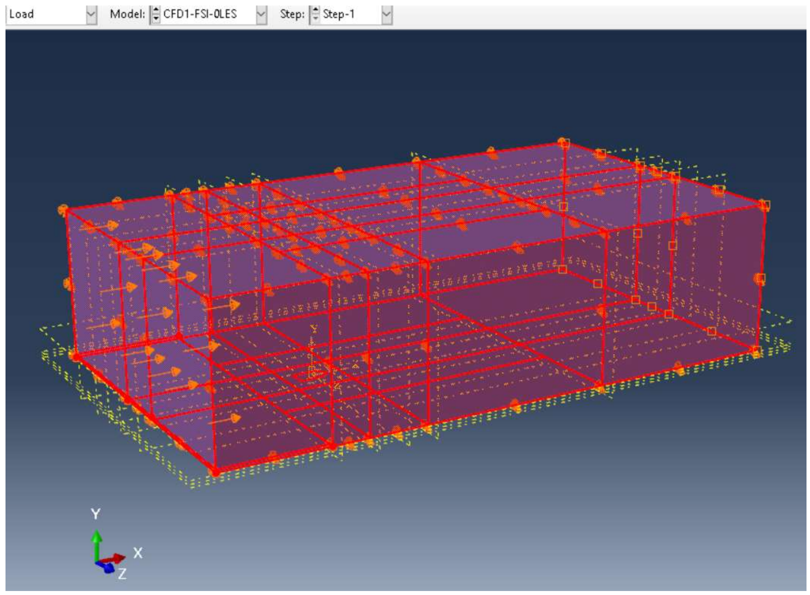

Figure 4.17 Boundary condition -ABAQUS /CFD

4.6.2 Structure

All six degree of freedoms of the bottom of the building are resisted against the motion of the structure. Figure 4.18 shows the structural model with the boundary conditions.

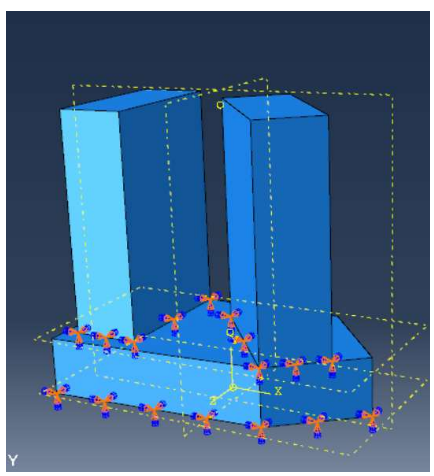

Figure 4.18 Constrains of structure- ABAQUS /Standard

4.7 Selection of Wind Profile

BS-EN1991-1-4:2005 with SLS EN 1991-1-4:2019 & AS/NZS 1170.2:2011 specified their wind profile using natural logarithmic expression. Nevertheless, CP3 CHAPTER V-2:1972 uses power law expression to describe the vertical distribution of the horizontal mean wind velocity. The expression for the log wind profile is presented in BS-EN1991-1-4:2005 code comprising few factors such as roughness length, terrain factor etc. However, such kind of an expression is not specified in AS/NZS 1170.2:2011 code. Therefore, designers are free to use the general log wind profile equation, which consists the frictional velocity & Von-Karman constant. Also, it is always better to express the wind profile of the ABL (Atmospheric Boundary Layer) by logarithmic equation compared to power law equation, if the surface roughness and stability information are available.S2 factor values are given in Table 4.6.

Appendix A.3, A.4 of CP3 CHAPTER V-2:1978 define wind profile as follows.

$$V_{Ht} = \frac{V_{Et}}{V_{E3}} \frac{V_{E3}}{V_{10,3}} V_{10,3} \left(\frac{H-Y}{10}\right)^{\alpha} \tag{1}$$

where,

V_{Ht} = t s speed at height H in appropriate category

$V_{10,3}$ = 3 s speed at 10 m height in open terrain category

Y = level corresponding to general roof top level or obstruction level

V_{Ht} = t s speed at height H in appropriate category

$V_{10,3}$ = 3 s speed at 10 m height in open terrain category

Y = level corresponding to general roof top level or obstruction level

= 10 m (taken for this case study)

E = effective height 10 m above Y

$\frac{V_{Et}}{V_{E3}}$ = ratio of the t s to 3 s wind at an effective height

$\frac{V_{E3}}{V_{10,3}}$ = conversion factor to ensure that at or near gradient wind height all 3s wind speed are the same whatever the roughness category.

α = power law exponent

Table 4.6 Values for S_2 factors

Category	Y (metres)	E (metres)	$\left(\frac{V_{E3}}{V_{10,3}}\right)$	$\left(\frac{V_{Et}}{V_{E3}}\right)$			α		
				t (seconds)			t (seconds)		
				3	5	15	3	5	15
1	0	10	1.00	1.00	.95	0.90	0.080	0.090	0.100
2	2	12	0.98	1.00	.95	0.90	0.085	0.095	0.105
3	10	20	0.95	1.00	.95	0.90	0.090	0.100	0.110
4	25	35	0.94	1.00	.95	0.90	0.090	0.105	0.115

BSEN 1991-1-4:2005 calculates wind profile with expression 4.3 of Cl.4.3.1 as follows.

$$V = V_b\, C_0(z)\, k_r \ln\left(\frac{z}{z_0}\right) \quad (2)$$

$k_r = (\frac{z_0}{z_{0,II}})^{0.07}$; for $Z_{min} < Z < Z_{max}$

$= 0.19\,(\frac{0.3}{0.05})^{0.07} = 0.215$ (Expression .4.5 of Cl.4.3.2 BS-EN1991-1-4:2005)

where,

z_0 = roughness length. (z_0 values are given in Table 4.6)

k_r = terrain factor depending on the roughness length

$z_{0,II}$ = 0.05 (terrain category II)

z_{min} = minimum height defined in table 4.1. (z_{min} values are given in Table 4.6)

z_{max} = maximum height taken as 200 m

V_b = Basic wind velocity

= 22.11 m/s (taken from manual calculation considering the altitude correction factor)

$C_o\,(z)$ = Orography factor –should be calculated as per Clause 4.3.3 of BS-EN1991-1-4 :2005. Recommanded value is 1.0.

Table 4.7 Terrain categories and terrain parameters

Terrain category		z_0 m	z_{min} m
0	Sea or coastal area exposed to the open sea	0,003	1
I	Lakes or flat and horizontal area with negligible vegetation and without obstacles	0,01	1
II	Area with low vegetation such as grass and isolated obstacles (trees, buildings) with separations of at least 20 obstacle heights	0,05	2
III	Area with regular cover of vegetation or buildings or with isolated obstacles with separations of maximum 20 obstacle heights (such as villages, suburban terrain, permanent forest)	0,3	5
IV	Area in which at least 15 % of the surface is covered with buildings and their average height exceeds 15 m	1,0	10
NOTE: The terrain categories are illustrated in A.1.			

$V \quad = V_b \ k_r \ln(\frac{z}{z_0})$; (Expression .4.3 of Cl.4.3.1 BS-EN1991-1-4:2005)

$V \quad = 22.11 * 0.215 * ln(\frac{z}{0.3}) = 4.76 * ln(\frac{z}{0.3})$

AS/NZS 1170.2:2011 defines the wind profile as follows.

$$V_H = \frac{U^*}{\mathcal{K}} \ln\left(\frac{z}{z_0}\right) \tag{3}$$

where,

U^* = Frictional velocity

K = Von Karman's constant = 0.4

Z_0 = Roughness length values are given in Table 4.8.

Table 4.8 Roughness length for terrain categories

ROUGHNESS LENGTHS FOR TERRAIN CATEGORIES	
Terrain category	Roughness length (m)
1	0.002
2	0.02
3	0.2
4	2.0

$$V_H = 7.125 \, ln(z) + 11.476$$

Table 4.9 Inflow wind profiles according to three international wind codes

Code	Basic Wind Speed	Wind Profile
CP3 CHAPTER 2:1978	38 ms^{-1}	$V_{Ht} = \frac{V_{Et}}{V_{E3}} \frac{V_{E3}}{V_{10,3}} V_{10,3}(\frac{H-Y}{10})^{\alpha}$ $= 0.9*0.95*38* (\frac{H-10}{10})^{0.11}$ $= 32.5* (\frac{H-10}{10})^{0.11}$ (Appendix A.3, A.4 CP3 CHAPTER V-2:1978)
BS-EN1991-1-4:2005 with SLS-EN1991-1-4:2019	22 ms^{-1}	$V = V_b\, C_0(z)\, k_r \ln(\frac{z}{z_0})$ $k_r = (\frac{z_0}{z_{0,II}})^{0.07} = 0.19\,(\frac{0.3}{0.05})^{0.07} = 0.215$ (Expression .4.5 of Cl.4.3.2 BS-EN1991-1-4:2005) $V = 4.76 * ln(\frac{z}{0.3})$ (Expression .4.3 of Cl.4.3.1 BS-EN1991-1-4:2005)
AS/NZS 1170.2:2011	38 ms^{-1}	$V_H = \frac{U^*}{\mathcal{K}} \ln\left(\frac{z}{z_0}\right)$ U* - Frictional velocity K - Von Karman's constant = 0.4 $V_H = 7.125 \ln\left(\frac{z}{0.2}\right)$

Wind profiles as per three different wind loading codes (Table 4.9) are presented in graphically in below Figure 4.19.

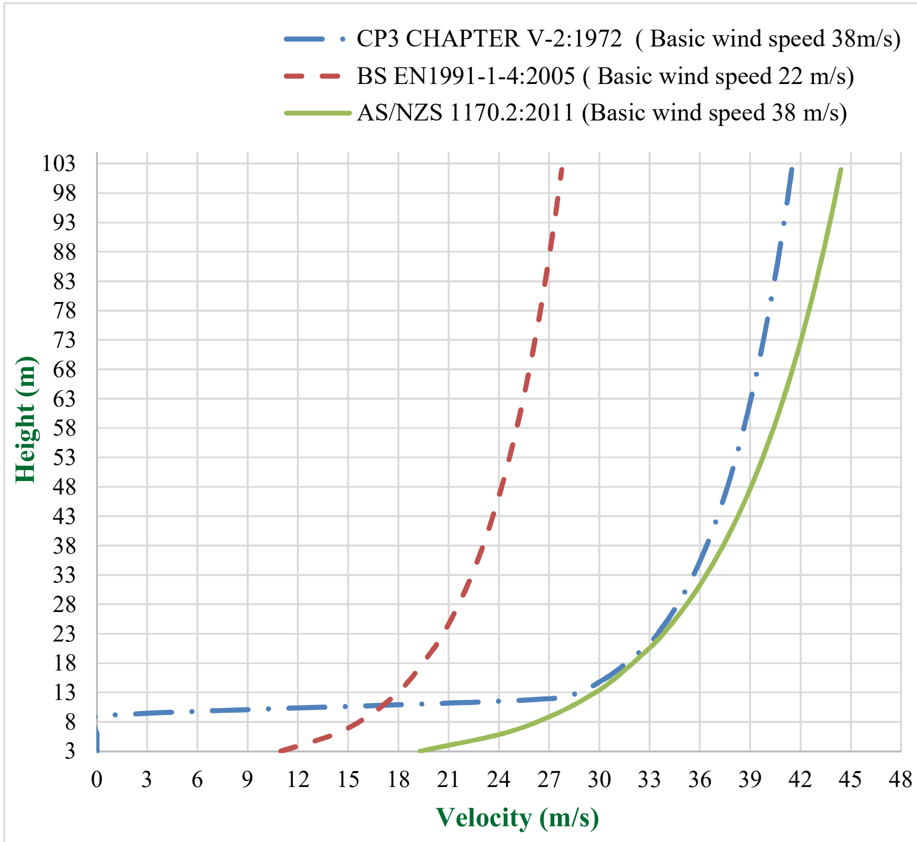

Figure 4.19 Inflow velocity profile according to three wind codes

4.8 Comparison between the Actual Wind Profile (Based on Power Law or Logarithmic) and Manually Calculated Wind Profile

Inflow velocity profile obtained from manual calculation (Expression 1) and power law equation (Expression 2) are presented in same graph as shown in Figure 4.20 in order to endorse the comparison between simulation results (along wind pressure) and the code based calculation.

Inflow Velocity Profile (CP3: Chapter V-2:1972)

$V_s = V\, S_1 S_2 S_3\, S_4$; Clause. 4.3 (2) of CP3: Chapter v-2:1972 - **(Exp. 1)**

$V_{Ht} = \frac{V_{Et}}{V_{E3}} \frac{V_{E3}}{V_{10,3}} V_{10,3}(\frac{H-Y}{10})^{\alpha}$; Appendix A.3, A.4 CP3 CHAPTER V-2:1978)

- **(Exp. 2)**

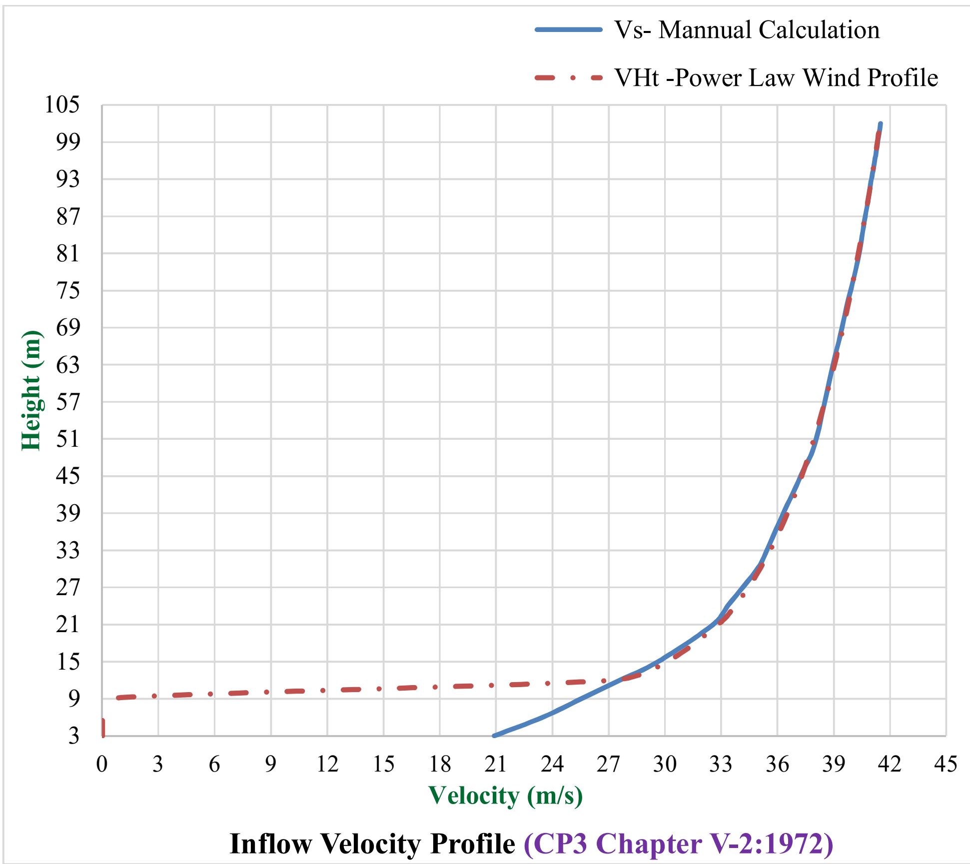

Figure 4.20 Inflow velocity profile graph as per CP3 Chapter V-2:1972

The significant different is shown between manual calculation wind profile and the actual wind profile (power law wind profile) up to 10m height. From 10 m upward both lines (V_s and V_{Ht}) are almost overlaid each other while having small deviation factor of 0.06 (height between 12m-24m).

Same comparative study is performed for other two codes of practice as well.

Inflow Velocity Profile (BS-EN1991-1-4:2005)

$V = C_o(z)V_{b,0}\ C_{dir}\, C_{season}$ Clause. 4.3 of BS-EN 1991-1-4:2005) - **(Exp. 1)**

$V = V_b\, C_0(z)\, k_r \ln(\frac{z}{z_0})$; Expression .4.5 of cl.4.3.2 BS-EN1991-1-4:2005

- (Exp. 2)

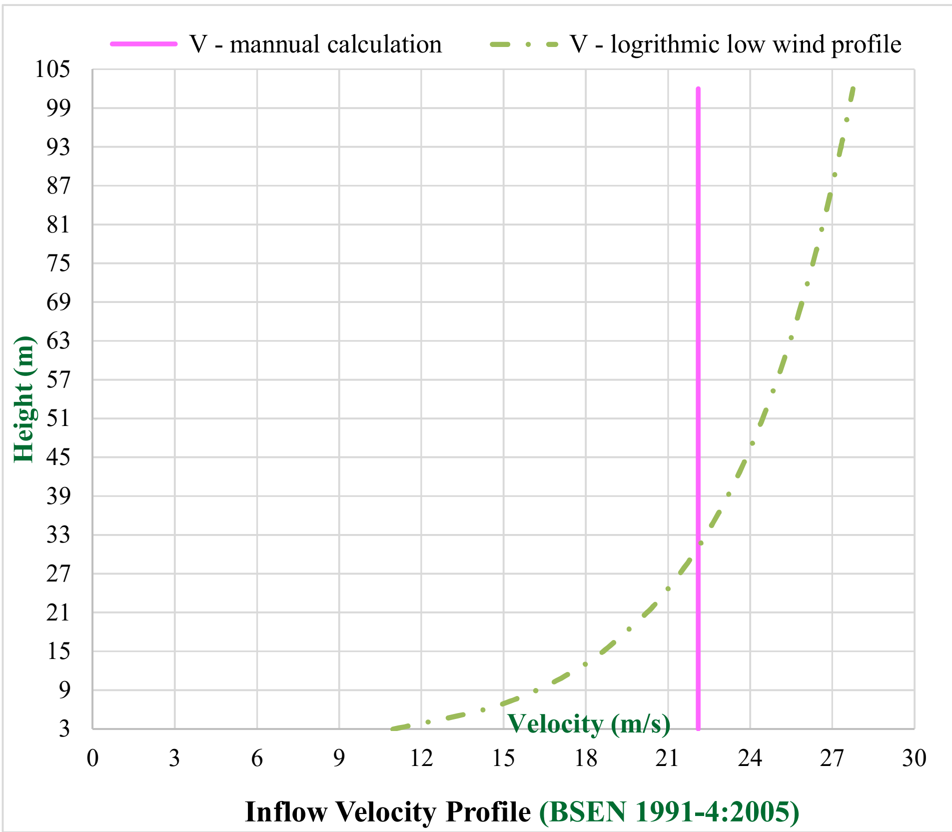

Figure 4.21 Inflow velocity profile graph as per BS-EN1991-1-4:2005

In BS-EN1991-1-4:2005, wind loads are calculated according to the dividing by parts rule which related with the building dimensions , hence the significant deviation is observed from manual calculated wind speed with actual wind speed (logarithmic wind profile) as shown in above Figure 4.21.

Inflow Velocity Profile (AS/NZS 1170.2:2011)

$$V_{sit,\beta} = V_R M_d (M_{z,cat} M_s M_t)$$; Clause of 2.2 of AS/NZS 1170.2:2011 **(Exp. 1)**

$$V_H = \frac{U^*}{\mathcal{K}} \ln\left(\frac{z}{z_0}\right)$$ - **(Exp. 2)**

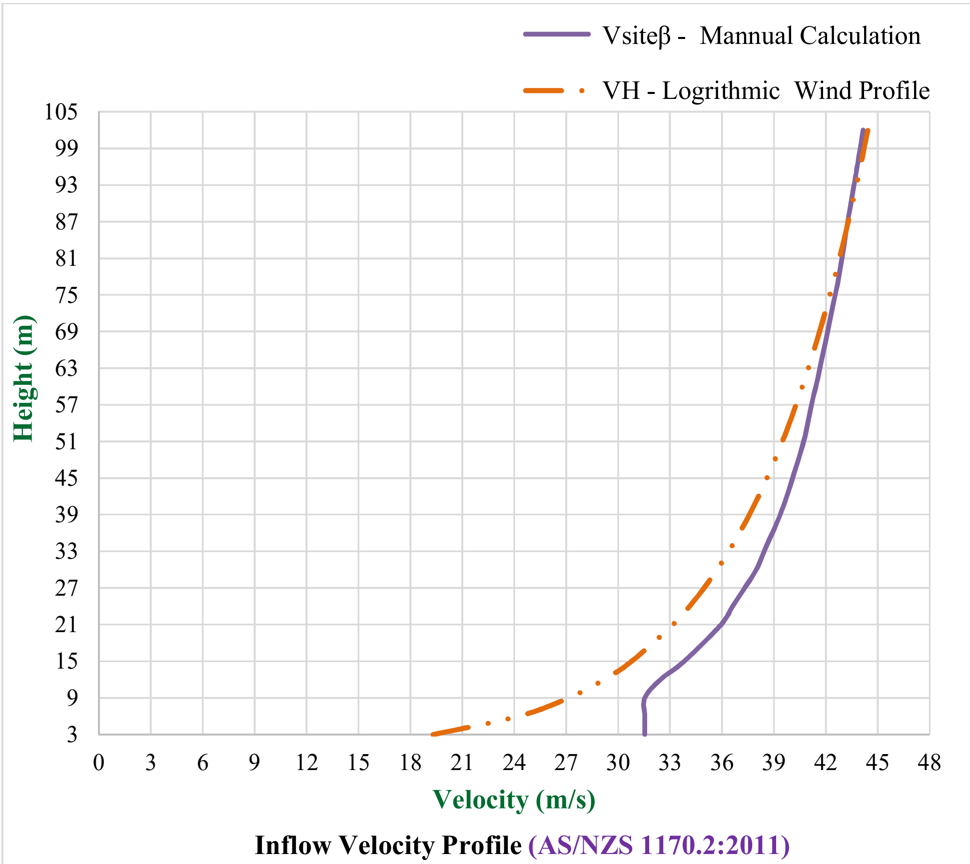

Figure 4.22 Inflow velocity profile graph as per AS/NZS 1170.2:2011

The significant different is shown between manual calculation wind profile and the actual wind profile (shown in Figure 4.22) up to 10 m height. From 10 m upward, difference between the manual calculation wind speed and actual wind speed (power law wind profile) is gradually reducing. The manual calculation wind profile deviated from the actual wind profile with the maximum deviation factor of 0.09 at the lower level (10 m).

4.9 Turbulence Models

As described in Section 2.2.5.2, different types of turbulent models can be used to find the flow variables in a turbulent flow. Therefore, numerical simulation has been performed using S-A model available in ABAQUS software. Additional inflow parameters required for each turbulent model are mentioned in below.

4.9.1 Spalart –Allmaras (S-A)

As described in Section 2.2.5.3, following simple expression is used to calculate the kinematic eddy viscosity.

$$Viscosity\ Ratio = \frac{Kinmatic\ Eddy\ Viscosity}{Dynamic\ Viscosity}$$

The value of eddy viscosity ratio plays in a vast range depending on the application. In general, eddy viscosity ratio should be ranged from 1-10 for the external flows such as flow around cars, aircrafts and submarine or structures etc. and 10-100 for the internal flows such as pipe flow. (ANSYS FLUENT user guidelines). The viscosity ratio should be increased with the increase of Reynolds's number (Re) in the application. In this case study, ANSYS FLUENT user guidelines is followed to estimate the kinematic eddy viscosity, thus the available parameters are inadequate for the calculation process. Similarly, it is recommended to use the aforementioned viscosity ratios in the situations, where the user cannot guess the level of turbulent in the simulation.

Upper limit of the viscosity ratio (10) for the external flows has been selected to create the critical environmental condition with the strong effect of turbulent viscosity. Roughness of the structure wall is not implemented in the simulation. Additional inflow parameters used for the analysis are given in Table 4.10 and Figure 4.23.

Table 4.10 Additional inflow parameters for turbulent models-ABAQUS/CFD

Turbulent model	Spalart-Allmaras **(S-A)**
Additional Input Parameter	Viscosity Ratio =10 Kinematic Eddy viscosity =10*kinematic viscosity(√) 10*1.7885 E-05 =1.7785E-04 (ANSYS FLUENT)

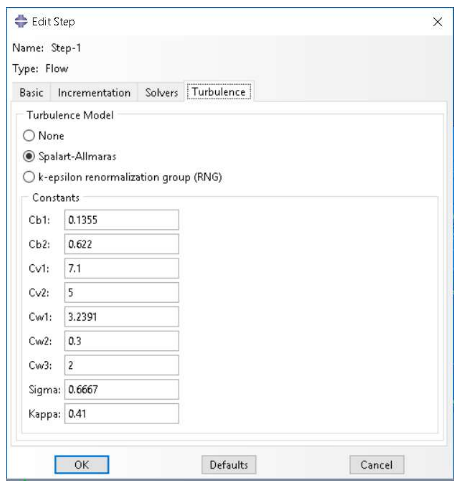

Figure 4.23 S-A turbulent ABAQUS /CFD

4.10 Coupling Type – Fluid and Solid

Different mesh sizes (fluid domain and structure domain) and different numerical methods cause difficulties in coupling fluid dynamic and structure dynamic codes. Generally, finite-volume approach is employed in fluid dynamic codes and finite-element (FE) approach is employed in structure dynamics codes. Therefore, intermediate layer is used to interpolate and exchange the data between the grids in fluid domain and structure domains to solve the problem (Aksenov, et al., 2004). Accordingly, FSI is created between the fluid and the structure by defining the co-simulation boundary in both domains. The more details of coupling are contained in Section 2.2.6.

However, in this research, two way coupling method is used, which means the fluid pressure acting on the structure is transferred to the structure solver and the structure displacement is also transferred to the fluid solver (Benra, et al., 2011). In addition, FSI supports to maintain the accuracy of governing equations. Figures 4.24 (a) and (b) show the co-boundary in fluid domain and co-boundary in structure domain respectively.

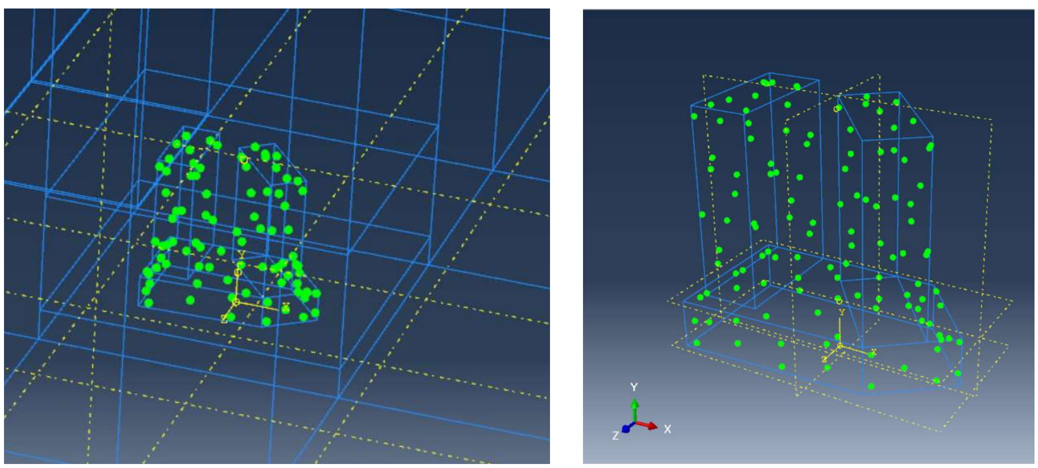

(a) (b)

Figure 4.24 (a) Co- boundary in fluid domain (b) Co- boundary in structure domain

Advanced parameters used for the analysis are described in Annex D.

Results are presented graphically in Chapter 5.

4.11 Summary

- A known case study is performed in order to identify and avoid the modeling and numerical approximation errors.
- Numerical simulation has been performed for two orthogonal wind directions (0^0 and 90^0) using S-A turbulent model.
- Simulation has been carried out for three different meshes (Coarse, medium and fine) in order to verify the accuracy of the results with the computational time.
- Two –way coupling method is used for CFD simulation

5. RESULTS AND DISCUSSION

Chapter 5 presents the comparison between three different wind loading codes when assessing wind loads and their effects on tall buildings. Further, this Chapter presents the wind loading results by Codes of practice and the numerical modeling in the same graph. Finally, the Chapter concludes the more suitable wind loading code to assess complex –building wind environment and the advantages of CFD analysis opposed with manual calculations in terms of accuracy of results, time, and cost.

5.1 Parametric Study between Wind Profiles by Codes of Practice

In this section, all the relevant features/parameters needed for the assessment of along wind loads according to different codes/standards are closely studied and compared. Moreover, Figure 4.19 in Chapter 4.7 clearly revealed that the discrepancies between three wind codes due to different parameters and different conditions introduced by them.

Similarities and discrepancies among three codes of practice are discussed by comparing the numbers which are used to estimate the along wind force in this case study. Followings features/parameters are identified as decisive and discussed in Tables 5.1 to 5.4.

- <u>Limitations of applicability in codes of practice</u>

  Different limitations are specified in three different codes during applications. In general, all the codes are applicable for the buildings up to 200m height. In addition, AS/NZS 1170.2:2011 code can be applied for the buildings with aspect ratio less than 6. All three codes cannot be applied for unusual site locations. In CP3 CHAPTER V-2:1972, the wind induced forces such as vortex shedding, aero-elastic effects are not considered for the wind load calculation. In addition, CP3 CHAPTER V-2:1972 cannot be applied, if structural properties of a building such as damping, weight and stiffness etc. are caused to make them liable for dynamic loadings. Particularly, BS-EN1991-1-4:2005 with NA present the wind load calculation procedure while offering the freedom for others to change the parameters as per their country context. Hence, the designers would have opportunity to prepare the NA which perfectly match with their country context by altering the factors such as the terrain roughness factor, terrain roughness correction exposure factor etc.

Table 5.1 Parameters comparison

Code	CP3 CHAPTER V-2:1972	BS-EN 1991-1-4:2005	AS/NZS 1170.2:2011
Basic wind speed for zone 3 (ms^{-1})	38	22	38
Terrain category	3	III	3
Roughness length	Not specified	0.3	0.2
Obstruction height considered(m)	Y=10	h_{avg} = 10	Not specified

- Basic wind speed with averaging time

  In CP3 Chapter V-2:1072, basic wind speed considers the 3s gust wind speed at 10m height in open terrain with no obstructions. But in BS-EN1991-1-4:2005 with SLS EN 1991-1-4:2019 consider characteristic 10 minutes mean wind velocity at 10 m (33 ft) height for terrain category II. AS/NZS 1170.2:2011 code defines 3-second gust wind speed at a height of 10 m above the ground relates to the terrain category 2. Therefore, the 3 *s* gust wind speed can be converted to 10 minute mean wind speed by combination of two methods suggested by Cook (1999) and IECUK. ICEUK proposed to use 1.06 conversion factor to convert mean hourly wind speed in to 10 minute mean speed.

- Terrain category and Roughness length

  CP3 chapter V-2:1072 and AS/NZS 1170.2:2011 introduced 4 terrain categories and BS-EN1991-1-4:2005 introduced 5 terrain categories including category 0 for sea, coastal area exposed to the open sea. Both category 0 and I in BS-EN1991-1-4:2005 are fallen in to category 1 in other two codes. Also, the roughness length for each terrain category is defined in BS-EN 1991-1-4:2005 and AS/NZS 1170.2:2011 and the values are always higher in BS-EN 1991-1-4:2005 compared to AS/NZS 1170.2:2011. Furthermore, all the codes addressed the influence of the change of the terrain category including lagging length. Among those codes BS-EN 1991-1-4:2005 and AS/NZS 1170.2:2011discussed this matter in detail.

- Obstruction height

  In BS-EN1991-1-4:2005, influencing area of the neighbouring structures and their average heights are considered in order to calculate the displacement height due to the wind act as if the ground level is upheaved . Even though, this is applicable only for the terrain category IV, wind effect due to neighbouring structures is taken in to account in this case study for the sake of representing the actual environmental condition. Also, the average roof top level of neighbouring structures is taken in to account in CP3 Chapter V-2:1972 when calculating the S_2 factor for terrain category 3 and 4. This is expressed by $\frac{V_{Et}}{V_{E3}}\frac{V_{E3}}{V_{10,3}}(\frac{H-Y}{10})^{\alpha}$ and Y represents the general roof top level. However, AS/NZS 1170.2:2011 didn't go in to that depth and only option would be the selection of terrain category which fits for the actual obstruction heights criterion.

- Wind Profile

Table 5.2 Wind profile comparison

Code	Wind Profile	V
CP3 CHAPTER V-2:1972	Power law	$V_{Ht} = \frac{V_{Et}}{V_{E3}} \frac{V_{E3}}{V_{10,3}} V_{10,3} (\frac{H-Y}{10})^{\alpha}$
BS-EN 1991-1-4:2005	Logarithmic	$V_m = V_{b,0}\ k_r \ln(\frac{z}{z_0})$
AS/NZS 1170.2:2011	Logarithmic	$V_H = \frac{U^*}{\mathcal{K}} \ln(\frac{z}{z_0})$

BSEN 1991-1-4:2005 and AS/NZS 1170.2:2011 specified their wind profile using natural logarithmic expression. Nevertheless, CP3 CHAPTER V-2:1972 used power law expression to describe the vertical distribution of the horizontal mean wind speed. BS-EN1991-1-4:2005 code built its' expression using terrain factor which depends on the roughness length. However, AS/NZS 1170.2:2011 didn't specify such kind of an expression by itself and the designers can use the general log wind profile equation consisting frictional velocity and Von-Karman constant. Log wind profile is well suited to represent atmospheric boundary layer with terrain roughness effect. But, those features are represented in power law wind profile.

Table 5.3 Parameters comparison

Code	CP3 CHAPTER V-2:1972	BS-EN 1991-1-4:2005	AS/NZS 1170.2:2011
Average recurrence Interval	50yrs $S_3 = 1$	50yrs $C_{prob} = 1$	50yrs V_{50}
Wind direction adjustment factor	$S_4 = 1$	$C_{dir} = 1$	$M_d = 1$
Wind adjustment factor for seasonal variation	Not specified	$C_{season} = 1$	Not specified
Correction factor for altitude	Not specified	$C_{alt} \leq 1.5$ (Max.)	Not specified
Topography/Orography factor	$S_1 = 1$	$C_0 = 1$	$M_t = 1$
Gust factor	Not specified	$C_s C_d$	C_{dyn}

- Average recurrence interval

  In this case study average recurrence interval is taken as 50 years. However, Different wind loading codes addressed this matter in a different way. CP3 CHAPTER V-2:1972 introduced statistical based factor named S3 which represents the wind exposure period and the safety of the structure. AS/NZS 1170.2:2011 presented the different regional wind speed with respect to the different average recurrence intervals such as V50, V100 etc. Moreover, BS-EN1991-1-4:2005 introduced the C_{prob} probability factor consisting the shape parameter and the exponent of n (=0.5).

- Wind Directional factor

  All the codes of practice introduced the wind direction adjustment factor when estimating the wind loads on structure. Among them, AS/NZS 1170.2:2011 recommended to calculate the $V_{site,\beta}$ for 8 cardinal directions and select the maximum one as a $V_{des,\Theta}$. In this case study the recommended value is 1.0.

- Seasonal factor

  Only BS-EN1991-1-4:2005 introduced the wind seasonal factor when estimating the wind loads on structure. In this case study the recommended value is 1.0.

- Altitude Correction factor

  Similar to above, only BS-EN1991-1-4:2005 introduced the altitude correction factor to count the variation of the wind velocity (w.r.t mean sea level) corresponds to the structure location. Altitude correction factor is particularly useful when calculating the wind loads for the buildings locate in hill country.

- Topography / Orography factor

  All three codes introduced the orography factor to account the orography factor to account the inflow velocity increment due to the upwind terrain slope.

- Gust Factor

  Both BS-EN1991-1-4:2005 and AS/NZS 1170.2:2011 use random vibration gust effect approach for evaluating the fluctuating component of flow variables as well as dynamic behaviour (dynamic loading) of the structure. BS-EN1991-1-4:2005 specified it as a "structural factor" (C_sC_d). Structural factor can be decomposed in to two factors, size factor (C_s) and dynamic factor (C_d).Dynamic factor is used to account the structure vibration due to turbulence occurring. Size factor represents the wind effect if the wind performs to have maximum wind pressure on structure in non- simultaneously. Furthermore, structural factor is specified using several other factors such as turbulent Intensity, peak factor for the upwind velocity fluctuations, background factor, and resonant response factor.

Table 5.4 Parameters comparison

Code	CP3 CHAPTER V-2:1972	BS-EN1991-1-4:2005	AS/NZS 1170.2:2011
Turbulence Length Scale	Not specified	$L_z = L_t(\frac{z}{z_t})^{\alpha}$; z> z_{min} α = 0.67+0.05ln(z_0) Z_0 = 0.3 ,α = 0.60 , L_z = 199	$L_z = 85(\frac{h}{10})^{0.25}$ L_z = 152
Peak factor for the upwind velocity fluctuations	Not specified	$k_p = \sqrt{2\ln vT} + \frac{0.6}{\sqrt{2\ln vT}}$ or k_p =3 (larger one) T= 600 s	g_v = 3.7
Peak factor for resonant	Not specified	$R^2 = \frac{\pi^2}{2\delta} S_L(z_s, n_{1,x}) R_h(\eta_h) R_b(\eta_b)$ (Annex B) $R^2 = \frac{\pi^2}{2\delta} S_L(z_s, n_{1,x}) K_s(n_{1,x})$	$g_R = \sqrt{2log_e(600n_a)}$
Background factor	Not specified	$B^2 = \frac{1}{1+0.9(\frac{b+h}{L(z_s)})^{0.63}}$ (Annex B) $B^2 = \frac{1}{1+\frac{3}{2}\sqrt{\left(\frac{b}{L(z_s)}\right)^2 + \left(\frac{h}{L(z_s)}\right)^2 + (\frac{b}{L(z_s)}\frac{}{L}}}$ (Annex C)	$B_s = \frac{1}{1+\frac{\sqrt{0.26(h-s)^2+0.46b_{sh}^2}}{L_h}}$
Pressure co-efficient	C_{pe}	C_{pe}	C_{fig}

As shown in Table 5.4, BS-EN1991-1-4:2005 provides two methods to calculating structural factor in Annex B and Annex C. However, AS/NZS 1170.2:2011 defined it as a dynamic response factor (C_{dyn}). Similar to BS-

EN1991-1-4:2005, dynamic response factor is expressed using same factors like turbulent Intensity, peak factor for the upwind velocity fluctuations, background factor, peak factor for the resonant response etc. But, CP3 CHAPTER V-2:1972 use quasi-static approach for simulate the dynamic behaviour of the structure.

- Turbulence length scale

  BS-EN 1991-1-4:2005AS/NZS 1170.2:2011 specified the turbulence length scale factor to account the turbulent effect of the fluid flow.

- Peak factor for the upwind velocity fluctuations

  AS/NZS 1170.2:2011 specified the peak factor value in straight. However, BS-EN1991-1-4:2005 provided an expression related with up-wind crossing (v) and averaging time for mean wind velocity (T).

- Peak factor for resonant response

  AS/NZS 1170.2:2011 specified the peak factor for resonant response related with natural frequency of vibration (1st mode). However, BS-EN1991-1-4:2005 provided two expressions to calculate the resonance response related with vibration modes.

- Background factor

  Both BSEN 1991-1-4:2005 and AS/NZS1170.2:2011 specified the background factor related with structure dimensions and turbulence length scale.

- Aerodynamic Influence- Pressure co-efficient (External)

  Aerodynamic influences are accounted by use of external pressure coefficient. CP3 CHAPTER V-2:1972, BS-EN1991-1-4:2005 directly specified the average pressure co-efficient factor and the local pressure co-efficient factors. However, AS/NZS 1170.2:2011 specified the aerodynamic shape factor with combination of several other factors such as external pressure co-efficient, area reduction factor, local pressure factor, porous cladding reduction factor etc.to account the other special effects also.

Therefore, both BS-EN1991-1-4:2005 with SLS EN 1991-1-4:2019 and AS/NZS 1170.2:2011 showed the similarities when calculating the dynamic component of the flow variables and the dynamic behaviour of the structure. But CP3 CHAPTER V-2:1972 used very simple method (quasi-static) for evaluating the dynamic performance.

5.2 Comparison of Along Wind Pressure Estimated on 31 Storey Apartment Building with Codes of Practice

Static based along wind pressure is calculated for the selected apartment building according to CP3 Chapter V – Part2:1972, BSEN 1991-1-4:2005 and AS/NZS 1170.2:2011.The calculation has been carried out for windward, leeward and side face of the Tower1 under two orthogonal wind directions as shown in Figure 5.1(a) and (b). The results are presented graphically in below Figures 5.2 to 5.4.

Wind directions

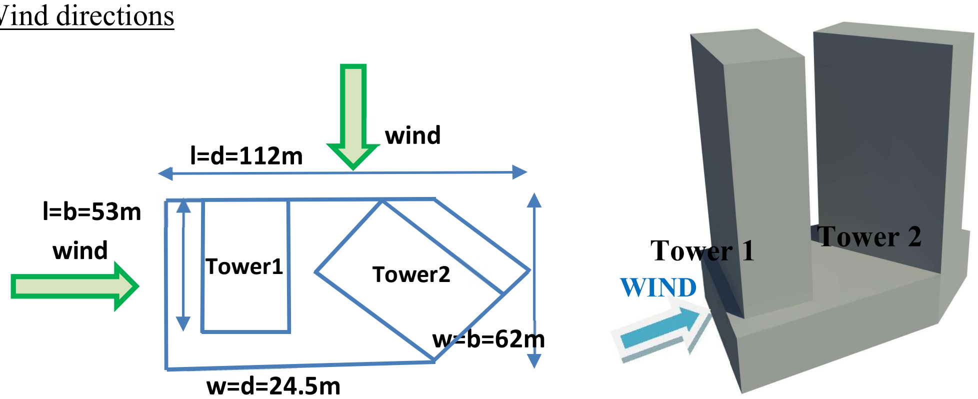

(a) (b)

Figure 5.1 (a) Wind directions (b) 3-D view

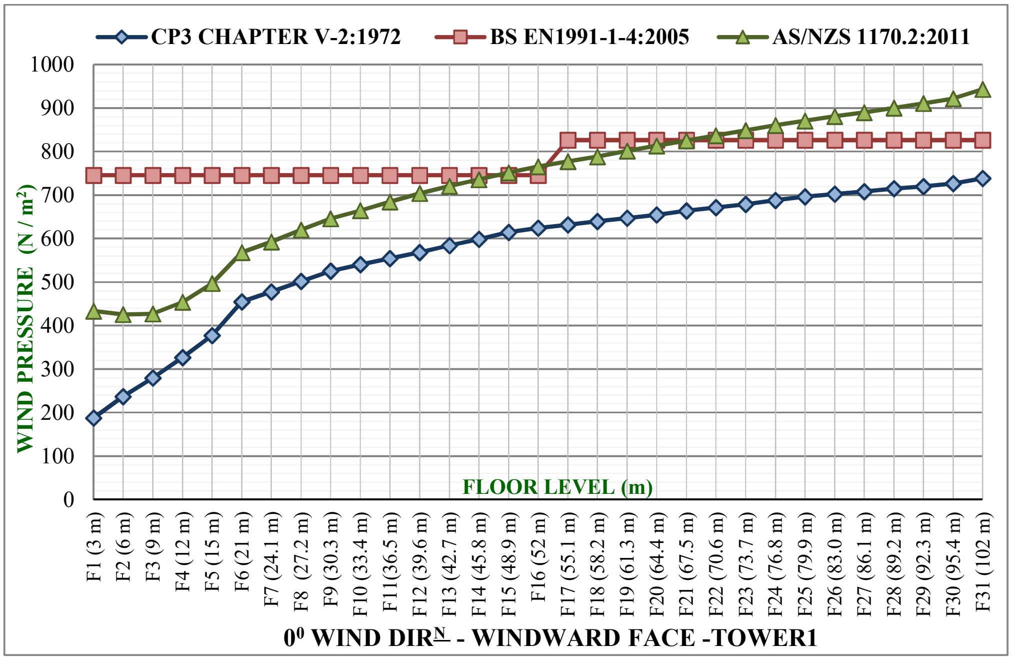

Figure 5.2 Along wind pressure variation on windward face-Tower-1

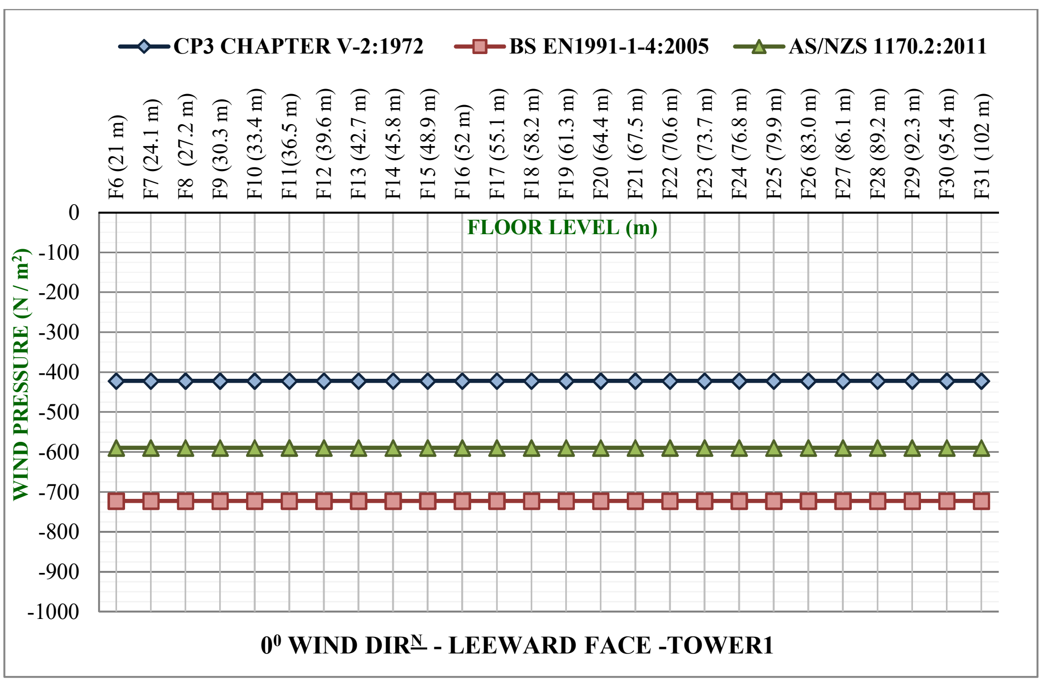

Figure 5.3 Along wind pressure variation on Leeward face-Tower1

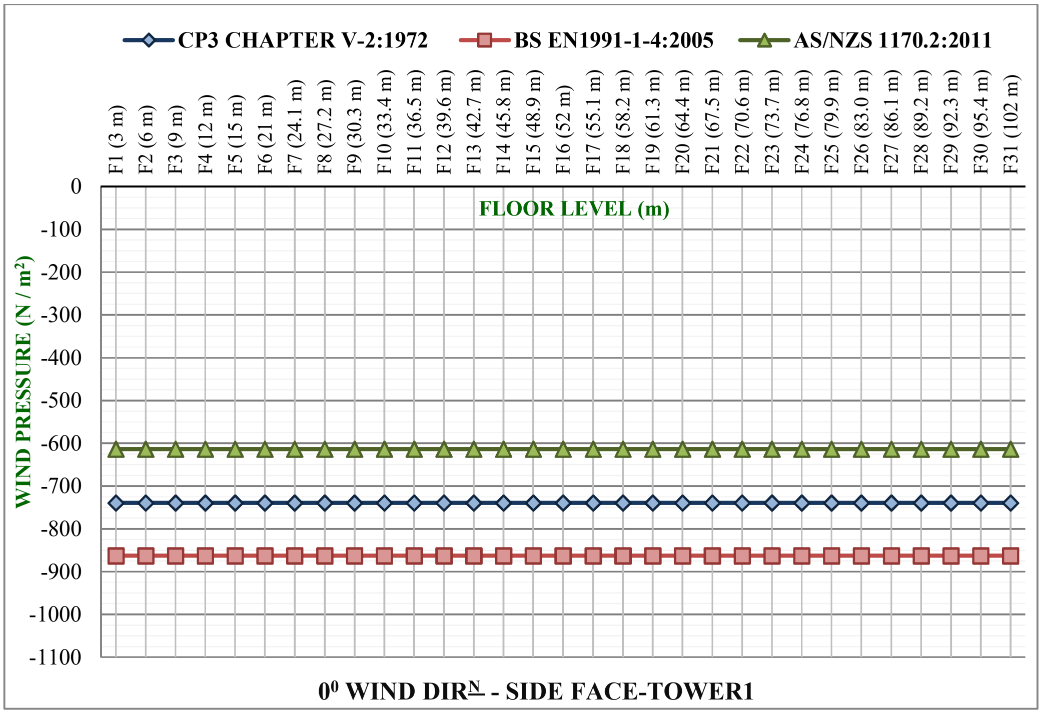

Figure 5.4 Along wind pressure variation on side face-Tower1

In Section 5.1, parametric study has been carried out for three different international wind codes to identify the commonalities and differences among them. Since different wind codes use different approaches to account the fluctuating flow variables, which cause to construct three different wind pressure distribution lines for the same building face. Therefore, compromising the dynamic effect by an “equivalent static force” or similar factor is much more important part in the wind loading codes.

Furthermore, it can be observed that the along wind pressure increases smoothly with the elevation of the building according to CP3 Chapter V – Part2:1972 and AS/NZS 1170.2:2011. However, in BS-EN1991-1-4:2005 the wind loads calculation procedure is built on the dividing by parts – rule, which makes the pressure distribution profile different. As shown in Figure 5.2 to,5.4 the along wind pressure is constant up to the height equal to b (b= 52m = width of the building face which perpendicular to 0^0wind direction) and then exhibits rapid increment in next floor level (F17 -55.1m)and again remains as constant for upper part of the building.

It can be observed that CP3 Chapter V – Part 2:1972 exhibits the lowest along wind pressure values for windward and leeward faces compared to other two wind loading codes. Percentage of pressure variation in BS-EN1991-1-4:2005 and AS/NZS 1170.2:2011 are calculated with respect to the pressures in CP3 Chapter V – Part2:1972 for the ease of reference.

Pressure value by BS EN or AS/NZS = x

Pressure value by CP3 Chapter V-2:1972 = y

$$Pressure\ variation\ = (\,x - y)\ /y\ * 100\%$$

Figure 5.2 shows the considerably higher pressure values in windward face calculated following AS/NZS 1170.2:2011 and BS-EN1991-1-4:2005 compared to CP3 Chapter V– Part2:1972 between the Floor levels 1 – 6. Furthermore, it is observed that the along wind pressure values of AS/NZS 1170.2:2011 on windward, leeward and side face increased by average of 24% (Floor level 7-31) and 39% and decreased by 17% respectively. In case of BS-EN1991-1-4:2005, the pressure values of windward, leeward and side face increased by average of 27% (Floor level 7-31), 42% and 17% in that order. The reason is that in BS-EN1991-1-4:2005 and AS/NZS 1170.2:2011 well apprise the dynamic phenomena (wind fluctuation and structure vibration) compared to CP3Chapetr V-2:1972.

Besides, BS-EN1991-1-4:2005 shows somewhat higher pressure values for windward ((Floor level 1-15), leeward and side face compared to AS/NZS 1170.2:2011 code. The pressure values on windward ((Floor level 1-15), leeward and side face calculated following BS-EN1991-1-4:2005 are greater by average of 30%, 22% and 40% compared to Australian code values (AS/NZS 1170.2:2011). One of the reason for that deviation is the dissimilarities in factors amongst the codes used for their calculation.

Wind in 90^0 direction

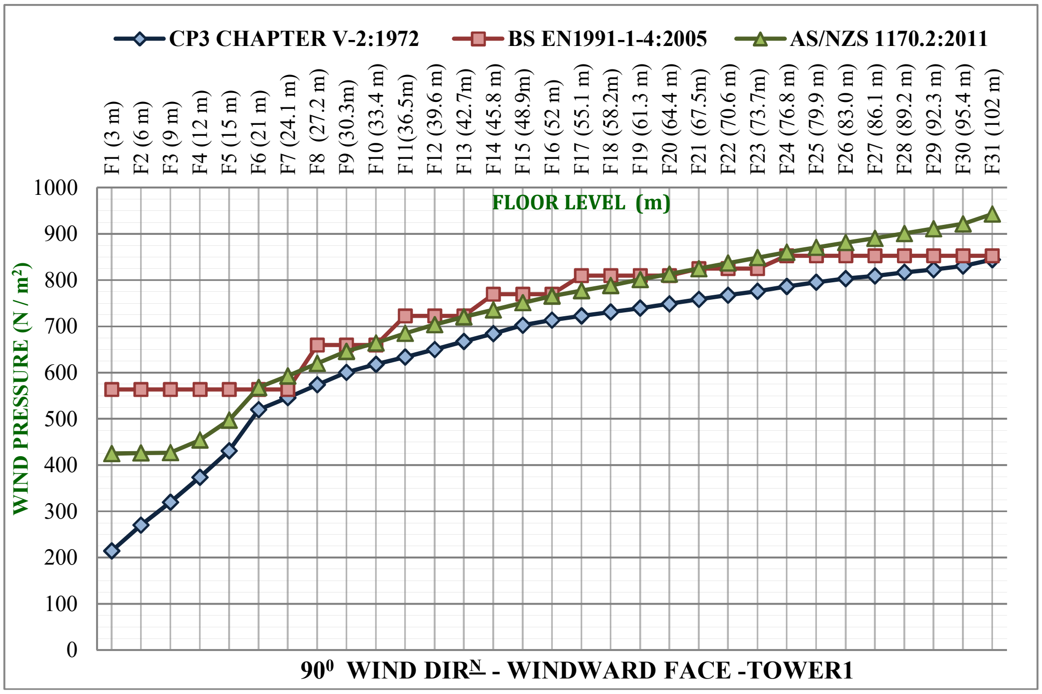

Figure 5.5 Along wind pressure variation on windward face –Tower1

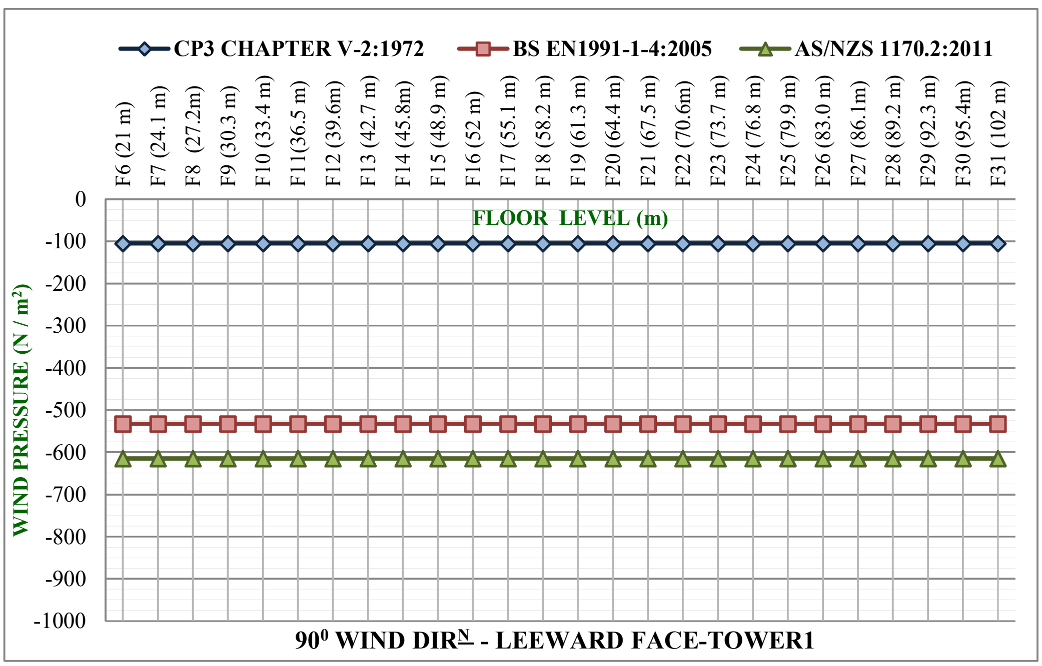

Figure 5.6 Along wind pressure variation on Leeward face –Tower1

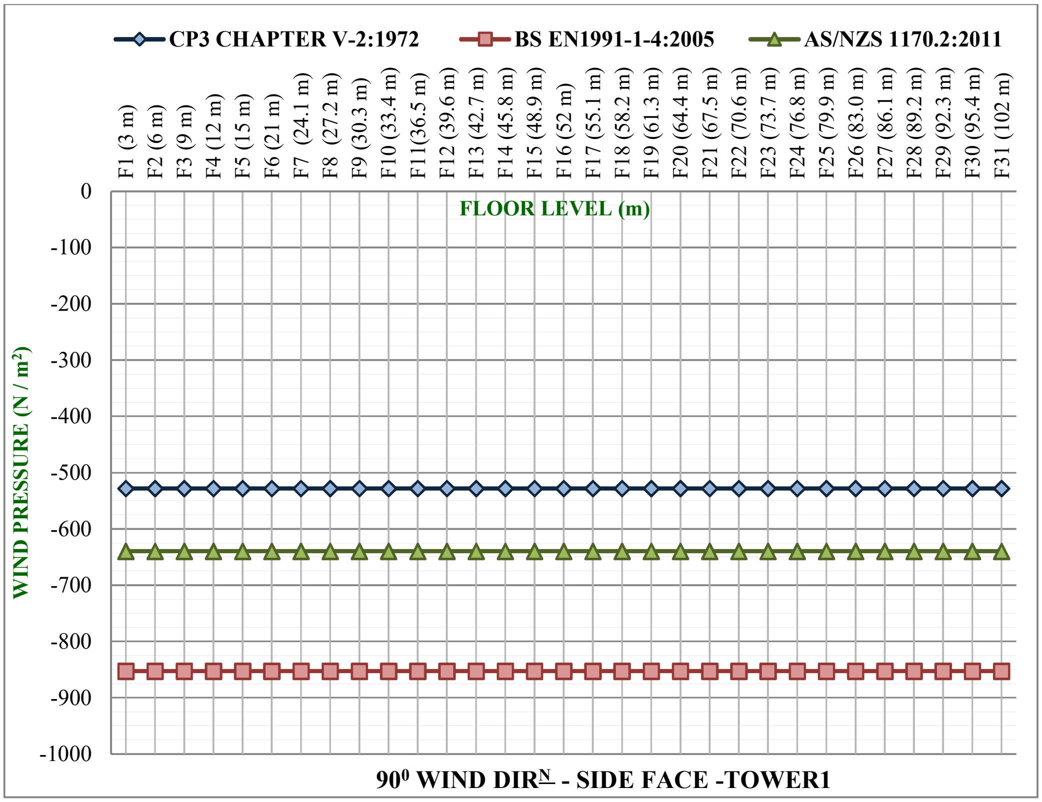

Figure 5.7 Along wind pressure variation on side face –Tower1

Figures 5.5 to 5.7 show the comparison of the along wind pressure distribution obtained from three different international wind codes on windward, leeward and side face respectively. In case of wind angle of 90^0, it can be observed that the similar wind distribution pattern as described in previous pages.

Similar to Figures 5.2, Figure 5.5 also shows the considerably higher pressure values in windward face obtained from BS-EN1991-1-4:2005 and AS/NZS 1170.2:2011 compared to CP3 Chapter V– Part2:1972 between the Floor levels 1 – 6. In addition, it is observed that the along wind pressure values of AS/NZS 1170.2:2011 on windward and side face increased by average of 8% (Floor level 7-31) and 17% respectively. In case of BS-EN1991-1-4:2005, the pressure values of windward and side face are higher by average of 8% (Floor level 7-31), 62% in that order. However, in case of leeward pressure distribution, pressure values by BS-EN1991-1-4:2005 and AS/NZS 1170.2:2011 are 4.8 times and 4 times higher than the CP3 Chapter V– Part2:1972 values. This is caused mainly due to much low pressure coefficient (-0.1) specified for leeward face in the code of CP3 Chapter V– Part2:1972 compared to Australian wind loading code. In CP3 Chapter V– Part2:1972 specified the external pressure co-efficient relating with the building dimensions such as height to width ratio (h/w) and the length to width ratio (l/w) of the building. Furthermore, it is observed that if the width of the building face which perpendicular to wind flow direction is having lesser horizontal dimension compared to other one (1.5 < l/w <4) the leeward face is experiencing the much lower suction according to CP3 Chapter V– Part 2:1972. However, it is important to revisit and revise such factors with the support of experimental works and numerical simulations.

Similar to 0^0 wind direction, BS-EN1991-1-4:2005 shows somewhat higher pressure values for windward ((Floor level 1-16) and side face compared to AS/NZS 1170.2:2011 code. The pressure values of windward and side face by BS-EN1991-1-4:2005 are greater by average of 10%, 33% compared to Australian code values (AS/NZS 1170.2:2011). However, in case of leeward, Australian code values are 13% lesser than the BS EN code values. The same reasoning mentioned for 0^0 wind angle are applicable for the deviation here as well.

5.3 Wind Flow Patterns around the Building

Numerical Simulation has been carried out for the same building using two way-coupling method and S-A turbulent models available in ABAQUS software. Same wind flow directions has been considered here as well. Inflow velocity profile has been obtained according to the wind loading codes. Results are summarised and presented graphically in below Chapters.

As described in Section 2.2.1, different wind flow patterns such as near wake flow, turbulence wake, horse-vortex system, flow separation, reverse flow, reattachment of the flow are observed around the building (Figures 5.8, 5.9 and 5.10).

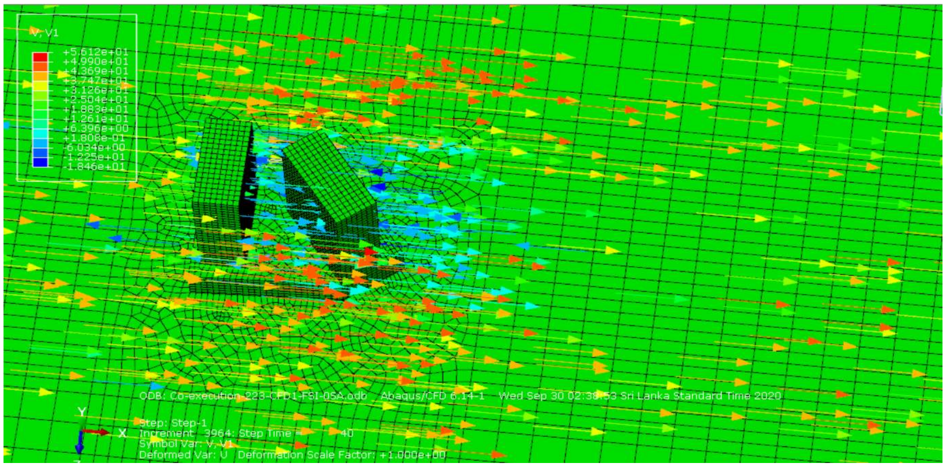

Figure 5.8 Velocity field around the building – V1

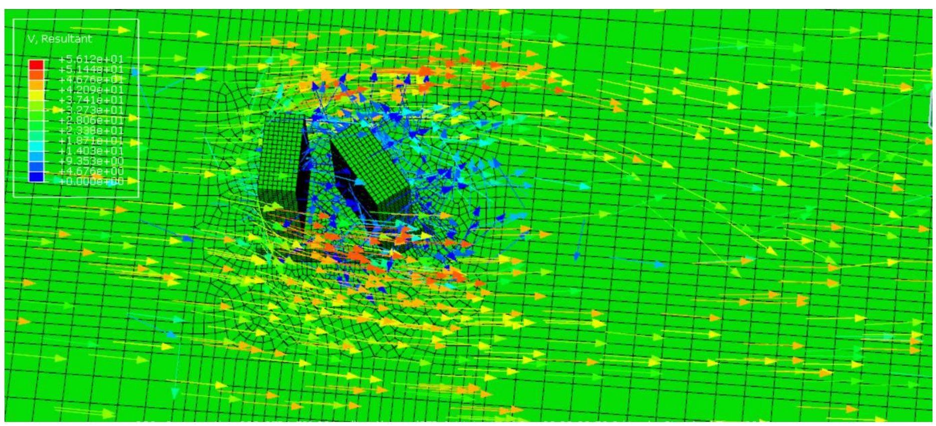

Figure 5.9 Different wind flow pattern around the building

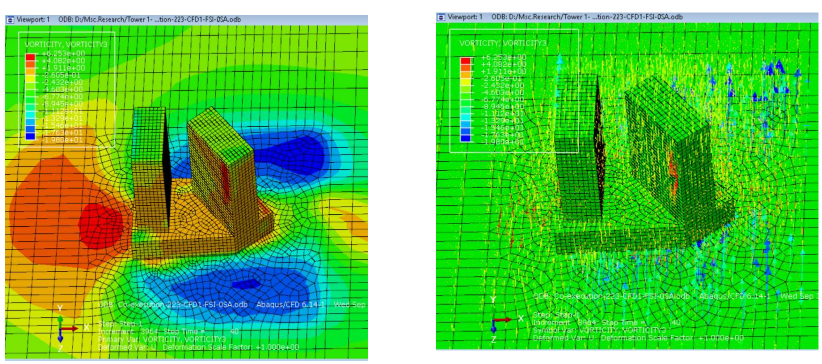

Figure 5.10 Vorticity (vorticity 3) around the building

5.4 Wind Loads on the Building

As described in Chapter 1.1, with the increment of wind velocity, wind pressure on the building increases proportionally with the square of the mean wind velocity ($P \alpha V^2$). However, the pressure varies dynamically with respect to the degree of shielding provided by other buildings and topographical features. Therefore, in this case study, the resulting wind load on the structure is observed throughout the period of 0 - 40 second to in order to check whether the structure undergoes on a static effect or dynamic effect by the wind.

Therefore, few points along the structure height are selected to observe the fluctuations of along wind and crosswind forces with the time.

5.4.1 Wind loads on the structure - 0^0 wind direction (AS/NZS 1170.2:2011)

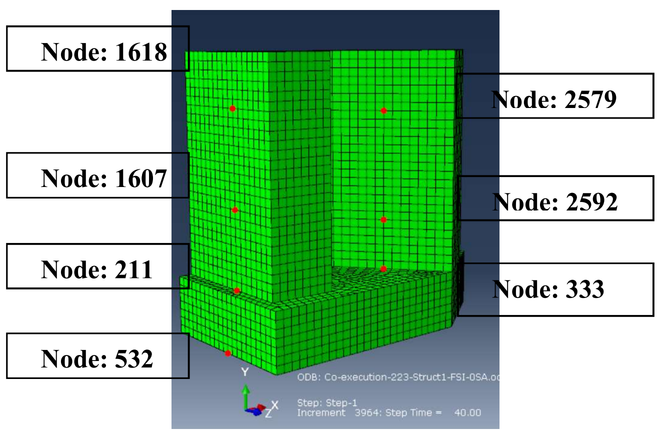

Figure 5.11 Force measured nodes –Tower 1 and 2

As shown in Figure 5.11, few nodes are chosen to observe the variation of forces with the time.

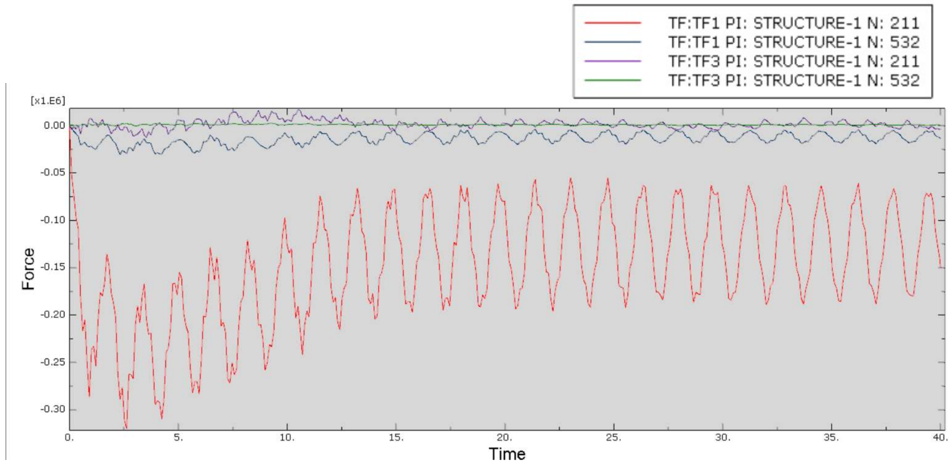

Figure 5.12 Along wind (TF1) and crosswind force (TF3)-Tower 1 –Lower part

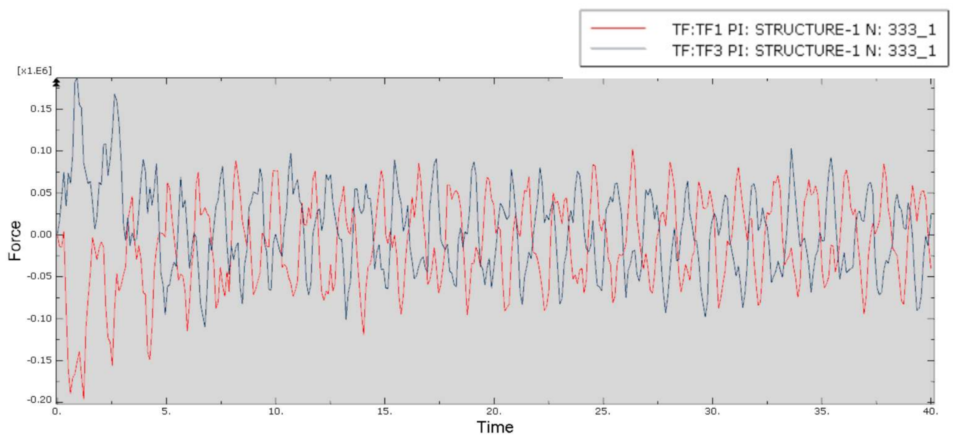

Figure 5.13 Along wind (TF1) and crosswind (TF3) force -Tower 2 –Lower part

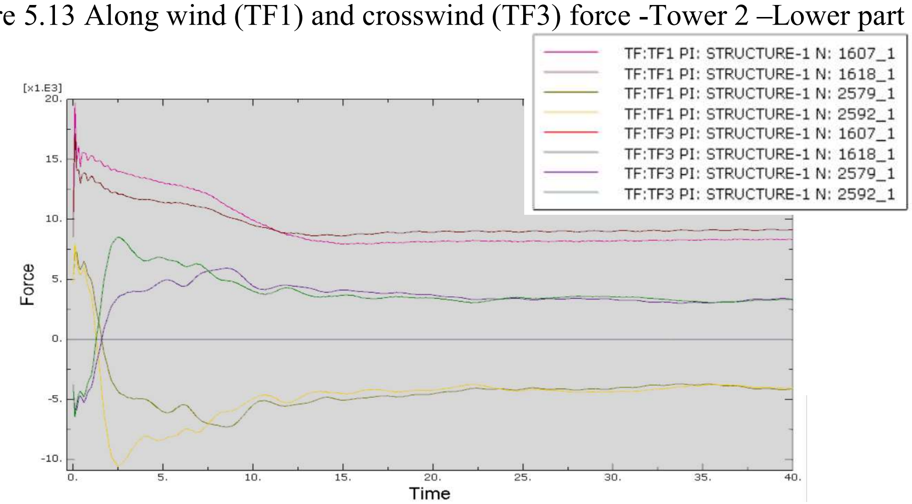

Figure 5.14 Along wind (TF1) and crosswind (TF3) force – Tower 1 and 2 –Upper part

As shown in Figure 5.12 and 5.13, the lower part (0-21 m) of the structure experiences the dynamic loading. Additionally, Tower 2 undergoes both along wind and crosswind forces compared to Tower 1. Gustiness or turbulent characteristics of the wind is one of the reason for the dynamic load at the lower part. However, the gustiness decreases with the height and it remains constant after gradient height. Therefore, at the upper part of both Towers experience static loads as shown in Figure 5.14.

5.4.2 Wind loads on the structure - 90^0 wind direction (AS/NZS 1170.2:2011)

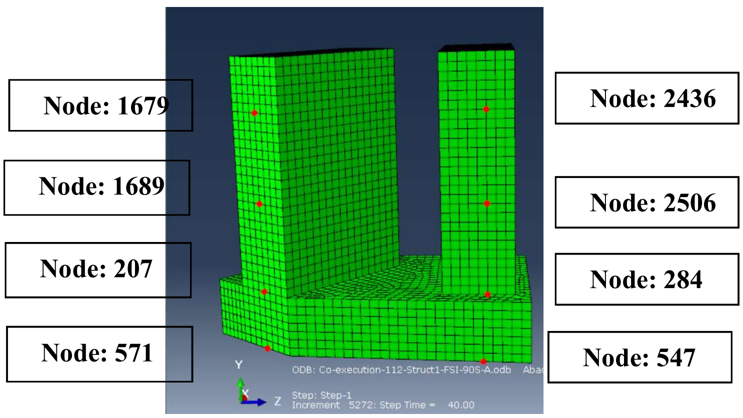

Figure 5.15 Force measured nodes –Tower 1 & Tower 2

Similarly, few nodes are chosen from the 90^0 building configuration to observe the variation of forces with the time. (Figure 5.15)

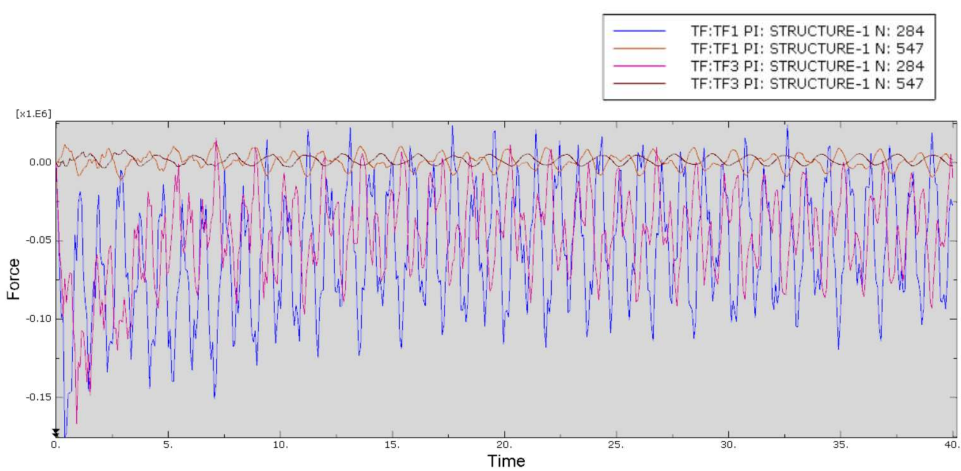

Figure 5.16 Along wind (TF1) and crosswind (TF3) force -Tower 1 –Lower part

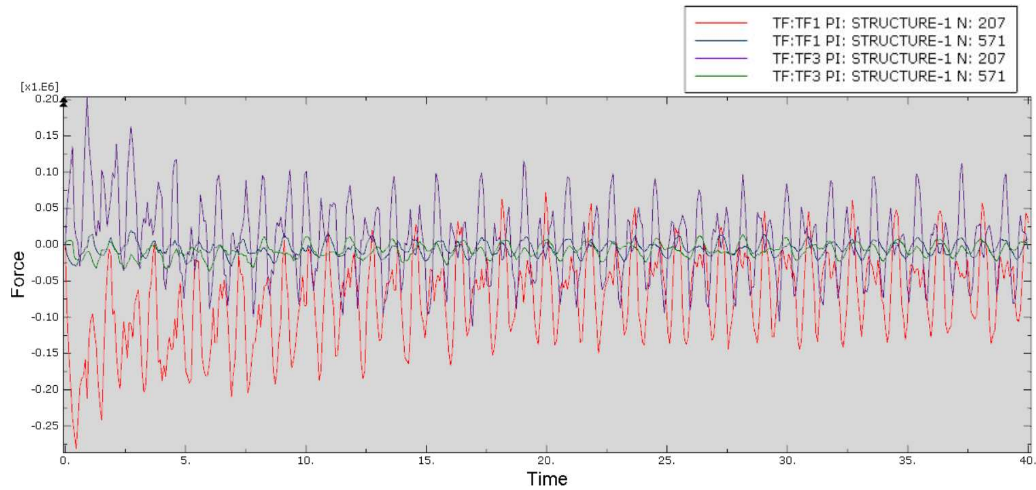

Figure 5.17 Along wind (TF1) and crosswind (TF3) force –Tower 2- Lower part

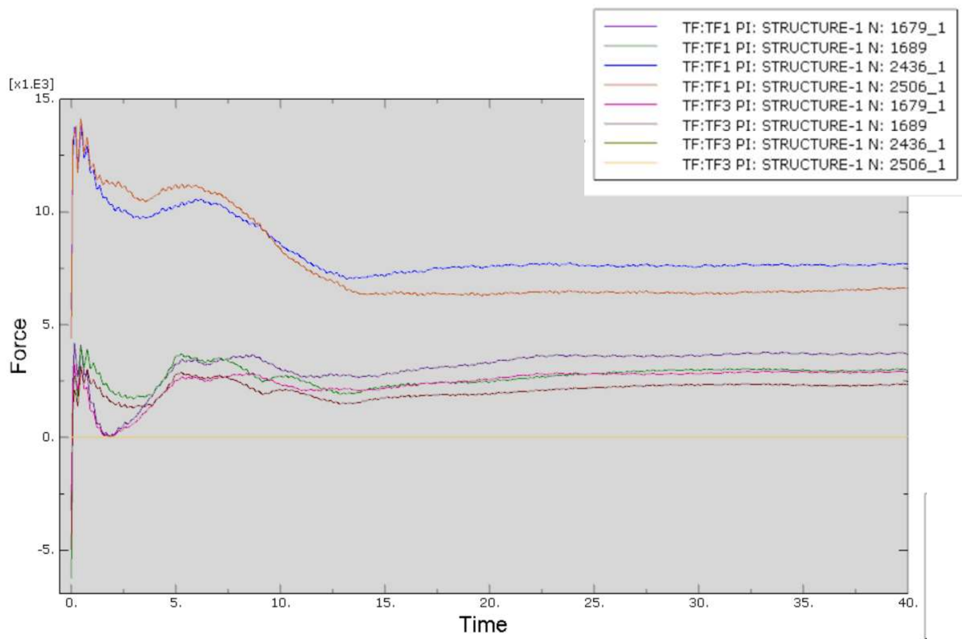

Figure 5.18 Along wind (TF1) and crosswind (TF3) force – Tower 1 and 2 –Upper part

Similar to Chapter 5.4.1, the lower part (0-21 m) of the structure experiences the dynamic loading (Figures 5.16 and 5.17). Particularly, Tower 1 and 2 undergoes both along wind and crosswind forces. Gustiness or turbulent characteristics of the wind is one of the reason for the dynamic load at the lower part. However, the gustiness decreases with the height and it remains constant after gradient height. Therefore, at the upper part of both Towers experience static loads as shown in Figure 5.18.

5.5 Building Performance under Wind Action (wind-induced vibration)

5.5.1 Displacement of the structure - 0^0 wind direction (AS/NZS 1170.2:2011)

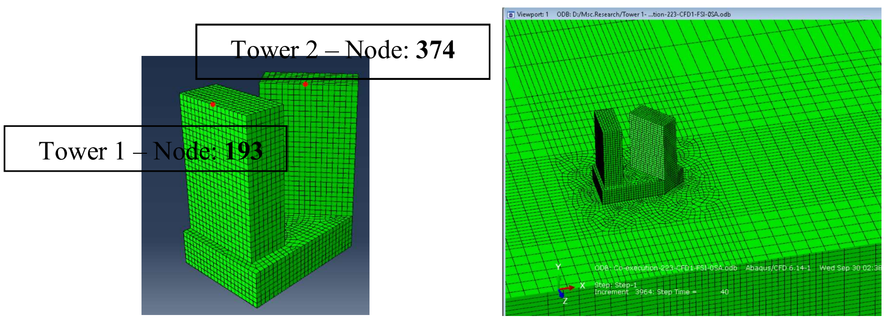

Figure 5.19 Displacement measured nodes & building configuration

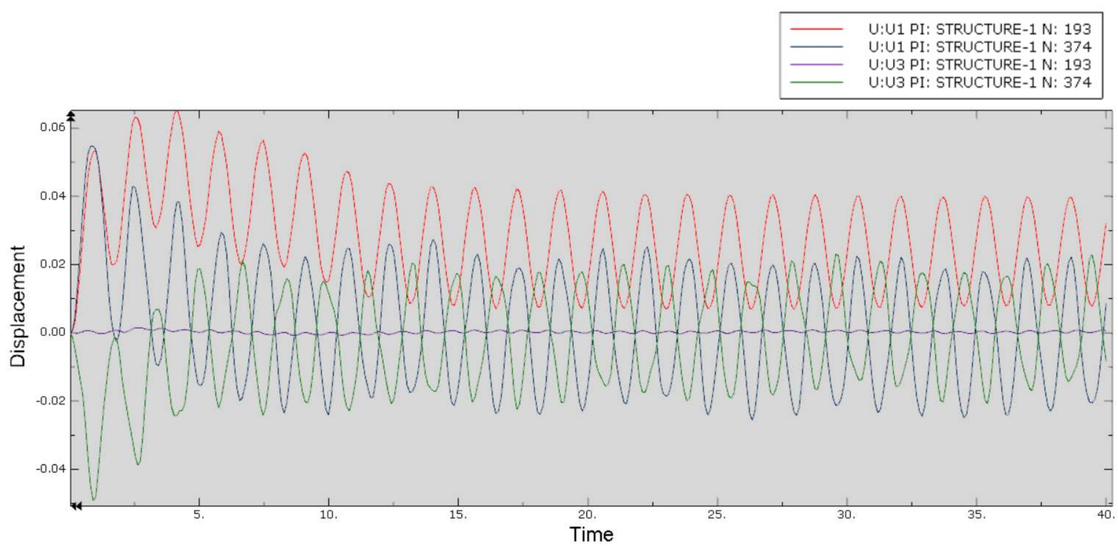

Figure 5.20 Displacement graph for U1 (X dir$^{\underline{n}}$) and U3 (Z dir$^{\underline{n}}$) (units – m , sec)

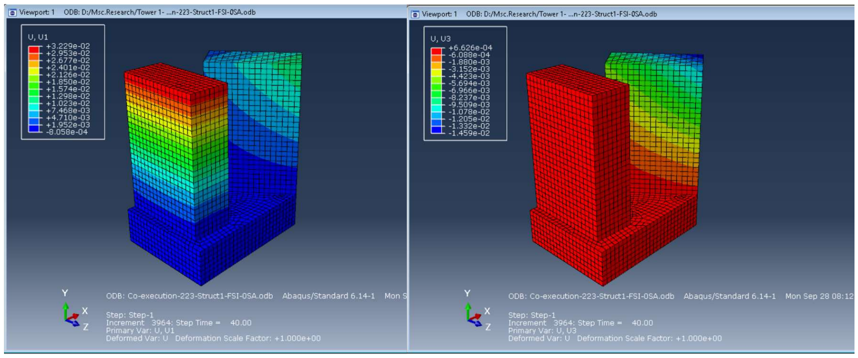

Figure 5.21 Displacement - U1 (X dir^{n}) and U3 (Z dir^{n})

Figure 5.20 illustrates the displacement of Tower 1 (Top node -193) and Tower 2 (Top node - 374) with the time. As shown in Figures 5.20 and 5.21, Tower 1 oscillated only for the along wind direction (red line) and hit the maximum of 40 mm. Nevertheless, displacement of the Tower 1 in crosswind direction (purple line) is negligible. However, Tower 2 vibrated in a sinusoidal manner and the displacement components are in both along wind (blue line) and crosswind (green line) directions. The maximum displacements for U1 (x direction) and U3 (z direction) are 27 mm and 22 mm. Moreover, displacement of the Tower 2 is lesser than the Tower 1 in order to shielding effect from the Tower 1 against the wind loadings. Generally, configuration of the Tower 2 (approximately 30^{0} angle) subjected to the direction of the wind flow may cause to have the vibration components in both directions. Vortices development especially around the Tower 2 may be another reason for its vibration in crosswind direction (Figure 5.10).

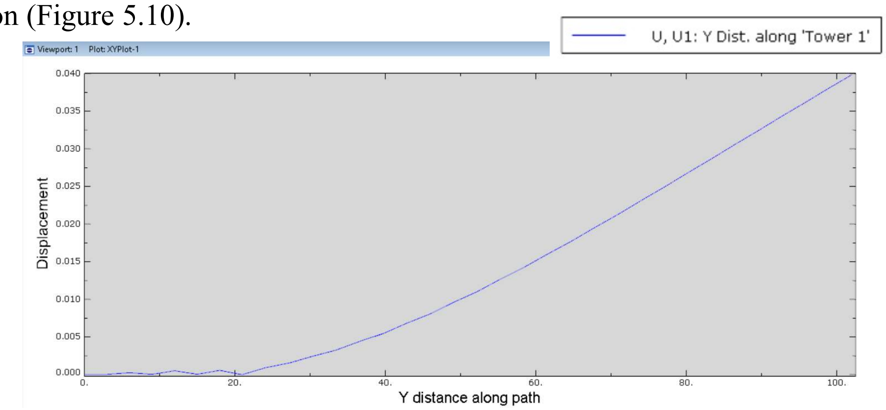

Figure 5.22 Displacement –Tower1 - U1 (X dir^{n})

5.5.2 Displacement along the Structure Height -Tower 1

Figure 5.22 illustrates the deflection of the Tower 1, which is considered for the wind pressure comparison. It is observed that the deflection of the structure up to 21m height is negligible due to its geometry. From 21m height where the building is separated in to two Towers, deflection of the Tower 1 gradually increased and ended up in 40mm.

5.5.3 Displacement of the structure- 90^0 wind direction (AS/NZS 1170.2:2011)

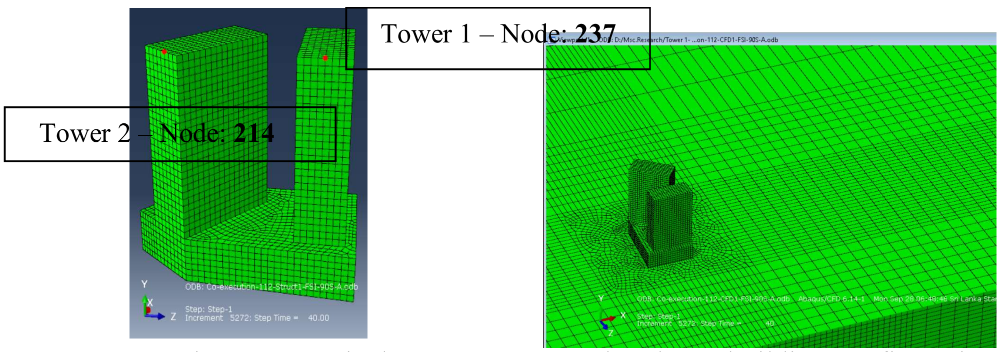

Figure 5.23 Displacement measured nodes & building configuration

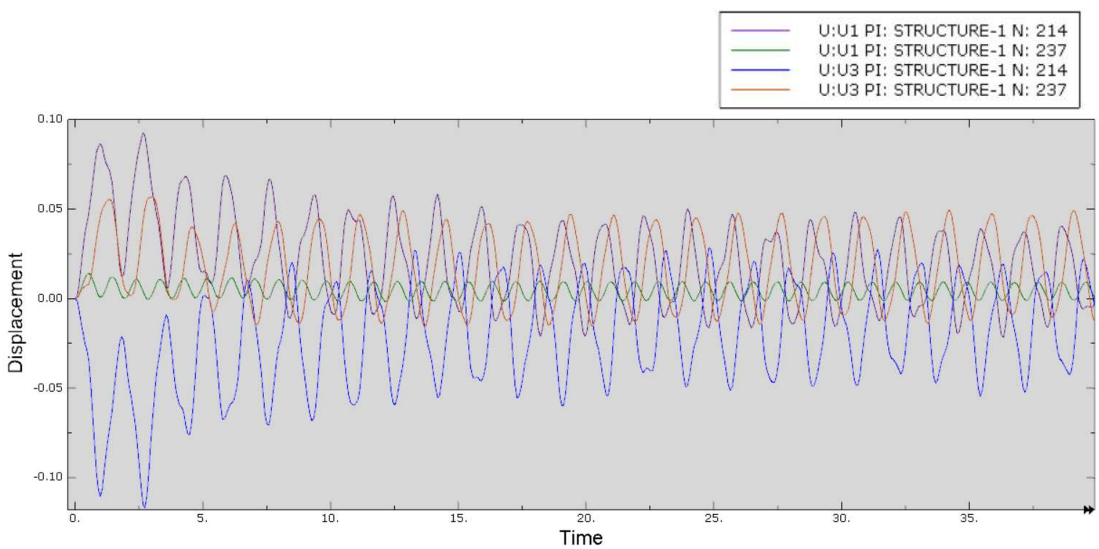

Figure 5.24 Displacement graph for U1 (X dir^n) and U3 (Z dir^n) (units – m , sec)

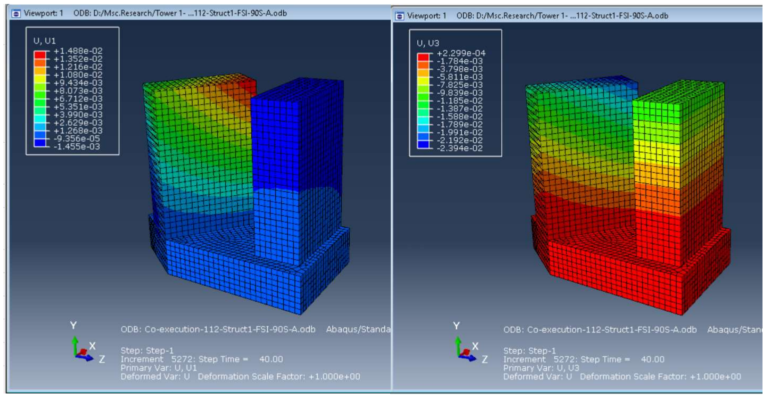

Figure 5.25 Displacement graph for U1 (X dir$^{\underline{n}}$) and U3 (Z dir$^{\underline{n}}$) (units – m , sec)

Figure 5.24 illustrates the displacement of Tower 1 (Top node -237) and Tower 2 (Top node 214) with the time. As shown in Figures 5.24 and 5.25, Tower 1 vibrated mainly in crosswind direction (brown line) and hit the maximum of 48 mm. Nevertheless, Tower 1 showed narrow band motion in along wind direction (green line) and the displacement is much lower (7 mm) compared to crosswind direction. The main reason for the vibration caused in crosswind direction is vortex shedding.

When the wind runs into a tall building, it separates in to two streams along the side of the building. In general, it creates the vortices along each side faces, which are identical in shape and size. However, in this case study different magnitudes of the vortices occurred in the opposite sides as shown in Figure 5.26 (b). Therefore, vortices, which are stronger than the other side, force the Tower 1 to sway to the other side. The tower 1 sways back to its original position and beyond by virtue of its elasticity. Then, succeeding vortices cause to push Tower 1 further to the opposite side. However, in this case study, oscillation continued due to the differences in wind pressure along the opposite side of the Tower 1 as shown in Figure 5.26 (a). As anticipated, negative pressure occurred one side face of Tower1, conversely, positive pressure occurred the opposite side, where the Tower 2 exists. Therefore, the Tower 1 continued to sway in the direction perpendicular to wind's main stream.

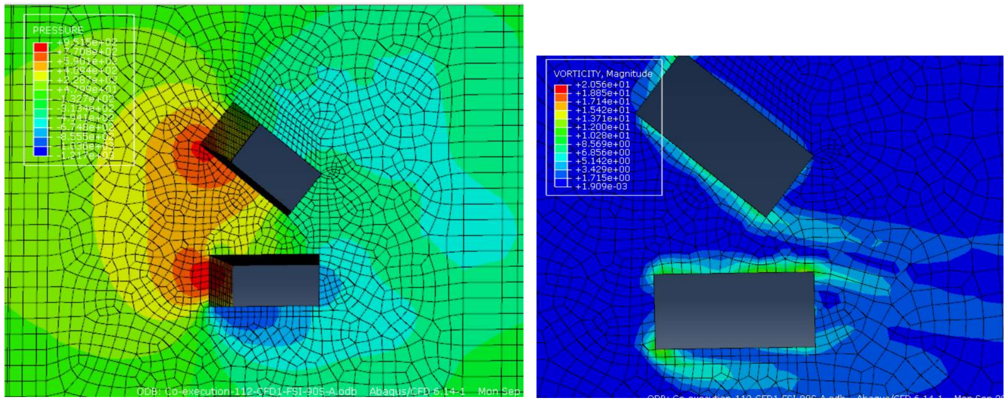

(a) (b)

Figure 5.26 (a) Wind pressure variation around the structure (b) vortices around Tower 1

In case of Tower 2, it vibrated in a sinusoidal manner and the displacement components are in both along wind (purple line) and crosswind (blue line) directions. The maximum displacements for U1 (x direction) and U3 (z direction) are 45 mm and 54 mm. Generally, configuration of the building (approximately 30^0) with the wind direction may cause to have vibration components in both directions. In addition, vortices development around the Tower 2 may cause for its vibration in crosswind direction (Figure 5.24).

5.5.4 Displacement along the structure height - Tower 1

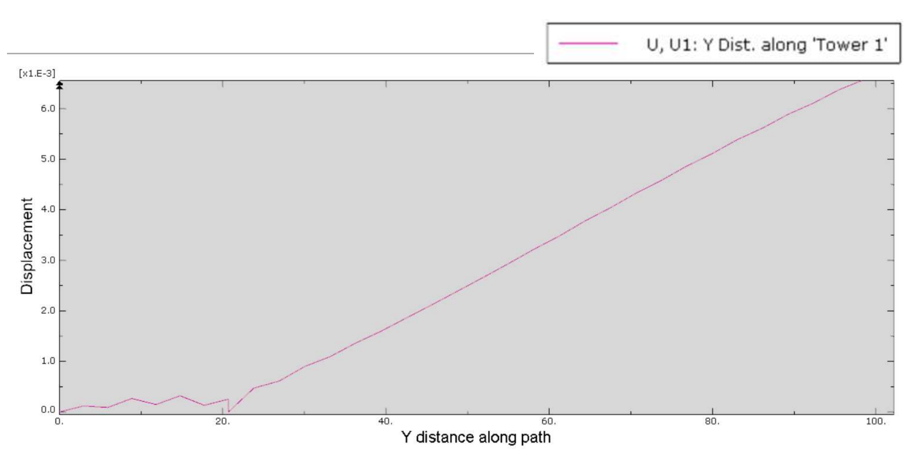

Figure 5.27 Displacement–Tower1 - U1 (X dir^{n})

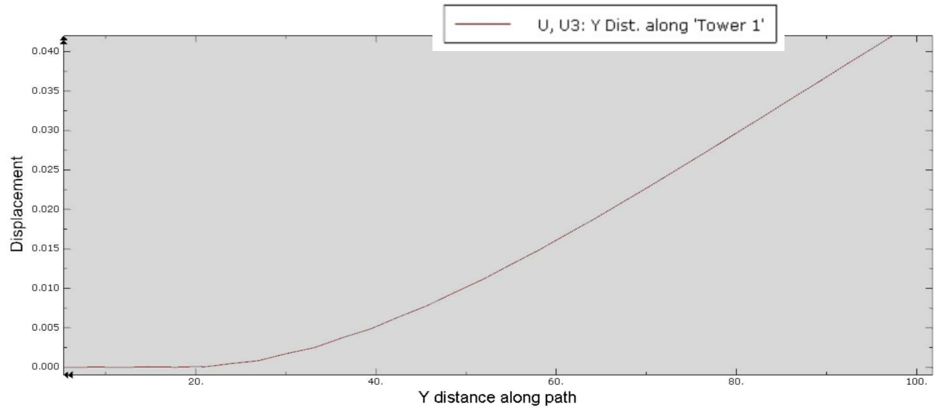

Figure 5.28 Displacement–Tower1 – U3 (Z dir$^{\underline{n}}$)

Figures 5.27 and 5.28 illustrate the deflection of the Tower 1 in U1 (along wind) U3 (crosswind) directions. It is observed that the deflection of the structure up to 21 m height is negligible due to its geometry. From 21m height where the building is separated in to two Towers, deflection of the Tower 1 gradually increased and it behaves as a freestanding cantilever beam.

5.6 Comparison of Along Wind Pressure Results

Figures 5.29 (a) and (b) show the 0^0 along wind pressure in S-A turbulent model on windward, side wall and leeward respectively.

<u>0^0 Wind direction - CP3 CHAPTER V-2:1972</u>

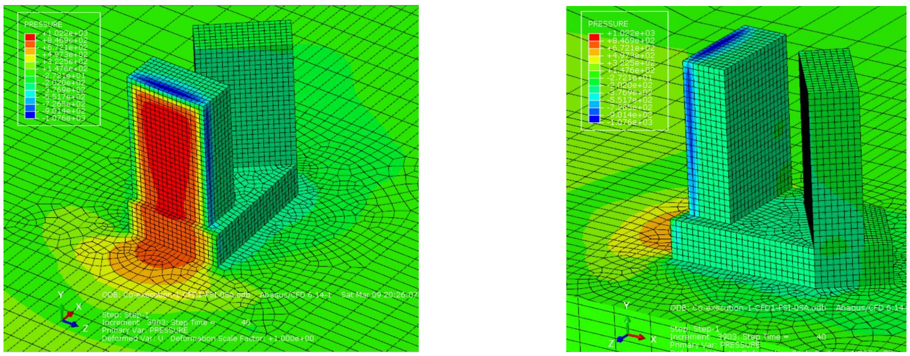

(a) (b)

Figure 5.29 S-A - 0^0 along wind pressure on (a) windward and side wall (b) leeward

<u>Wind in 90^0 direction</u>

Figures 5.30 (a) and (b) show the 90^0 along wind pressure in S-A model on windward, side wall and leeward respectively.

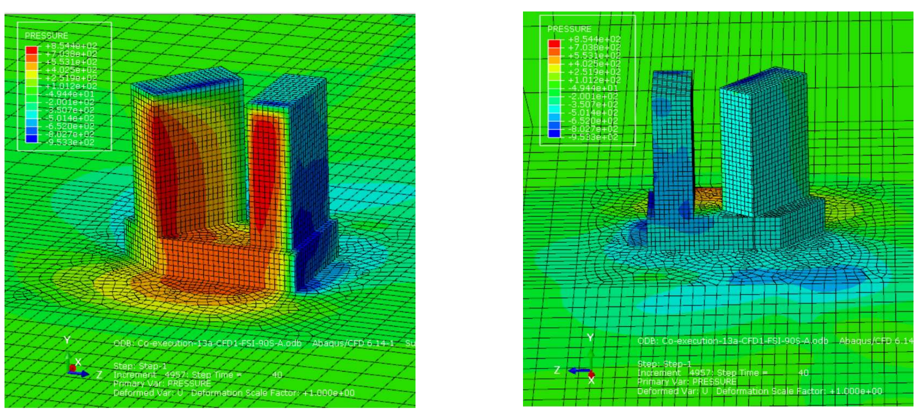

(a) (b)

Figure 5.30 S-A - 90^0 along wind pressure on (a) windward and side face (b) leeward

Wind in 0^0 direction - CP3 CHAPTER V-2:1972

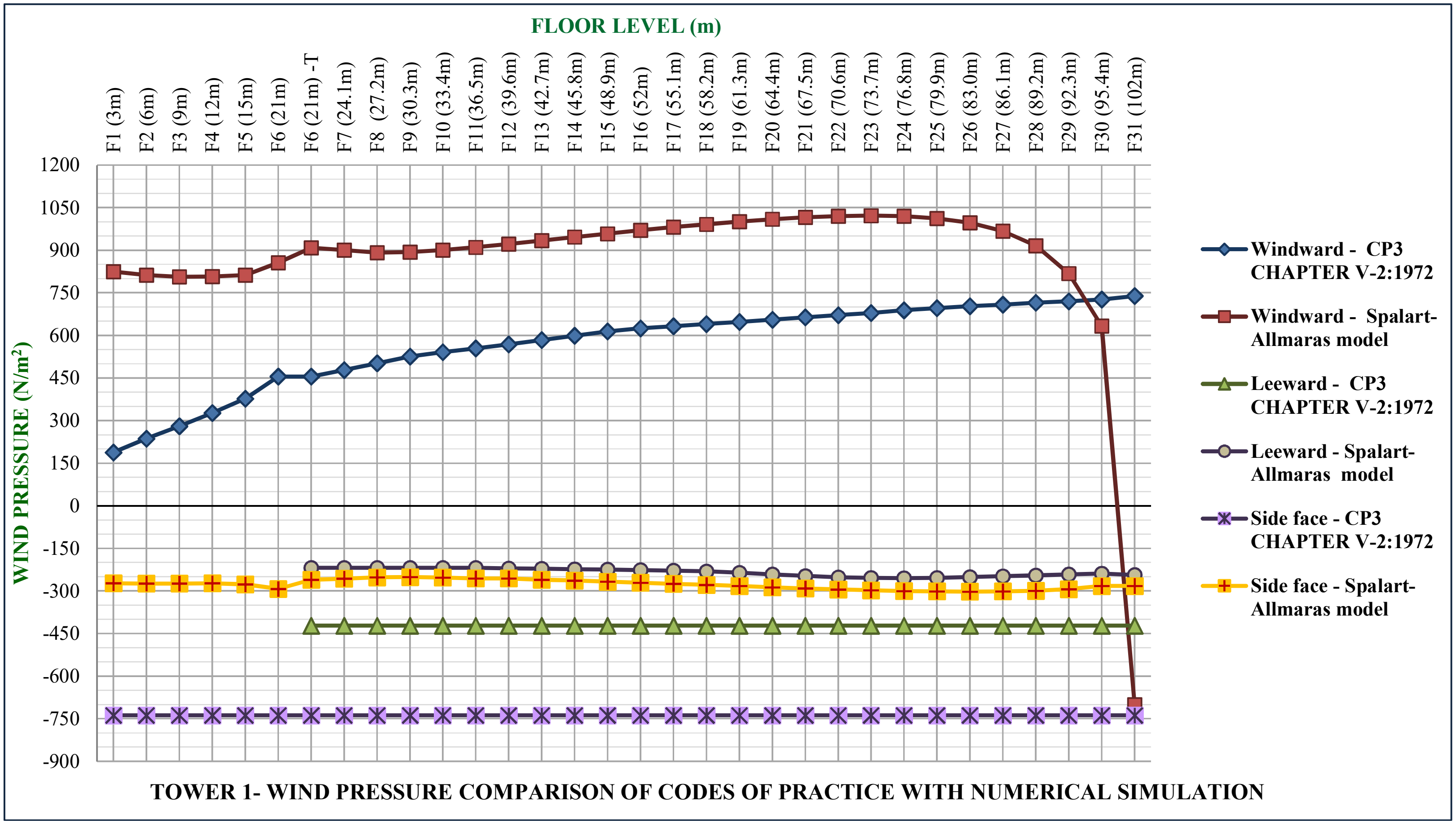

Figure 5.31 0^0Wind pressure comparison of CP3 Chapter V-2:1972 with CFD model

Wind in 90^0 direction - CP3 CHAPTER V-2:1972

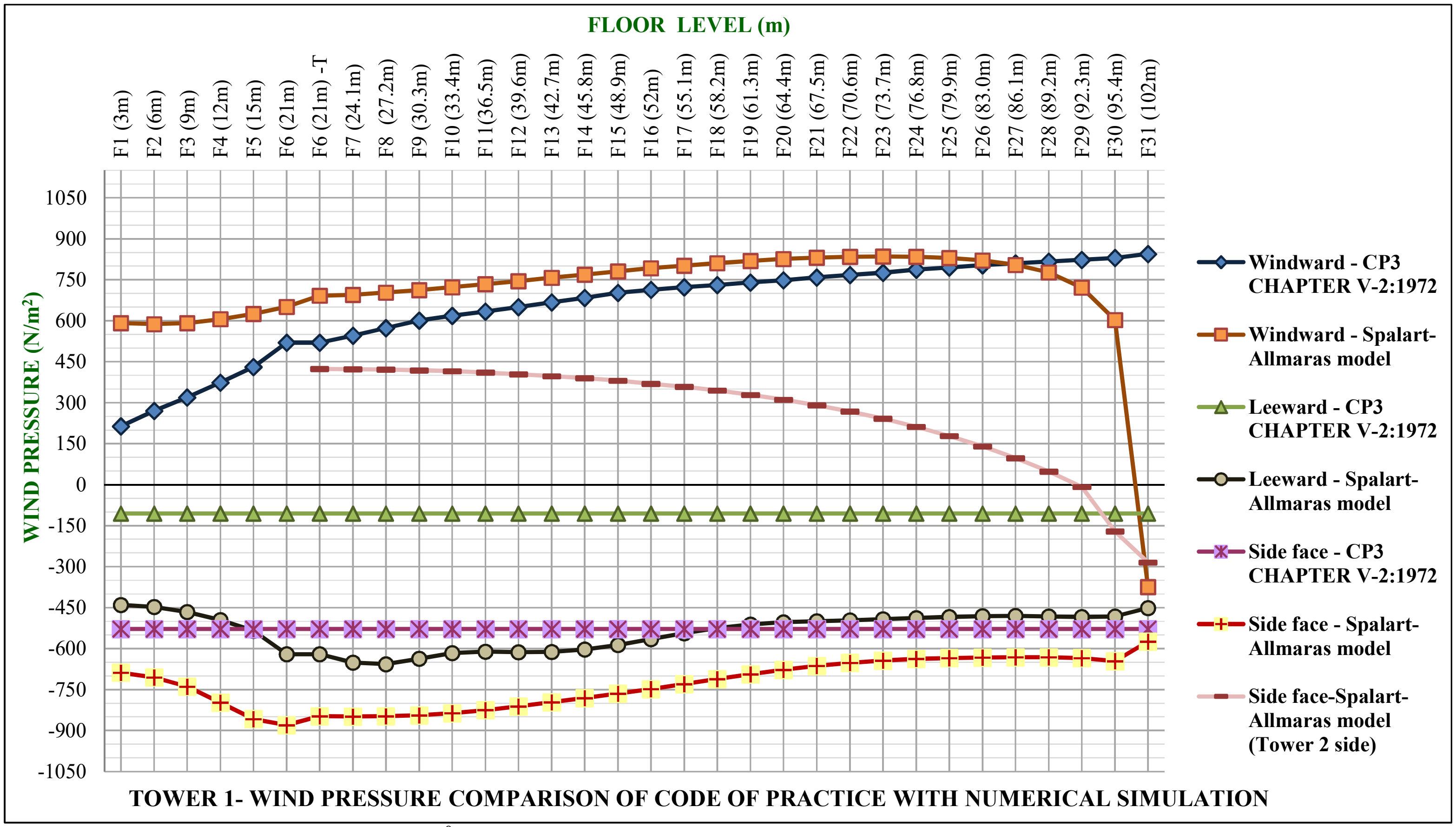

Figure 5.32 90^0 Wind pressure comparison of CP3 Chapter V-2:1972 with CFD model

Wind in 0^0 direction - BS-EN1991-1-4:2005

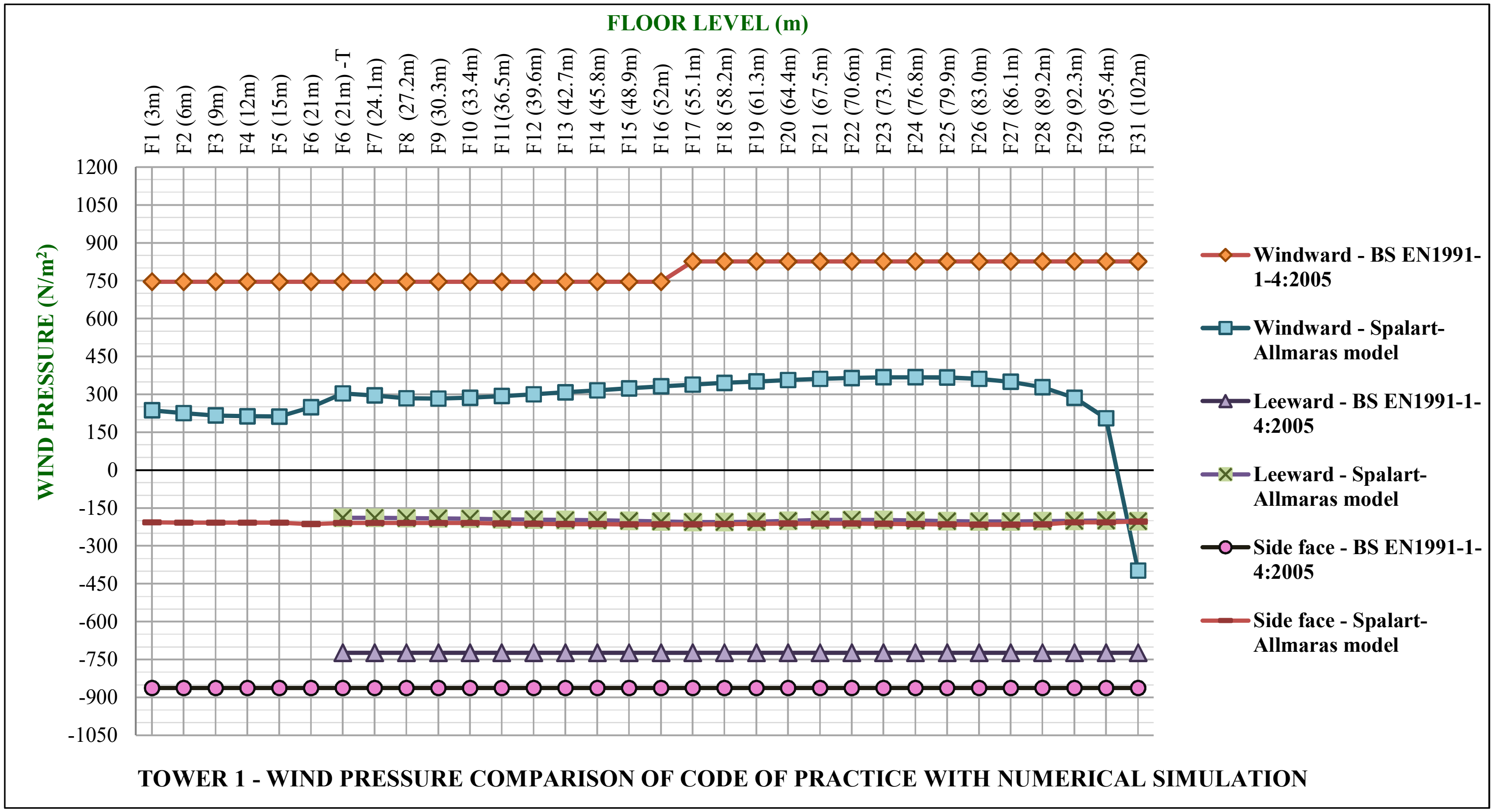

Figure 5.33 0^0Wind pressure comparison of BS EN 1991-1-4:2005 with CFD model

Wind in 0^0 direction - BS-EN1991-1-4:2005

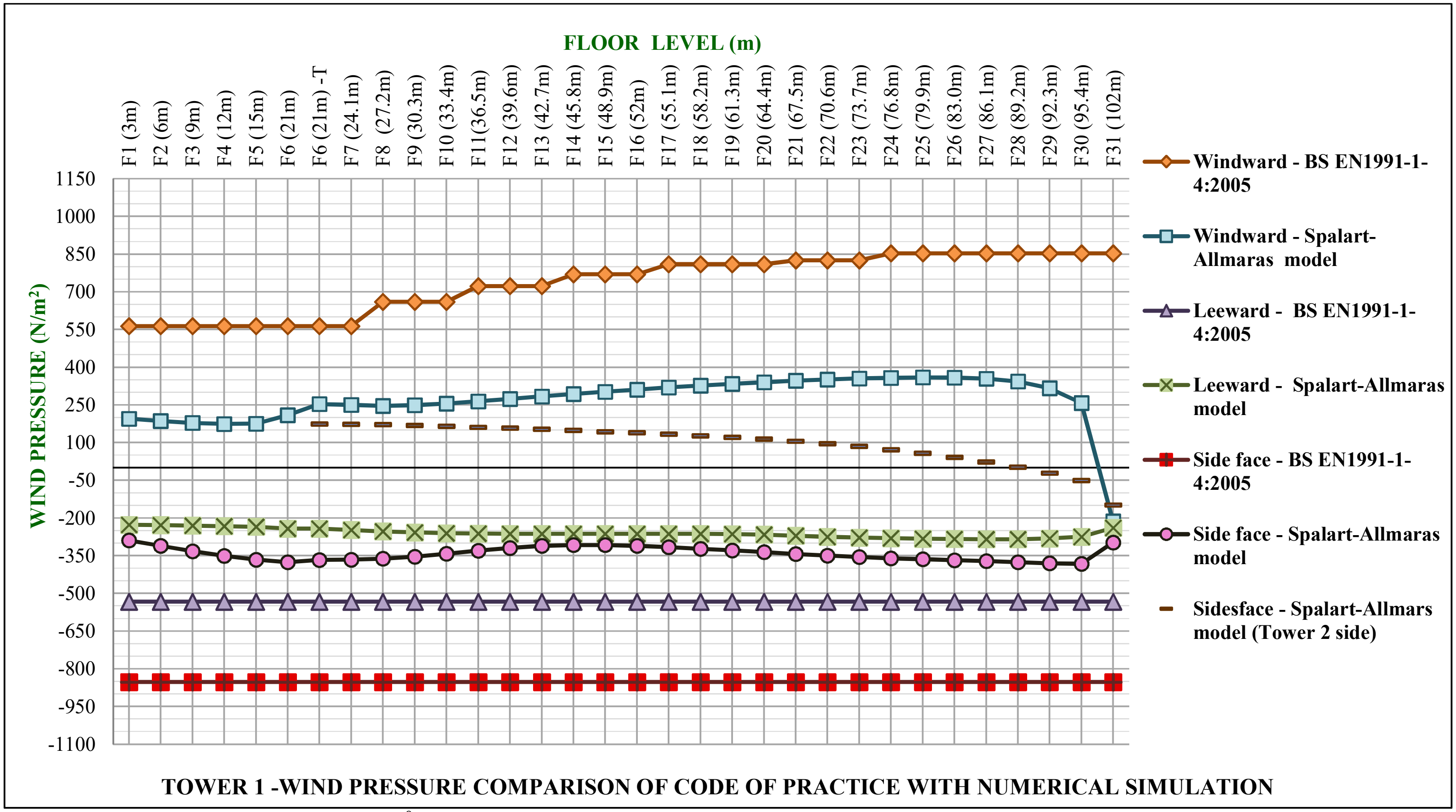

Figure 5.34 90^0Wind pressure comparison of BS EN 1991-1-4:2005 with CFD model

Wind in 0^0 direction - AS/NZS 1170.2:2011

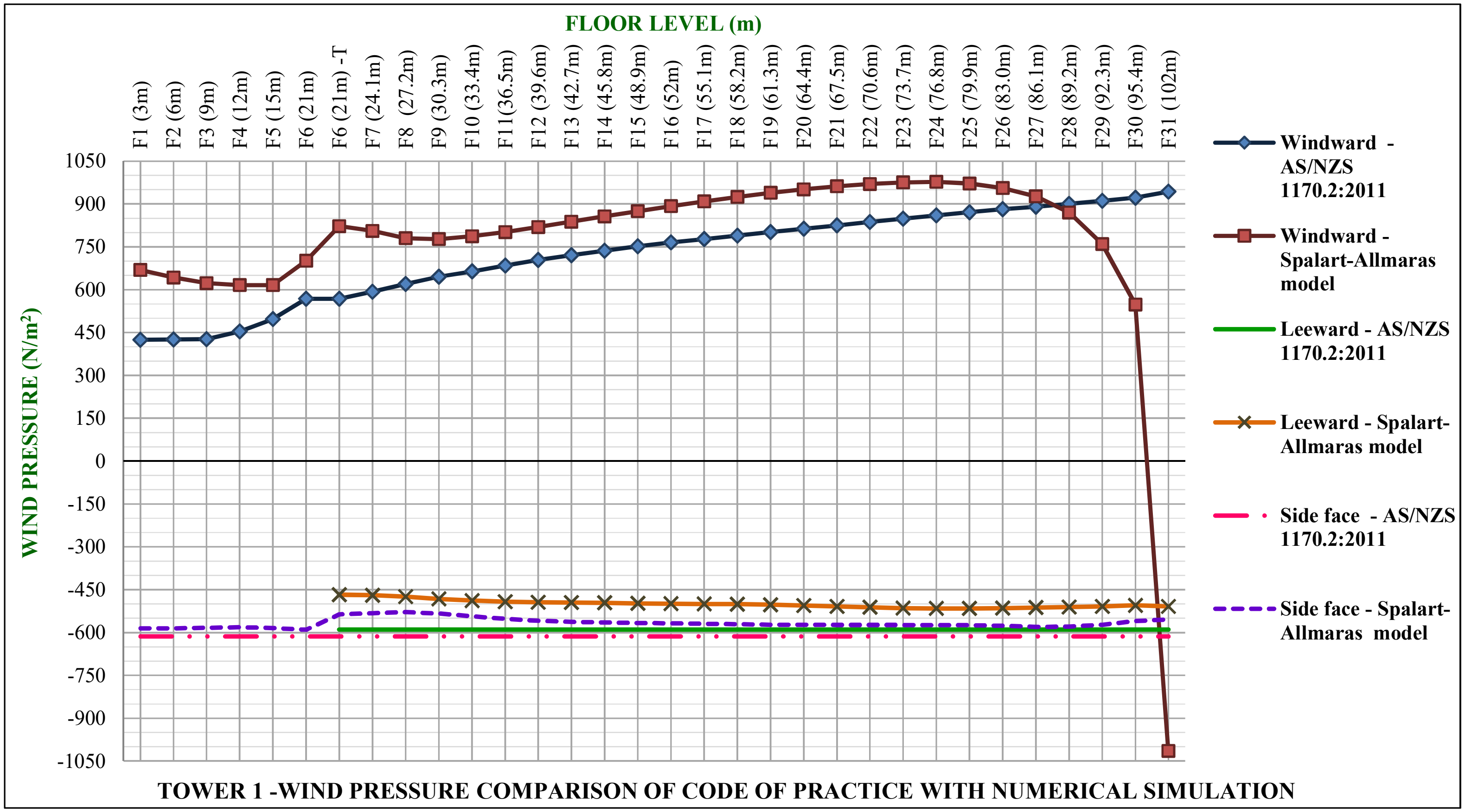

Figure 5.35 0^0Wind pressure comparison of AS/NZS 1170.2:2011 with CFD model

Wind in 90^0 direction - AS/NZS 1170.2:2011

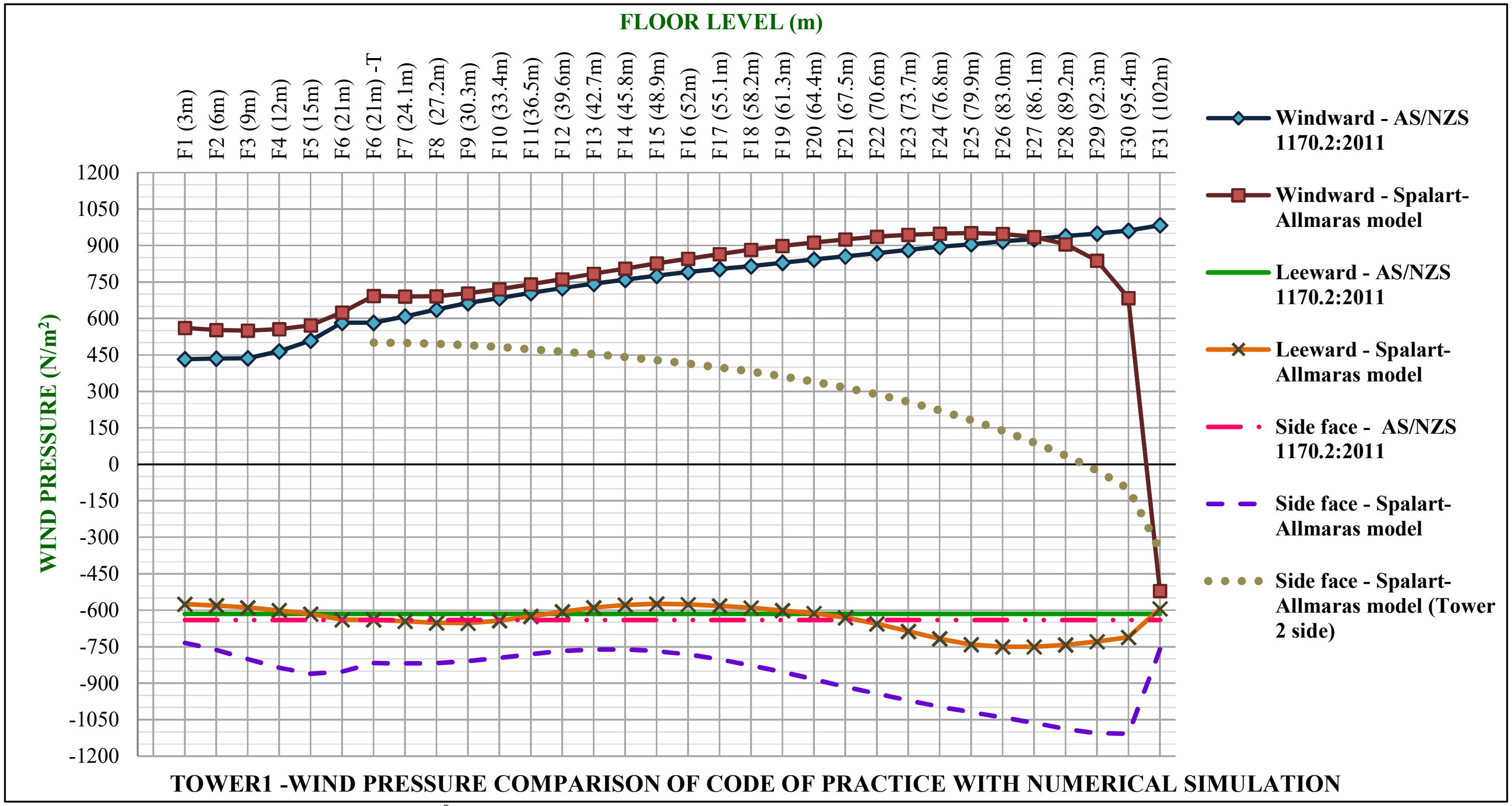

Figure 5.36 90^0Wind pressure comparison of AS/NZS 1170.2:2011 with CFD model

Based on the comparison between manual calculation and the simulation results for wind in 0^0 and 90^0 directions, the following conclusions can be drawn.

Evaluating the numerical simulation results obtained for all three wind loading codes, it is observed that the windward pressure reached its maximum at the 2/3 rd of the Tower1 (floor level 24 -76.8m -4/3 rd of the total building height) as shown in Figures 5.31, 5.32, 5.33, 5.34, 5.35 and 5.36. Then, windward pressure started to decline and ended up with higher negative value (suction) at the top of the building (close to Floor 31). This is caused mainly due to the layer separation of the wind flow at and around the top of the building. However, according to the wind loading code calculations, maximum pressure occurs at the top of the building. Also, it is observed that the computed values on leeward and side faces in 0^0 wind angle are fairly constant with the height of the building in S-A turbulent model. However, two difference wind pressures are observed the opposite side faces of the Tower 1. As anticipated, negative pressure occurred one side face of Tower1, conversely, positive pressure occurred the opposite side, where the Tower 2 exists as shown in Figures 5.32, 5.34 and 5.36. Furthermore, it is observed that the Tower 2 is shielded from the Tower 1 in 0^0 wind direction.

CP3 CHAPTER V-2:1978

As shown in Figures 5.31 and 5.32, numerical simulation results for windward pressure show always higher value than the manual calculations between the floors 1 to 6. This is caused mainly due to edge effect, building irregularities and the downdraught effect. Furthermore, similar sort of outcome is shown from the computed results obtained by BS-EN1991-1-4:2005 and AS/NZS 1170.2:2011 codes as well (Figure 5.33, 5.34, 5.35 and 5.36). “Downdraught” effect causes when the wind hits on an obstacle and then it tries to move up, down and around the obstacle. As a result, wind speed at ground level increases and eventually higher pressure occurs at the lower portion of the building. Besides, building irregularities (at 6^{th} floor) such as projecting out is caused to have a localized turbulence. Turbulence causes to speed-up the wind, and then increases the wind pressure in particular area of the building. In addition, simulation results clearly shows rapid increment of the windward pressure at the location where the Tower 1 has started to rise up independently (21 m height - at the starting level of Tower1). Edge effect is the reason for this.

0^0 wind direction

Figure 5.31 illustrates that the computed results show always higher value than the manual calculation between the floor levels 7 to 29. The simulation results increased by average of 54% than the manual calculations. It is observed that the aforementioned percentages are significantly higher, and cannot be simply neglected. As described in Section 2.2.4.2, CP 3 Chapter V-Part2:1972 uses the quasi-static method to evaluate the wind loadings on a building. The quasi-static approach is built on the assumption that the inertia force is negligible. Even though, quasi-static approach considers an equivalent additional static force to compensate the dynamic behavior of the structure, which is not adequate to get accurate solutions. Figure 5.31 reflects this phenomenon very well. Therefore, this method is usually failed to evaluate the wind flow variables such as buffeting characteristics, gustiness due to its extremely simplicity.

Conversely, it is observed that the simulation results on leeward and side face for S-A turbulent models show significantly lesser pressure values than the manual calculations according to Figure 5.31. Computed results on leeward and side face shows average of 44% and 62% lesser pressure values compared to values in code of practice.

90^0 wind direction

In case of 90^0 wind direction, simulation results increased by average of 12% than the manual calculation (Figure 5.32). Variation of the simulation results with the values in code of practice is less compared to 0^0 wind direction configuration. Shorter dimension of the building placed perpendicular to the wind direction might be the reason for this less variation. In addition, building configuration (both Towers are facing to the wind direction) to the wind direction may cause to have less variation.

However, leeward and side face pressure graphs (Figure 5.32) reflect the complexity of the velocity flow field behind the tower 1 varying with building height. Therefore, computed results on leeward faces for numerical models show extremely strengthen negative pressure value compared to the manual calculation. The negative pressure increased at the lower part of the building and it gradually reduced with the height of the building. Gustiness or turbulent characteristics of the wind is one of the reason for the higher negative pressure at the lower part. However, the gustiness decreases with the height and it remains constant after gradient height. Therefore, it is evident that the results obtained by simulation are able to show the gust effect at the lower part of the building. However, computed values in leeward face are approximately 4 times higher than the values obtained by code of practice. Similarly, simulation results for side face at the upper part (floors 12-30)) shows average of 30% respectively. Moreover, the computed value show average of 53% increment compared to manual calculation at the lower part of the building due to gust effect.

The reason for the extreme negative pressure values is the presence of the surrounding structures (Tower 2) and resulting complex flow interference due to “channelling” and wake effects on the Tower1 (Figure 5.38). Figure 5.37 illustrates the instantaneous vorticity formation, which indicates the development of flow vortices caused by the flow separations at sharp corners of the buildings. This effect is not accounted by the manual calculation. Furthermore, Tower 1 experiences localized turbulences due to the presence of adjacent building, Tower 2. Because, Tower 2 added an additional roughness effect to the environment compared with an isolated tower condition. However, negative pressure value reduced with the height of the building due to the reduction of the turbulent intensity.

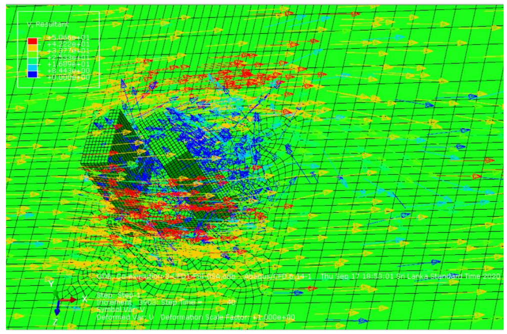

Figure 5.37 Complex velocity field behind the Tower 1- CP 3 Chapter V-Part2:1972

In general, numerical simulation results (S-A turbulent model) shows significant deviation with the manual calculations obtained by CP 3 Chapter V-Part2:1972. Finally, the study concludes that the CP3 Chapter V-Part2:1972 is incapable of evaluating the building-wind environment accurately.

BS-EN1991-1-4:2005

0^0 wind direction

In this case, it is observed that the S-A simulation results for all the building faces as shown in Figure 6.33 show lesser pressure values compared to calculation obtained by code of practice. The computed values on windward face show average of 61% reduction compared to the manual calculations. As well, values obtained by code of practice for leeward and side face are approximately 3.6 times and 4 times higher than the computed results

90^0 wind direction

Similar to above, it is observed that the S-A simulation results show lesser pressure values on all the faces compared with manual calculation. The computed values on windward face show average of 61% reduction compared to the manual calculations.

Moreover, it is observed that the values obtained by code of practice for leeward and side face are approximately 2.0 times and 2.5 times higher than the computed results.

AS/NZS 1170.2:2011

0^0 wind direction

As shown in Figure 5.35, it is observed that the maximum windward pressure in S-A model (971 N/m^2) well agreed with the maximum pressure in manual calculation. (943N/m^2) .However, it is observed that the computed results on windward face for both turbulent models increased by average of 12 % compared to manual calculations between the floors 7-30.

However, it is observed that pressures in leeward and side face show almost constant value along the structure height (Figure 5.35).The computed values on leeward and side face show average of 15% and 8% reduction compared to values obtained by codes of practice.

90^0 wind direction

Similar to above, the maximum windward pressure value in S-A models (951 N/m^2) showed bit of lesser value compared to the manual calculation. (983N/m^2) .However, it is observed that the computed results on windward face increased by average of 5% than the manual calculation between the floor levels 7 to floor level 29 (Figure 5.36).

However, pressure graphs for leeward and side face (Figure 5.36) reflect the complexity of the velocity and vortices formation around the Tower 1. Therefore, computed results are not followed the straight line as previous. However, simulation results in leeside at lower part varied within the range of +4% and -4%. But, in upper part (Floor 21-30) computed values increased by average of 15%. However, simulation results for side face showed considerably higher value (negative value) than the manual calculation. Computed results increased by average of 36% than the manual calculation.

The reason for this is the presence of the surrounding structures (Tower 2).Therefore, the facts described in Chapter 5.6 - CP3 Chapter V-2:1972 for 90^0 wind direction are applicable for this as well.

In general, it is observed that manual calculation obtained by CP 3 Chapter V Part 2:1972 showed always lesser values compared to numerical results. Because, CP 3 Chapter V-2:1972, quasi-static method is used to calculate the wind loadings on a building as described in section 2.2.4.2. Even though the code states that, the applicable height limit for a building is up to 200 m, the quasi-static approach is not suitable for evaluating the wind loads on tall buildings. For the reason that, the quasi-static approach is built on the assumption that, the inertia force is negligible. If the load is gradually applied on the structure, the structure undergoes gentle deformation resulting the zero inertia force. However, the medium and high-rise buildings are experiencing the dynamic effect (local turbulences, vortices) induced by the wind. Hence, the structure tends to vibrate and the inertia force cannot be negligible. Even though the quasi-static approach considers an additional static force to calculate the dynamic component, it is evident that the simulation results are able to show the incompetence of CP3 Chapter V-Part2:1972 for assessing the fluctuating component of fluid properties and dynamic behavior of the structure.

In BS-EN1991-1-4:2005, S-A turbulent models demonstrated noticeably low-pressure values in all the cases. As described in Chapter 2.2.5.1, term 'Reynolds Stresses' was defined as a function of mean flow variables in RANS approach. Therefore, all the fluctuating flow variables are being calculated based on the mean flow variables as velocity, pressure etc. In BS-EN1991-1-4:2005, velocity profile is based on the 10 minutes wind velocity. Hence, it will lead to underestimate the total wind pressure (mean + fluctuating). This will be one of the reason for the lesser pressure values in numerical simulation, thus the wind profile uses for the numerical simulation for BS-EN1991-1-4:2005 should be carefully selected and adjusted accordingly.

Furthermore, in manual calculation, BS-EN1991-1-4:2005 shows somewhat higher pressure values compared to AS/NZS 1170.2:2011 code values for both wind directions. However, pressure values obtained by Australian wind loading code well agreed with the numerical simulation results in most of the places. As described in Section 2.2.4.4, gust effect factor method is employed to calculate the both fluctuating flow components and dynamic behavior of the structure. Therefore, it is observed that the AS/NZS 1170.2:2011 code well represents the dynamic phenomena.

Ultimately, the results conclude that AS/NZS 1170.2:2011 wind loading code is more capable of predicting the wind-building environment in most of the cases. Therefore, AS/NZS 1170.2:2011 can be applied for most of the cases without any uncertainty.

5.7 Velocity Field Development around the Building (AS/NZS 1170.2:2011)

Development of flow field around the building with respect to the elevation is shown by the following series of figures. S –A turbulent model with inflow velocity profile obtained from AS/NZS 1170.2:2011 has been selected to study on this.

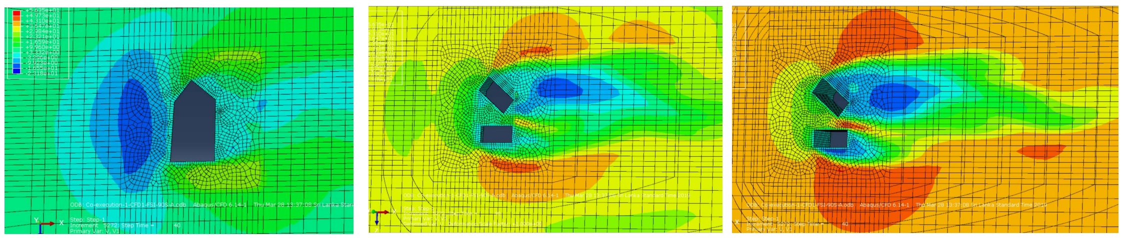

(a) (b) (c)

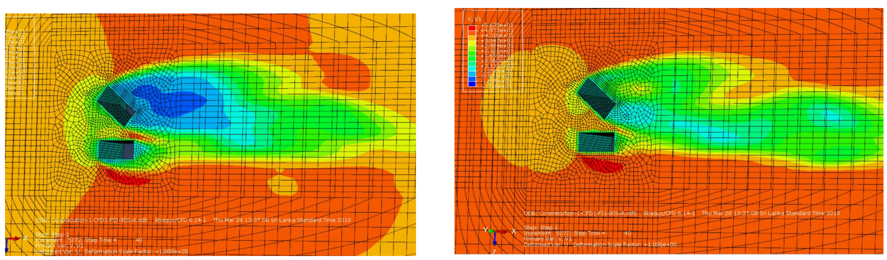

(d) (e)

Figure 5.38 Velocity field (V1) (a) H=1 m (b) H=21 m (c) H = 60 m (d) H = 80 m (e) H =101 m

Above serious of figures exhibited the enlargement of wake field and the velocity increment with the height of the building. Furthermore, Figure 5.38(c) and (d) clearly show the velocity increment due to the "channelling effect" due to the closely spaced towers. The inflow velocity of 42 ms^{-1} (as per the code evaluation) at the 80 m height from the ground level has increased up to 56 ms^{-1} in between the towers due to the reduction of the free flow area. Figures 5.38 (c) to (e) show the inflow velocity increment at the sides' wall (left side of the Tower 1 and right side of the Tower 2) of the building since the flow tends to move by omitting the obstacle. Therefore, the inflow velocity increased up to around 56 ms^{-1} particularly in left side of the Tower 1. Furthermore, above Figure shows the velocity increment at the edges of both Towers.

5.8 Pressure Field Development around the Building (AS/NZS 1170.2:2011)

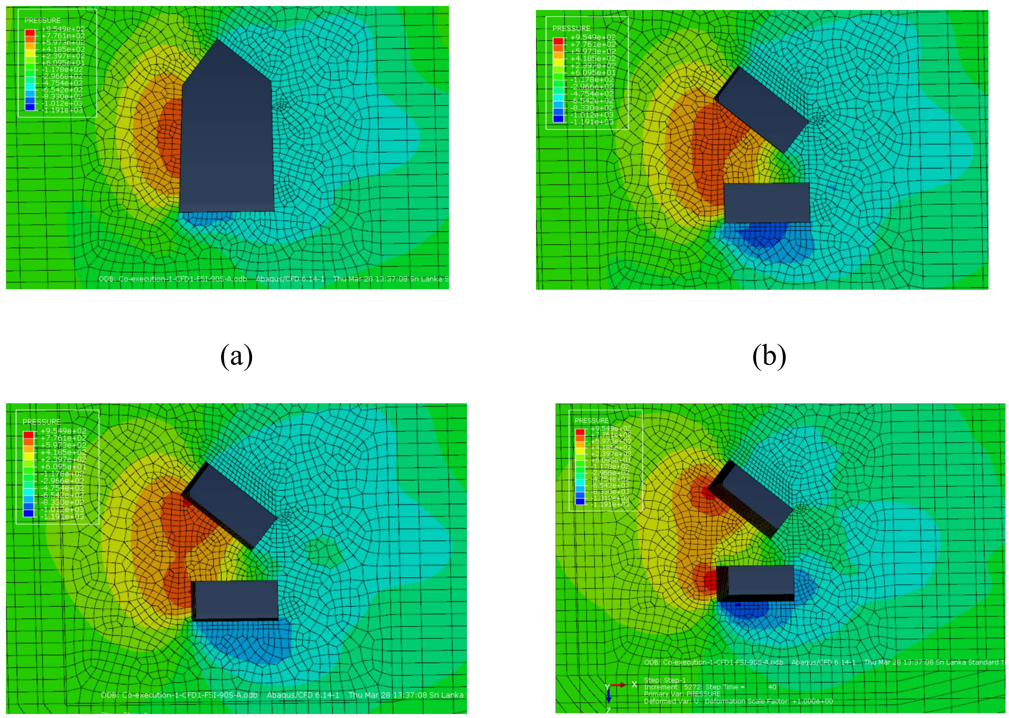

(a) (b)

(c) (d)

Figure 5.39 Pressure development (P) (a) H = 1 m (b) H = 22 m (c) H = 40 m (d) H = 80 m

It is observed the shear layer separation and the separation bubble formation at the zone of behind the building (Figures 5.39 (a) to (d)). Among those two Towers, maximum negative peak pressure occurred behind the Tower1 compared to Tower2.

Approximately, similar kind of structures arrangement (90^0 wind direction) used for this reaesrch has been used by Terazaki and Nakamura (2009, 2010) (closely spaced two high-rise buildings) for their wind tunnel test. Correspondingly, the researchers observed the extremely strengthen negative peak pressure value leeside of the building compared to the isolated model case. This helps to validate this model results up to certain extent.

By considering all the above facts, the study revealed the strength of CFD software when evaluating the wind loads and their effects on high-rise building accurately. Even though AS/NZS 1170.2:2011 wind loading code is capable of evaluating the dynamic loading on the building up to certain extent, actual fluid flow behaviour around the building can be performed by CFD tool. Moreover, special features such as edge effect, shear layer separation, wake formation, complex flow field and vortices formation at leeside of the building, stagnation point etc. can be clearly observed in the numerical simulation. In addition, building performance under wind action can be observed. Especially in this case study, additional roughness effect caused due to the presence of adjacent building can be observed. In addition, CFD tool is strengthened by various solution approaches such as 1-qeuation (S-A), 2-equation (k-ε), 2-equation (k-ω) etc. Therefore, the designer has freedom to choose the suitable turbulent model relates to the application. However, wind tunnel testing can also be used to evaluate the wind loadings on the structure. Then again, wind tunnel testing is inexpedient in terms of cost and time. Major advantages of CFD simulation over other conventional methods such as code based calculation (manual),wind tunnel testing are cost effective , time saving , can easily modify the inflow parameters and model geometry, greater accuracy of results and ability to study the vast range of flow parameters and their effects. Ultimately, CFD can be used to accomplish the goal of “aerodynamic shaped structure” while fulfilling the aesthetical perspectives.

In this case study, S-A turbulent model is used to perform in order to evaluate the flow parameters. S-A turbulent model is designed for wall bounded flows with mild separations and recirculation. In addition, S-A turbulent model well performs even for the large meshed models. On the other hand S-A model is low cost turbulent model, which needs less time, less computational configurations etc. compared to LES turbulent model. As a result of it, S-A model uses for most of the industrial applications.

5.9 Summary

- Different flow features such as vortices, wake formations, vortices can be clearly observed by the numerical simulation results that is more suitable to assess the complex geometries.
- Building performance under wind action can be observed by the CFD simulation.
- AS/NZS 1170.2:2011 can be applied for most of the cases without any uncertainty.
- AS/NZS 1170.2:2011 uses advanced techniques for assessing the flow variables.
- S-A turbulent uses for most of the industrial applications due to its well performance for poor mesh quality and less computer configuration compared to LES. Moreover. S-A is mainly designed for wall bounded flows.

6. CONCLUSION AND RECOMMANDATIONS

6.1 Conclusions

Static based wind force acting on the 102 m height tall building for two orthogonal directions are estimated based on CP3 Chapter V-2:1972, BSEN 1991-1-4:2005 with SLS EN 1991-1-4:2019, AS/NZS1170.2:2011A.Then, the comparative study has been carried out between the estimated forces based on three wind loading codes while identifying commonalities and differences among codes. Numerical simulation is performed for the same building under similar wind flow directions using RANS approach (S-A turbulent model) available in ABAQUS software. The input wind profile is specified utilizing same three wind codes CP3 CHAPTER V-2:1978, BS-EN1991-1-4:2005 & AS/NZS 1170.2:2011. Altogether six different models have been set for the analysis.

However, material property modification is done following other references such as code of practice of Earthquake actions in Australia: AS 1170.4-2007 due to lack of available data. Hence, seismic mass is used as the mass of the structure (building) and which is calculated according the code of practice of Earthquake actions in Australia: AS 1170.4 -2007. Furthermore, corresponding E value which represents the stiffness of the whole structure is calculated with the help of a FE Model as described in Section 4.4. In case of mesh sensitivity, performance of three different meshes are evaluated to find the optimal mesh. For the reason that, if the mesh is finer it will lead to get more accurate results. Conversely it will take more computational time and end up with the higher computational cost. Therefore, optimal mesh is found which helps to reduce the computational time without losing the accuracy of results. Three different meshes coarse mesh (239,095 elements), medium mesh (455,737elements), and fine mesh (602,307) are performed for the evaluation. However, medium mesh (455,737elements) is selected for this case study considering above facts.

CFD tool is strengthened by various solution approaches such as RANS and LES etc. RANS approach is selected for this case study, since LES requires high quality mesh, higher computational time etc.

Results obtained from numerical simulation are compared with the code based calculations.

Based on the comparative study, the following conclusions can be drawn.

- Both BS-EN1991-1-4:2005 and AS/NZS 1170.2:2011 used gust effect factor method for calculating the fluctuating component of the flow variables and the structure vibration. Therefore, both codes showed similarities when calculating the dynamic component of the flow variables and the dynamic behavior of the structure. But CP3 CHAPTER V-2:1972 used very simple method (quasi-static) for evaluating the dynamic performance.
- Along wind pressure increases smoothly with the elevation of the building according to CP3 Chapter V–Part2:1972 and AS/NZS 1170.2:2011. However, in BS-EN1991-1-4:2005 the wind loads calculation procedure is built on the dividing by parts – rule, which makes the pressure distribution graph containing straight lines.
- Wind pressures calculated by CP3Chapetr V-2:1972 show significantly lesser values compared to other two wind loading codes in most of the cases.
- In code based calculation, BS-EN1991-1-4:2005 shows somewhat higher pressure values compared to AS/NZS 1170.2:2011 code values for both wind directions.
- Computed results for S-A model showed significant deviation with the code based calculations obtained by CP3 Chapter V-Part2:1972. Therefore, CP3 Chapter V-Part2:1972 is incapable of evaluating the building-wind environment accurately due to its simple calculation method.

- Numerical simulation results obtained from BS-EN1991-1-4:2005 for both wind directions, showed noticeably lesser pressure values on all the faces. In BS-EN1991-1-4:2005, velocity profile is based on the 10 minutes wind velocity and all the fluctuating flow variables are being calculated based on the mean flow variables in accordance with RANS equations. This will be one of the reason for the underestimation of the total wind pressure (mean + fluctuating).
- Manual calculation obtained from AS/NZS 1170.2:2011 showed good agreement with the numerical simulation results for both turbulent models in most of the places. AS/NZS 1170.2:2011 wind loading code is capable of evaluating the dynamic phenomena (wind fluctuation + structure vibration) up to certain extent compared to other two wind loading codes. Therefore, AS/NZS 1170.2:2011 can be applied for most of the cases without any uncertainty.
- Actual fluid flow behaviour around the building can be performed by CFD software. Special flow features such as edge effect, shear layer separation, wake formation, vortices can be observed along with building performance through numerical simulation. This helps to predict the building-wind environment accurately.
- S-A turbulent model is suitable for this kind of applications. Because, it is designed for wall bounded flows with mild separations and recirculation. Also, S-A turbulent model well performs even for the poor mesh quality. Suitability of the selected turbulent model mainly depends on the application.

6.2 Recommendations for Future Works

It recommended to

- Conduct more comparative studies between the codes of practices and numerical simulations for tall-buildings with different heights and aspects ratios.
- Expand numerical simulations for tall-buildings with different heights and shapes
- Study the behavior of different turbulent models to identify their suitability relates to the application.
- Include effects of different surrounding buildings.
- Use the latest wind loading map developed for Sri Lanka (using wind data obtained by 23 weather stations) for different codes of practice (Maduranga & Lewangamage, 2018).

REFERENCES

1. Rouse, M., 2014. *computational fluid dynamics (CFD).* [Online].
2. Ahmed, L., 2018. Dynamic Measurements for Determining Poisson's Ratio of Young Concrete. *Nordic Concrete Research ,* 11 May, Issue Publ. No. NCR 58 – ISSUE 1– Article 6 , pp. 95-106.
3. Aksenov, A., Dyadkin, D., Luniewski, T. & Pokhilko, V., 2004. *Fluid Structure Interaction analysis using Abaqus and FlowVision.* s.l., s.n.
4. Alaghmandan, M. & Elnimeiri, M., 2013. Reducing Impact Of Wind On Tall Buildings Through Design And Aerodynamic Modifications. *AEI 2013,* pp. 847-856.
5. Anon., 1978. *Design manual "Design building for high winds ".* Sri Lanka: s.n.
6. Anon., 2007 (Amendment No.1 (August 2015)). *Structural Design Actions - Part 4 -Earthquake actions in Austalia :AS 1170.4 -2007.* s.l.:1170.4-2007, AS.
7. Anon., 2012. *Turbulence Part 2 - Wall Functions and y+ Requirements.* [Online]
   Available at: https://www.computationalfluiddynamics.com
8. Anon., 2014. *ABAQUS 6.14 User Documentation.* s.l.:Simulia.
9. Anon., 2014. *ANSYS-Turbulence Modeling-Introduction to ANSYS Fluent.* [Online].
10. Anon., 2017. [Online]
    Available at: https://www.researchgate.net/post
11. Anon., 2018. *Log wind profile.* [Online]
    Available at: https://en.wikipedia.org/
12. Anon., 2019. *Effect of Wind Design of High Rise Buildings.* [Online]
    Available at: https://ukdiss.com
13. Anon., 2019. *IESL Guide Lines.* [Online]
    Available at:
    https://iesl.lk/index.php?option=com_content&view=article&id=43:iesl-guidelines&catid=19&lang=en&Itemid=162

14. Anon., 2020. *Fluid Dynamics.* [Online]
Available at: https://en.wikipedia.org
15. Anon., 2020. *List of tallest structures in Sri Lanka.* [Online]
Available at: https://en.wikipedia.org/
16. Anon., 2020. *Planetary boundary layer.* [Online]
Available at: https://en.wikipedia.org/
17. Anon., 2020. *Reynolds number.* [Online]
Available at: https://en.wikipedia.org
18. Anon., 2020. *Y+ range recommendations in documentation.* [Online]
Available at: https://www.simscale.com/
19. Anon., n.d. *British Standard: Eurocode 1: "Actions on Structures – Part1- 4: General actions - wind actions; BS EN 1991-1-4:2005 – Sri Lankan National Annex ".* s.l.:s.n.
20. Anon., n.d. *British Standard: Eurocode 1: "Actions on Structures – Part1- 4: General actions - wind actions; BS EN 1991-1-4:2005 ".* London: British Standard Institution.
21. Anon., n.d. *CP3 Chapter V: 1972, "Code of Basic data for the design of buildings chapter V. Loading, Part 2, Wind Loads".* London: British Standard Institution.
22. Antipin, A. et al., 2014. *Numerical Simulation of Wind Loads on High-Rise Buildings.* Melbourne, s.n.
23. AS/NZS1170.2, 2011. *Australian and New Zealand standards: "Structural design actions Part 2: wind actions; AS/NZS1170.2:20011".* s.l.:s.n.
24. Becker, S., Lienhart, H. & Durst, F., 2002. Flow around three-dimensional obstacles in boundary layers. *Wind Engineering and Industrial Aerodynamics,* Volume 90, pp. 265-279.
25. Bendini, L., 2019. *High-rise building or skyscraper: what's the difference.* [Online].
26. Benra, F.-K.et al., 2011. A Comparison of One-Way and Two-Way Coupling Methods for Numerical Analysis of. *Journal of Applied Mathematics,* August.Volume 2011.

27. Bernek, W. & Koten, V., 1979.
28. Blocken, B., Stathopoulos, . T., Carmeliet, J. & Hensen , J., 2011. Application of CFD in building performance simulation for the. *Journal of Building Performance Simulation, Vol. 4, No. 2, June 2011, 157–184,* June, Volume Vol. 4, No. 2, p. 157–184.
29. Bwail, K., 2019. *Why Tall Buildings Need Wind Load Analysis.* [Online].
30. Elshaer, A. et al., 2016. LES Evaluation of Wind-induced Responses for an Isolated and a Surrounded Tall Building. *Engineering Structures115(2016),* pp. 179-195.
31. Emeis, S. & Turk, M., 2007. Comparison of logarithmic wind profiles and power law wind profiles and their applicability for offshore wind profiles. February.
32. Franke, J. et al., 2014. *Recommendations on the use of CFD in wind engineering.* s.l., s.n., pp. 1-11.
33. Gaudio, . R., Miglio, . R. & Dey, S., 2010. Non Universality of Von Kármán's κ in Fluvial Streams. *ournal of Hydraulic Research, International Association for Hydraulic Research (IAHR),* 48(5), pp. 658-663.
34. Gerges, R. R. & Benuska, K., 2013. Across-Wind Response of High-Rise Buildings. *Structure,* July.
35. Haby, J., 2020. *Wind Speed increasing with Height.* [Online] Available at: https://www.theweatherprediction.com
36. Hall , J. J., 2005. High-Rise Building Definition, Development, and Use. In: *High-Rise Security and Fire Life Safety.* s.l.:High-Rise Building Fires. Quincy, MA: National Fire Protection Association, p. 1.
37. Hulle, B., 2012. *Study of Wake Region of a Typical Isolated Building:Part1 :Flow Visualization.* Rio De Janiro, s.n.
38. Irwin, P. A., 2009. Wind engineering challenges of the new generation of supertall buildings. *J. Wind Eng. Ind. Aerodyn. 97(2009) ,* pp. 328-334.
39. Jayasundara, , H. M., Koliyabandara , S. M. & Wijesundar, K. K., 2018. Wind Loads on Tall Buildings: A Comparative Study of the International Wind

Codes and Numerical Simulation. *Journal of the Institution of Engineers, Sri Lanka · July 2018 ,* June, Volume ENGINEER - Vol. LI, No. 03, , pp. 31-45.

40. Kumar, H. S. & Reddy, N. V., 2015. Estimation of Wind Forces on Square Tall Building with Acceptance Ratio 1:1:7 by ABAQUS. *International Research Journal of Engineering and Technology (IRJET),* 3(5), pp. 1581-1587.
41. Kwon, K. D. & Kareem, A., 2013. Comparative study of major international wind codes and standards for wind effects on tall buildings. *Engineering Structures 51 (2013),* pp. 23-35.
42. Lia, B., Liua, J., Luoa, F. & Manc, X., 2015. Evaluation of CFD Simulation Using Various Turbulence Models for Wind Pressure on Buildings Based on Wind Tunnel Experiments. *Procedia Engineering 121 (2015),* pp. 2209-2216.
43. Maduranga, W. S. & Lewangamage, C. S., 2018. Developement of Wind Loading Maps for Sri lanka for use with Different wind Loading Codes. *ENGINEER,* Ll(03), pp. 47-55.
44. Mendis, P. et al., 2007. Wind Loading on Tall buildings. *EJSE special issue; Loading on structures,* pp. 41-54 .
45. Mendis, P., Ngo, T., Haritos, N. & Hira, A., 2007. *Wind Loading on Tall Buildings.* s.l., s.n., p. 53.
46. Moghaddam, E. H., Amindeldar, S. & Besharatizadeh, A., 2011. New approach to natural ventilation in public buildings inspired by iranian's traditional windcatcher. *Procedia Engineering 21 - 2011 International Conference on Green Buildings and Sustainable Cities,* p. 42 – 52.
47. Mohamed, . A., 2013. *On Mesh Convergence and Accuracy Behaviour for CFD Applications,* s.l.: s.n.
48. Mohotti, D., Mendis, P. & Ngo, T., 2013. *Application of Computational Fluid Dynamics (CFD) in Wind Analysis of Tall Buildings.* Kandy, s.n.
49. Olenko, V. & Puzyrev, P., 2013. *Study of Wind Effects on Unique Buildings.* s.l., s.n.
50. Revuz, J., Hargreaves , D. & Owen, J., 2010. *Domain size for Computational Fluid Dynamics modelling of tall buildings.* Bristol, s.n., pp. 273-276.

51. Reynolds, O., 1895. On the Dynamical Theory of Incompressible Viscous Fluids and the Determination of the Criterion. *Philosophical Transactions of the Royal Society of London A. 186,* pp. 123-164.

52. Sadh, A. & Pal, A., 2018. A Literature Study of Wind Analysis on High Rise Building. *International Journal of Advanced Engineering Research and Science (IJAERS),* 5(11), pp. 263-266 .

53. Schmitt, F. G., (2007. About Boussinesq's turbulent viscosity hypothesis: historical remarks and a direct evaluation of its validity. *C. R. Mécanique 335,* pp. 617-627 .

54. Smagorinsky, J., 1963. General Circulation Experiments with the Primitive Equations. *Monthly Weather Review,* 91 (3), pp. 99-164.

55. Spalart, P. & Allmaras, S., 1992. A One-Equation Turbulence Model for Aerodynamic Flows. *AIAA Paper 92-0439* .

56. Taranath, B. S., 1998. In: *Steel, Concrete, and Composite Design of Tall Buildings.* s.l.:McGraw-Hill Education.

57. Taranath, B. S., 2005. In: *Wind and Earthquake Resistant Buildings Structural Analysis and Design.* s.l.:Marcel Dekker.

58. Vafaeihosseini, E., Sagheb, A. & Ramancharla, P. K., 2012. *Analysis of Highrise Building using Computational Fluid Dynamics Approach: A Case Study on 38Storey High-rise Building.* s.l., s.n.

59. Weerasuriya, A. U., Lewangamage , C. S. & Jayasinghe , M. T., 2010. *Comparison of Five Major Wind Codes with Sri Lankan Context.* South Korea, s.n.

60. Yoshikawa, M. & Tamura, T., 2013. *LES for wind Loads Estimated by Unstructured Grid System.* Shanghai, s.n., pp. 1960-1965.

61. Yoshikawa, M. & Tamura, T., 2013. *Wind Tunnel Study of Wind Pressure Distribution on Xi'an's Tallest Building and the Finite Element Calculation and Analysis.* s.l., s.n., pp. 572-582.

62. Zhang, G., Dou, Z. & Li, J., 2013. *LES of Fluctuating Pressures on a High-Rise Building Influenced by Windward Building.* Chennai, s.n., pp. 920-929.

Appendix A:

Wind load calculation for 31 storey building according to CP3-CHAPTER V-2:1972

Reference	Calculations	Output

A.1 Calculation of wind force acoording to CP3:ChapterV-2:1972

Wind Loading : CP3 : Chapter V - Part 2 : 1972 has been used to calculate the characteristic wind pressure on windward ,leeward and side face for the Tower 1.

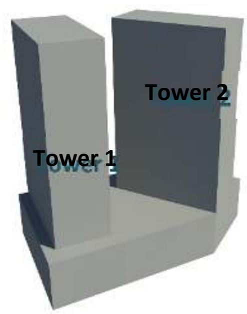

Fubdermental Basic wind speed in Zone 3 = 38 ms^{-1}

Cl.4.3.2 — $V_s = V_b\ S_1\ S_2\ S_3\ S_4$

Sample calculation at height of 3m from ground level.

Cl.5.4 — S_1 = Topography factor = 1

Table 3 — S_2 = Country with many wind breakers;small towns,outsirkit of large cities
Structural buildings with great horzontalor vertical dimension
is greater than 50m.
Class C
= 0.550

Cl.5.6 — S_3 = statistical concept factor = 1

Appendix L — S_4 = Directional factor = 1

$$\boldsymbol{V_s = V_b\ S_1\ S_2\ S_3\ S_4}$$

V_s = 38 x 1 x 0.550 x 1

= 20.9 ms^{-1}

$\boldsymbol{q = k V_s^2}$ k = 0.613

q = 267.8 N/m^2

Wind Load Calculation -CP3 ChapterV-2:1972	Page . No.	**1**	

Reference	Calculations	Output
	Presure Coefficient method (consider only external pressure co-efficient)	
Cl.4.3	$P = C_{pe*}\ q$	

From 0m -21m

Length of the towre 1 (l) = 112 m
Width of the tower1 (w) = 62 m

From 21m -102m

Length of the towre 1 (l) = 53 m
Width of the tower1 (w) = 24.5 m

Height of the building (h) = 102 m

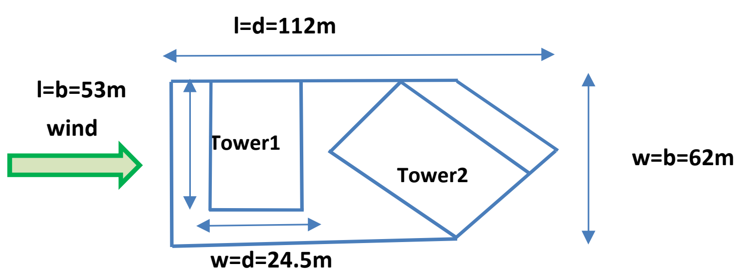

From 0m -21m

Building plan ratio	=	l / w =	1.81	**3/2 < l/w < 4**
Building height ratio	=	h / w =	1.65	**3/2 < h/w < 6**

From 21m -102m

Building plan ratio	=	l / w =	2.16	**3/2 < l/w < 4**
Building height ratio	=	h / w =	4.16	**3/2 < h/w <6**

C_{pe}			Pressure		
Windward	=	0.7	187.44	N/m^2	
Leeward	=	-0.7	-421.21	N/m^2	(Maximum value)
Side wall	=	-0.4	-738.88	N/m^2	(Maximum value)

Same Calculation Procedure has been used for calculating the wind pressure on the building when wind comes on 90^0 angle.
Summary of the calculation sheet is attached in next.

Wind Load Calculation -CP3 ChapterV-2:1972	Page . No.	2	

From 0-21m

h/w =1.80 3/2 < h/w < 6
l/w =1.64 3/2 < h/w < 4

From 24.1-102m
h/w =4.15 3/2 < h/w < 6
l/w =2.16 3/2 < h/w < 4

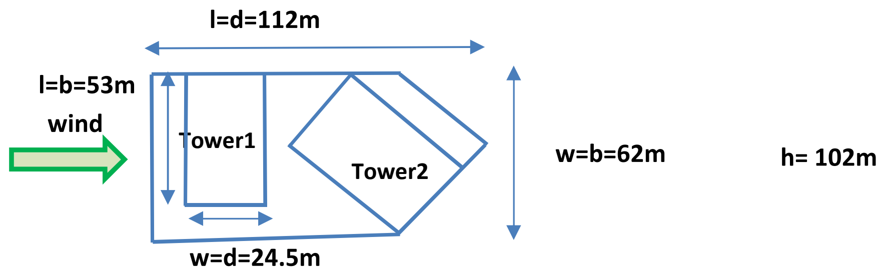

Wind X-direction		**α =0°**	**Tower1**			*Windward*	*Leeward*	*side wall*	*Windward*	*Leeward*	*Two sides*
Floor	***Height above ground***	***Effective Height***	***S2***	***Vs = V S1*S2*S3*S4***	***$q=kV_s^2$ (Pa)***	***C_{pe}***	***C_{pe}***	***C_{pe}***	***$P = C_{pe}*q$ (N/m^2)***	***$P = C_{pe}*q$ (N/m^2)***	***$P = C_{pe}*q$ (N/m^2)***
F1	3	3.0	0.550	20.90	268	0.7	-0.4	-0.7	187.44	-422.21	-738.88
F2	6	3.0	0.618	23.48	338	0.7	-0.4	-0.7	236.65	-422.21	-738.88
F3	9	3.0	0.672	25.54	400	0.7	-0.4	-0.7	279.81	-422.21	-738.88
F4	12	3.0	0.726	27.59	467	0.7	-0.4	-0.7	326.59	-422.21	-738.88
F5	15	3.0	0.780	29.64	539	0.7	-0.4	-0.7	376.98	-422.21	-738.88
F6	21	6.0	0.857	32.57	650	0.7	-0.4	-0.7	455.08	-422.21	-738.88
F7	24.1	3.1	0.878	33.36	682	0.7	-0.4	-0.7	477.66	-422.21	-738.88
F8	27.2	3.1	0.900	34.20	717	0.7	-0.4	-0.7	501.89	-422.21	-738.88
F9	30.3	3.1	0.921	35.00	751	0.7	-0.4	-0.7	525.59	-422.21	-738.88
F10	33.4	3.1	0.934	35.49	772	0.7	-0.4	-0.7	540.53	-422.21	-738.88
F11	36.5	3.1	0.946	35.95	792	0.7	-0.4	-0.7	554.51	-422.21	-738.88
F12	39.6	3.1	0.958	36.40	812	0.7	-0.4	-0.7	568.67	-422.21	-738.88
F13	42.7	3.1	0.971	36.90	835	0.7	-0.4	-0.7	584.20	-422.21	-738.88
F14	45.8	3.1	0.983	37.35	855	0.7	-0.4	-0.7	598.73	-422.21	-738.88
F15	48.9	3.1	0.996	37.85	878	0.7	-0.4	-0.7	614.67	-422.21	-738.88
F16	52.0	3.1	1.004	38.15	892	0.7	-0.4	-0.7	624.59	-422.21	-738.88
F17	55.1	3.1	1.010	38.38	903	0.7	-0.4	-0.7	632.07	-422.21	-738.88
F18	58.2	3.1	1.016	38.61	914	0.7	-0.4	-0.7	639.61	-422.21	-738.88

Wind X-direction	α =0°	Tower1				*Windward*	*Leeward*	*side wall*	*Windward*	*Leeward*	*Two sides*
Floor	***Height above ground***	***Effective Height***	***S2***	***Vs = V S1*S2*S3*S4***	***$q=kV_s^2$ (Pa)***	***C_{pe}***	***C_{pe}***	***C_{pe}***	***$P = C_{pe}*q$ (N/m^2)***	***$P = C_{pe}*q$ (N/m^2)***	***$P = C_{pe}*q$ (N/m^2)***
F19	61.3	3.1	1.022	38.84	925	0.7	-0.4	-0.7	647.18	-422.21	-738.88
F20	64.4	3.1	1.028	39.06	935	0.7	-0.4	-0.7	654.80	-422.21	-738.88
F21	67.5	3.1	1.035	39.33	948	0.7	-0.4	-0.7	663.75	-422.21	-738.88
F22	70.6	3.1	1.041	39.56	959	0.7	-0.4	-0.7	671.47	-422.21	-738.88
F23	73.7	3.1	1.047	39.79	970	0.7	-0.4	-0.7	679.23	-422.21	-738.88
F24	76.8	3.1	1.054	40.05	983	0.7	-0.4	-0.7	688.35	-422.21	-738.88
F25	79.9	3.1	1.060	40.28	995	0.7	-0.4	-0.7	696.21	-422.21	-738.88
F26	83.0	3.1	1.065	40.47	1004	0.7	-0.4	-0.7	702.79	-422.21	-738.88
F27	86.1	3.1	1.069	40.62	1012	0.7	-0.4	-0.7	708.08	-422.21	-738.88
F28	89.2	3.1	1.074	40.81	1021	0.7	-0.4	-0.7	714.72	-422.21	-738.88
F29	92.3	3.1	1.078	40.96	1029	0.7	-0.4	-0.7	720.05	-422.21	-738.88
F30	95.4	3.1	1.083	41.15	1038	0.7	-0.4	-0.7	726.75	-422.21	-738.88
F31	102	6.6	1.092	41.50	1056	0.7	-0.4	-0.7	738.88	-422.21	-738.88

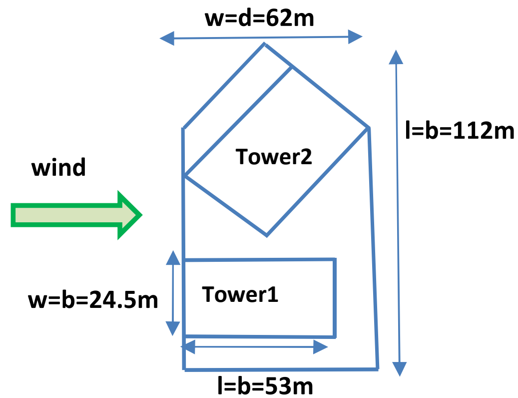

h= 102m

From 0-21m

h/w =1.80 3/2 < h/w < 6
l/w =1.64 3/2 < h/w < 4

From 24.1-102m

h/w =4.14 3/2 < h/w < 6
l/w =2.16 3/2 < h/w < 4

Wind X-direction	**α =90°**	Tower1				*Windward*	*Leeward*	*side wall*	*Windward*	*Leeward*	*Two sides*
Floor	***Height above ground***	***Effective Height***	**S2**	***Vs = V S1*S2*S3*S4***	***q=kV$_s^2$ (Pa)***	***C_{pe}***	***C_{pe}***	***C_{pe}***	***$P = C_{pe}*q\ (N/m^2)$***	***$P = C_{pe}*q\ (N/m^2)$***	***$P = C_{pe}*q\ (N/m^2)$***
F1	3	3.0	0.550	20.90	268	0.8	-0.1	-0.5	214.21	-105.55	-527.77
F2	6	3.0	0.618	23.48	338	0.8	-0.1	-0.5	270.45	-105.55	-527.77
F3	9	3.0	0.672	25.54	400	0.8	-0.1	-0.5	319.78	-105.55	-527.77
F4	12	3.0	0.726	27.59	467	0.8	-0.1	-0.5	373.24	-105.55	-527.77
F5	15	3.0	0.780	29.64	539	0.8	-0.1	-0.5	430.83	-105.55	-527.77
F6	21	6.0	0.857	32.57	650	0.8	-0.1	-0.5	520.09	-105.55	-527.77
F7	24.1	3.1	0.878	33.36	682	0.8	-0.1	-0.5	545.89	-105.55	-527.77
F8	27.2	3.1	0.900	34.20	717	0.8	-0.1	-0.5	573.59	-105.55	-527.77
F9	30.3	3.1	0.921	35.00	751	0.8	-0.1	-0.5	600.67	-105.55	-527.77
F10	33.4	3.1	0.934	35.49	772	0.8	-0.1	-0.5	617.75	-105.55	-527.77
F11	36.5	3.1	0.946	35.95	792	0.8	-0.1	-0.5	633.72	-105.55	-527.77
F12	39.6	3.1	0.958	36.40	812	0.8	-0.1	-0.5	649.90	-105.55	-527.77
F13	42.7	3.1	0.971	36.90	835	0.8	-0.1	-0.5	667.66	-105.55	-527.77
F14	45.8	3.1	0.983	37.35	855	0.8	-0.1	-0.5	684.27	-105.55	-527.77
F15	48.9	3.1	0.996	37.85	878	0.8	-0.1	-0.5	702.48	-105.55	-527.77
F16	52.0	3.1	1.004	38.15	892	0.8	-0.1	-0.5	713.81	-105.55	-527.77
F17	55.1	3.1	1.010	38.38	903	0.8	-0.1	-0.5	722.37	-105.55	-527.77

Wind X-direction	α =90°	Tower1				Windward	Leeward	Two sides	Windward	Leeward	Two sides
Floor	Height above ground	Effective Height	S2	Vs = V S1*S2*S3*S4	$q=kV_s^2$ (Pa)	C_{pe}	C_{pe}	C_{pe}	$P = C_{pe} * q\ (N/m^2)$	$P = C_{pe} * q\ (N/m^2)$	$P = C_{pe} * q\ (N/m^2)$
F18	58.2	3.1	1.016	38.61	914	0.8	-0.1	-0.5	730.98	-105.55	-527.77
F19	61.3	3.1	1.022	38.84	925	0.8	-0.1	-0.5	739.64	-105.55	-527.77
F20	64.4	3.1	1.028	39.06	935	0.8	-0.1	-0.5	748.35	-105.55	-527.77
F21	67.5	3.1	1.035	39.33	948	0.8	-0.1	-0.5	758.57	-105.55	-527.77
F22	70.6	3.1	1.041	39.56	959	0.8	-0.1	-0.5	767.40	-105.55	-527.77
F23	73.7	3.1	1.047	39.79	970	0.8	-0.1	-0.5	776.27	-105.55	-527.77
F24	76.8	3.1	1.054	40.05	983	0.8	-0.1	-0.5	786.68	-105.55	-527.77
F25	79.9	3.1	1.060	40.28	995	0.8	-0.1	-0.5	795.66	-105.55	-527.77
F26	83.0	3.1	1.065	40.47	1004	0.8	-0.1	-0.5	803.19	-105.55	-527.77
F27	86.1	3.1	1.069	40.62	1012	0.8	-0.1	-0.5	809.23	-105.55	-527.77
F28	89.2	3.1	1.074	40.81	1021	0.8	-0.1	-0.5	816.82	-105.55	-527.77
F29	92.3	3.1	1.078	40.96	1029	0.8	-0.1	-0.5	822.92	-105.55	-527.77
F30	95.4	3.1	1.083	41.15	1038	0.8	-0.1	-0.5	830.57	-105.55	-527.77
F31	102	6.6	1.092	41.50	1056	0.8	-0.1	-0.5	844.43	-105.55	-527.77

Appendix B:

Wind load calculation for 31 storey building according to BSEN1991-1-4:2005

Reference	Calculations	Output

B.1 Calculation of wind force acoording to BSEN 1991-1-4:2005

Wind Loading : BSEN 1991-1-4:2005 has been used to calculate the characteristic wind pressure on windward ,leeward and side face for the Tower 1.

Fubdermental Basic wind speed in Zone 3 = 22 ms^{-1}

Terrain category = III

Sample calculation at height of 3m from ground level.

SLSEN 4.2(1) P Note2 & SLSEN 4.2(2) P Note 1

$$V_{b,0} = V_{b,map}\ C_{alt}$$

$$C_{alt} = 1+0.001A$$

A = Altitude = 5m

C_{alt} = Altitude correction factor

C_{alt} = 1+0.001x5

= 1.005 ≤ 2 (maximum)

$V_{b,0}$ = 22 x (1.005)

= 22.11 ms^{-1}

Cl 4.2

$$V_b = V_{b,0}\ C_{dir}\ C_{season}$$

Note 2 Cl.2.4 — C_{dir} = Directional factor = 1.0

Note 3 Cl.2.4 — C_{season} = Seasonal factor = 1.0

V_b = 22.11 x1 x1

= 22.11 ms^{-1}

Cl.4.3.3 — $C_0(z)$ = Orogarphy factor = 1.0

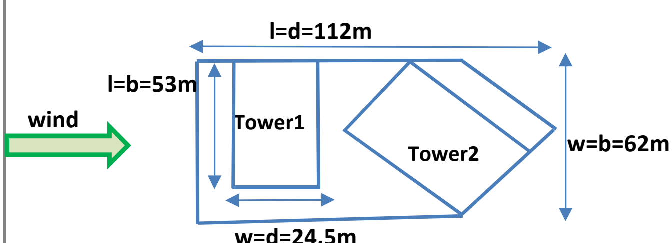

Fig 2.1 - building devided by part rule

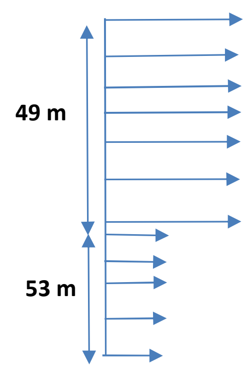

Wind Load Calculation -BSEN 1991-1-4:2005	Page . No.	7

Reference	Calculations	Output
Appendix A.4 &A.5 BSEN 1991-1-4:2005	h_{ave} = 10.0 m	
	x = 2*h_{avg} = 20 m	
	h_{dis} is lesser of 0.8h_{avg} or 0.6 h	
	0.8 h_{avg} = 8.0 m	
	0.6h = 61.2 m	
	h_{dis} = 8m	
	z-h_{dis} = 53 - 8 = 45 m	
Cl.4.10	$q_b = 0.5\ \rho\ V_m^2$	
	= 0.5 x 1.225 x 22.11^2	
	= 299.42 N/m^2	
Cl.4.5	$q_b = C_e(z)\ C_{e,T}(z)\ q_p$	
Fig. NA.5	$C_e(z)$ = Exposure factor = 3.6	
Fig. NA.8	$C_{e,T}(z)$ = Exposure correction factor = 1.0	
	q_b = 3.60 x 0.99 x 299.42	
	= 1067.14 N/m^2	
Cl.5.2	$W_e = C_{pe}\ q_p(z)$	

Wind Load Calculation -BSEN 1991-1-4:2005	Page . No.	8	

Reference	Calculations	Output
Cl.5.3 (3)	$\boldsymbol{F_w = C_s C_d W_e}$	
Figure D.2 Appendix D	C_sC_d = Structural factor = 0.91	
	$F_w = C_sC_d W_e$	
	= 0.91 x 1067	
	= 971.10	
	For leeward and sidewall = Maximum value of windward pressure	
	= (1067 ,1182)	
	h/d =4	

Wall Face	C_{pe}	Correlation factor	Pressure		
Windward	0.8	0.96	745.80	N/m^2	
Leeward	-0.7	0.96	-722.82	N/m^2	(Maximum value)
Side wall	-0.8	0.96	-826.08	N/m^2	(Maximum value)

Reference: Cl.7.2.1, Cl. 7.2.2(3) ,Figure7.5 & Table 7.1

Same Calculation Procedure has been used for calculating the wind pressure on the building when wind comes on 90^0 angle.
Summary of the calculation sheet is attached in next.

Wind Load Calculation -BSEN 1991-1-4:2005	Page . No.	9	

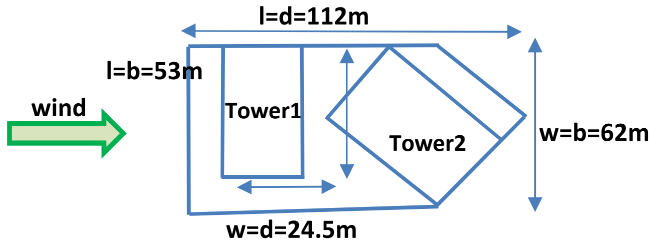

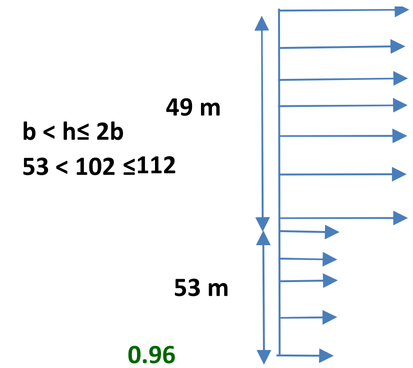

C_{pe} Note 3 : h/d =102/24.5=4

0.96

Wind 0^{0}-dir^{n} α =0° Tower1

Floor	Z (m)	Effective height	Z-h$_{dis}$ (m)	$V_b(z)$	$q_b=0.5\rho v_b^2$	$C_e(z)$	$C_e(T)$	$q_P = q_b x C_e(z) x C_e(T)$	Windward (C_{pe})	Leeward (C_{pe})	Two sides (C_{pe})	Windward we = $q_p(z_e)*C_{pe}$	Leeward we = $q_p(z_e)*C_{pe}$	Two sides we = $q_p(z_e)*C_{pe}$
F1	3	3.0	45.000	22.110	299.42	3.60	0.99	1067.1	0.8	-0.7	-0.8	745.8	-723.3	-862.9
F2	6	3.0	45.000	22.110	299.42	3.60	0.99	1067.1	0.8	-0.7	-0.8	745.8	-723.3	-862.9
F3	9	3.0	45.000	22.110	299.42	3.60	0.99	1067.1	0.8	-0.7	-0.8	745.8	-723.3	-862.9
F4	12	3.0	45.000	22.110	299.42	3.60	0.99	1067.1	0.8	-0.7	-0.8	745.8	-723.3	-862.9
F5	15	3.0	45.000	22.110	299.42	3.60	0.99	1067.1	0.8	-0.7	-0.8	745.8	-723.3	-862.9
F6	21	6.0	45.000	22.110	299.42	3.60	0.99	1067.1	0.8	-0.7	-0.8	745.8	-723.3	-862.9
F7	24.1	3.1	45.000	22.110	299.42	3.60	0.99	1067.1	0.8	-0.7	-0.8	745.8	-723.3	-862.9
F8	27.2	3.1	45.000	22.110	299.42	3.60	0.99	1067.1	0.8	-0.7	-0.8	745.8	-723.3	-862.9
F9	30.3	3.1	45.000	22.110	299.42	3.60	0.99	1067.1	0.8	-0.7	-0.8	745.8	-723.3	-862.9
F10	33.4	3.1	45.000	22.110	299.42	3.60	0.99	1067.1	0.8	-0.7	-0.8	745.8	-723.3	-862.9
F11	36.5	3.1	45.000	22.110	299.42	3.60	0.99	1067.1	0.8	-0.7	-0.8	745.8	-723.3	-862.9
F12	39.6	3.1	45.000	22.110	299.42	3.60	0.99	1067.1	0.8	-0.7	-0.8	745.8	-723.3	-862.9
F13	42.7	3.1	45.000	22.110	299.42	3.60	0.99	1067.1	0.8	-0.7	-0.8	745.8	-723.3	-862.9
F14	45.8	3.1	45.000	22.110	299.42	3.60	0.99	1067.1	0.8	-0.7	-0.8	745.8	-723.3	-862.9
F15	48.9	3.1	45.000	22.110	299.42	3.60	0.99	1067.1	0.8	-0.7	-0.8	745.8	-723.3	-862.9
F16	52.0	3.1	45.000	22.110	299.42	3.60	0.99	1067.1	0.8	-0.7	-0.8	745.8	-723.3	-862.9
F17	55.1	3.1	94.000	22.110	299.42	3.95	1.00	1182.7	0.8	-0.7	-0.8	826.6	-723.3	-862.9
F18	58.2	3.1	94.000	22.110	299.42	3.95	1.00	1182.7	0.8	-0.7	-0.8	826.6	-723.3	-862.9

Wind 0^0-dir^n	α =0°	Tower1							Windward	Leeward	Two sides	Windward	Leeward	Two sides
Floor	**Z (m)**	**Effective height**	**Z-h_{dis} (m)**	V_b(z)	$q_b=0.5pv_b^2$	C_e(z)	C_e(T)	$q_P=q_b x C_e(z) x C_e(T)$	(C_{pe})	(C_{pe})	(C_{pe})	we = q_p (z_e)*C_{pe}	we = q_p (z_e)*C_{pe}	we = q_p (z_e)*C_{pe}
F19	61.3	3.1	94.000	22.110	299.42	3.95	1.00	1182.7	0.8	-0.7	-0.8	826.6	-723.3	-862.9
F20	64.4	3.1	94.000	22.110	299.42	3.95	1.00	1182.7	0.8	-0.7	-0.8	826.6	-723.3	-862.9
F21	67.5	3.1	94.000	22.110	299.42	3.95	1.00	1182.7	0.8	-0.7	-0.8	826.6	-723.3	-862.9
F22	70.6	3.1	94.000	22.110	299.42	3.95	1.00	1182.7	0.8	-0.7	-0.8	826.6	-723.3	-862.9
F23	73.7	3.1	94.000	22.110	299.42	3.95	1.00	1182.7	0.8	-0.7	-0.8	826.6	-723.3	-862.9
F24	76.8	3.1	94.000	22.110	299.42	3.95	1.00	1182.7	0.8	-0.7	-0.8	826.6	-723.3	-862.9
F25	79.9	3.1	94.000	22.110	299.42	3.95	1.00	1182.7	0.8	-0.7	-0.8	826.6	-723.3	-862.9
F26	83.0	3.1	94.000	22.110	299.42	3.95	1.00	1182.7	0.8	-0.7	-0.8	826.6	-723.3	-862.9
F27	86.1	3.1	94.000	22.110	299.42	3.95	1.00	1182.7	0.8	-0.7	-0.8	826.6	-723.3	-862.9
F28	89.2	3.1	94.000	22.110	299.42	3.95	1.00	1182.7	0.8	-0.7	-0.8	826.6	-723.3	-862.9
F29	92.3	3.1	94.000	22.110	299.42	3.95	1.00	1182.7	0.8	-0.7	-0.8	826.6	-723.3	-862.9
F30	95.4	3.1	94.000	22.110	299.42	3.95	1.00	1182.7	0.8	-0.7	-0.8	826.6	-723.3	-862.9
F31	102	6.6	94.000	22.110	299.42	3.95	1.00	1182.7	0.8	-0.7	-0.8	826.6	-723.3	-862.9

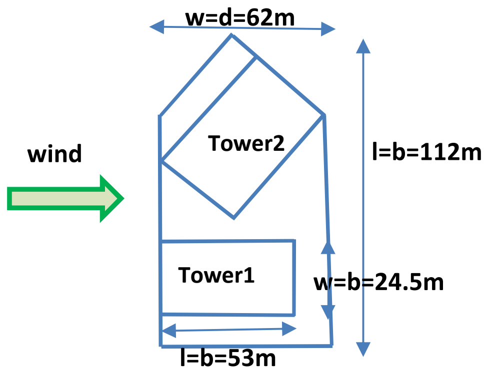

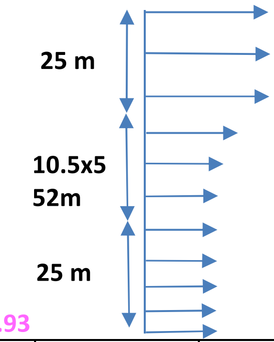

C_{pe} Note 3 : h/d =102/53=2

0.93

Wind X-dir^n α = 90^o Tower1

									Windward	Leeward	Two sides	Windward	Leeward	Two sides
Floor	Z (m)	Effective height	Z-h_{dis} (m)	$V_b(z)$	$q_b=0.5\rho v_b^2$	$C_e(z)$	$C_e(T)$	q_P= cscdxq$_b$xC$_e$(z)xC$_e$(T)	(C_{pe})	(C_{pe})	(C_{pe})	we = q_p (z_e)*C_{pe}	we = q_p (z_e)*C_{pe}	we = q_p (z_e)*C_{pe}
F1	3	3.0	17.000	22.11	305.533	2.90	0.90	797.44	0.8	-0.5	-0.8	563.6	-533.1	-853.0
F2	6	3.0	17.000	22.11	305.533	2.90	0.90	797.44	0.8	-0.5	-0.8	563.6	-533.1	-853.0
F3	9	3.0	17.000	22.11	305.533	2.90	0.90	797.44	0.8	-0.5	-0.8	563.6	-533.1	-853.0
F4	12	3.0	17.000	22.11	305.533	2.90	0.90	797.44	0.8	-0.5	-0.8	563.6	-533.1	-853.0
F5	15	3.0	17.000	22.11	305.533	2.90	0.90	797.44	0.8	-0.5	-0.8	563.6	-533.1	-853.0
F6	21	6.0	17.000	22.11	305.533	2.90	0.90	797.44	0.8	-0.5	-0.8	563.6	-533.1	-853.0
F7	24.1	3.1	17.000	22.11	305.533	2.90	0.90	797.44	0.8	-0.5	-0.8	563.6	-533.1	-853.0
F8	27.2	3.1	27.000	22.11	305.533	3.25	0.94	933.40	0.8	-0.5	-0.8	659.7	-533.1	-853.0
F9	30.3	3.1	27.000	22.11	305.533	3.25	0.94	933.40	0.8	-0.5	-0.8	659.7	-533.1	-853.0
F10	33.4	3.1	27.000	22.11	305.533	3.25	0.94	933.40	0.8	-0.5	-0.8	659.7	-533.1	-853.0
F11	36.5	3.1	37.000	22.11	305.533	3.45	0.97	1022.46	0.8	-0.5	-0.8	722.7	-533.1	-853.0
F12	39.6	3.1	37.000	22.11	305.533	3.45	0.97	1022.46	0.8	-0.5	-0.8	722.7	-533.1	-853.0
F13	42.7	3.1	37.000	22.11	305.533	3.45	0.97	1022.46	0.8	-0.5	-0.8	722.7	-533.1	-853.0
F14	45.8	3.1	47.000	22.11	305.533	3.60	0.99	1088.92	0.8	-0.5	-0.8	769.6	-533.1	-853.0
F15	48.9	3.1	47.000	22.11	305.533	3.60	0.99	1088.92	0.8	-0.5	-0.8	769.6	-533.1	-853.0
F16	52.0	3.1	47.000	22.11	305.533	3.60	0.99	1088.92	0.8	-0.5	-0.8	769.6	-533.1	-853.0
F17	55.1	3.1	57.000	22.11	305.533	3.75	1.00	1145.75	0.8	-0.5	-0.8	809.8	-533.1	-853.0

Wind X-dir^n		α = 90^o	Tower1						*Windward*	*Leeward*	*Two sides*	*Windward*	*Leeward*	*Two sides*
Floor	*Z (m)*	*Effective height*	*Z-h $_{dis}$ (m)*	$V_b(z)$	$q_b=0.5\rho v_b^2$	$C_e(z)$	$C_e(T)$	$q_P = c_s c_d \times q_b \times C_e(z) \times C_e(T)$	(C_{pe})	(C_{pe})	(C_{pe})	$we = q_p(z_e)*C_{pe}$	$we = q_p(z_e)*C_{pe}$	$we = q_p(z_e)*C_{pe}$
F18	58.2	3.1	57.000	22.11	305.533	3.75	1.00	1145.75	0.8	-0.5	-0.8	809.8	-533.1	-853.0
F19	61.3	3.1	57.000	22.11	305.533	3.75	1.00	1145.75	0.8	-0.5	-0.8	809.8	-533.1	-853.0
F20	64.4	3.1	57.000	22.11	305.533	3.75	1.00	1145.75	0.8	-0.5	-0.8	809.8	-533.1	-853.0
F21	67.5	3.1	67.000	22.11	305.533	3.82	1.00	1167.13	0.8	-0.5	-0.8	824.9	-533.1	-853.0
F22	70.6	3.1	67.000	22.11	305.533	3.82	1.00	1167.13	0.8	-0.5	-0.8	824.9	-533.1	-853.0
F23	73.7	3.1	67.000	22.11	305.533	3.82	1.00	1167.13	0.8	-0.5	-0.8	824.9	-533.1	-853.0
F24	76.8	3.1	94.000	22.11	305.533	3.95	1.00	1206.85	0.8	-0.5	-0.8	853.0	-533.1	-853.0
F25	79.9	3.1	94.000	22.11	305.533	3.95	1.00	1206.85	0.8	-0.5	-0.8	853.0	-533.1	-853.0
F26	83.0	3.1	94.000	22.11	305.533	3.95	1.00	1206.85	0.8	-0.5	-0.8	853.0	-533.1	-853.0
F27	86.1	3.1	94.000	22.11	305.533	3.95	1.00	1206.85	0.8	-0.5	-0.8	853.0	-533.1	-853.0
F28	89.2	3.1	94.000	22.11	305.533	3.95	1.00	1206.85	0.8	-0.5	-0.8	853.0	-533.1	-853.0
F29	92.3	3.1	94.000	22.11	305.533	3.95	1.00	1206.85	0.8	-0.5	-0.8	853.0	-533.1	-853.0
F30	95.4	3.1	94.000	22.11	305.533	3.95	1.00	1206.85	0.8	-0.5	-0.8	853.0	-533.1	-853.0
F31	102	6.6	94.000	22.11	305.533	3.95	1.00	1206.85	0.8	-0.5	-0.8	853.0	-533.1	-853.0

Appendix C:

Wind load calculation for 31 storey building according to AS/NZS 1170.2-2011

Reference	Calculations	Output
	C.1 Calculation of wind force acoording to AS/NZS1170.2:2011	
	Wind Loading : AS/NZS1170.2:2011 has been used to calculate the characteristic wind pressure on windward ,leeward and side face for the Tower 1.	
	Fubdermental Basic wind speed in Zone 3 = 38 ms^{-1}	
	Terrain category = 3	
	Importance level of structure = 2	
	Sample calculation at height of 3m from ground level.	
Table 3.1	$V_{site,\beta} = V_R M_d (M_{z,cat} M_s M_t)$	
Cl.3.3.2	M_d = Wind directional factor = 1	
Cl.4.3.1	M_s = Sheilding Multiplier = 1	
Cl.4.4	M_t = Topographical Multiplier = 1	
Cl 4.2 Table 4.1(A)	$M_{z,cat}$: Topographical Multiplier = 0.83	
	$V_{site,\beta} = V_R M_d (M_{z,cat} M_s M_t)$ = 38 x 1 (0.83 x 1x1) = 31.54 ms^{-1}	
	$f = (0.5 \rho_{air}) [V_{des\,\vartheta}]^2 C_{fig} C_{dyn}$	
Cl.5.2	C_{fig} = Aerodynamic Shape factor	
Section 6	C_{dyn} = Dynamic response factor	
Equ. 6.2(1)	$C_{dyn} = \frac{1 + 2I_h\sqrt{g_v^2 B_s + \frac{H_s g_R^2 S E_t}{\xi}}}{1 + 2g_v I_h}$	
	B_s = Bcakground resonance factor	
Equ. 6.2(2)	$B_s = \frac{1}{1 + \frac{\sqrt{0.26(h-s)^2 + 0.46 b_{sh}^2}}{L_h}}$	
	h = Total height = 102 m	
Fig 6.1	s = considering height = 3 m	

Wind Load Calculation -AS/NZS1170.2:2011	Page . No.	14	

Reference	Calculations	Output
	b_{sh} = Average bredth of height s and h = 53 m	
Equ. 6.2(3)	L_h = Turbulent length scale = $85*(h/10)^{0.25}$	
	= $85*(102/10)^{0.25}$	
	= 151.9	
	B_s = 0.71	
Equ. 6.2(4)	g_R = Peak ground for resonant response = $\sqrt{2log_e(600n_a)}$	
	n_a = Natutral frequancey of vibration (first mode) = 1 / 1.902 = 0.526 Hz	
	g_R = 3.39	
	S = Size reduction factor	
Equ. 6.2(5)	= $\frac{1}{[1+\frac{3.5n_a h(1+g_v I_h)}{V_{des,\theta}}][1+\frac{4n_a b_{0h}(1+g_v I_h)}{V_{des,\theta}}]}$	
	g_v = Factor for upwind velocity fluctuation = 3.7	
	I_h = Turbulent Intensity (z=h) = 0.165	
	S = 0.0579	
	E_t = (π/4) times the spectrum of turbulence in the approaching wind stream	
Equ. 6.2(6)	= $\frac{\pi N}{(1+70.8N^2)^{5/6}}$	
	N = Reduced frequancy	
	= $n_a L_h[1+g_v I_h]/V_{des,\theta}$	
	= 0.526 x 151.9 [1 + 3.7 x 0.165] /31.54	
	= 4.08	
	E_t = 0.035	
	ξ = Ratio of structural damping tp critical damping of structure	
	= 0.01	

Wind Load Calculation -AS/NZS1170.2:2011	Page . No.	15	

Reference	Calculations	Output
	$_h$ = height factor for the resonant response = $1+(s/h)^2$	
	$$C_{dyn} = \frac{1 + 2I_h\sqrt{g_v^2 B_s + \frac{H_s g_R^2 S E_t}{\xi}}}{1 + 2g_v I_h}$$	
	= 0.968	
Cl.5.2	$C_{fig,e} = C_{p,e} K_a K_{c,e} K_l K_p$	
Table 5.4	K_a = Area reduction factor = 1.0 Side wall = 0.8	
Table 5.5	$K_{c,e}$ = Combination factor = 0.9	
Table 5.6	K_l = Local pressure factor = 1.0	
Table 5.4.5	K_p = Porous cladding factor = 1.0	
	$C_{fig,\,e}$ = C_{pe} x 0.9 Windward & leeward	
	$C_{fig,\,e}$ = C_{pe} x 0.72 side wall	

Wall Face	C_{pe}	Pressure N/m^2	
Windward	0.8	424.50	
Leeward	-0.5	589.5	(Maximum value)
Side wall	-0.7	613.1	(Maximum value)

Same Calculation Procedure has been used for calculating the wind pressure on the building when wind comes on 90^0 angle.
Summary of the calculation sheet is attached in next.

Wind Load Calculation -AS/NZS1170.2:2011	Page . No.	16	

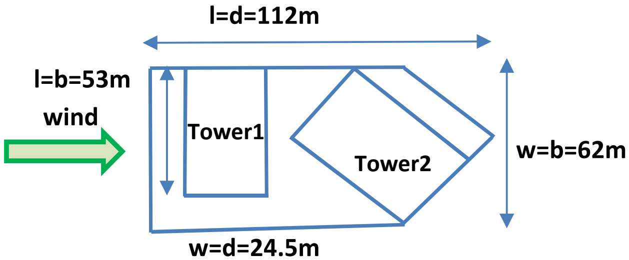

h > 25m			C_{pe}	0.8	Windwa Table 5.2(A)
d/b	24/53	< 1	C_{pe}	-0.5	Leewarc Table 5.2(B)
Horizontal distance 0 to1h wind ward edge			C_{pe}	-0.65	Side wal Table 5.2(C)

Wind X-direction α =0° Tower1

Floor	z (m)	Effective Height	$M_{z,cat}$	$V_{site\theta}$	s	B_{sh}	g_R	N	E_t	S	H_s = 1+(s/h)	g_R^2 * S*E_t /£	C_{dyn}	windward C_{fig}	Leeward C_{fig}	Side wall c_{fig}	windward P= 0.5*P_{air} $(V_{des\theta})^2$ C_{dyn} C_{fig}	Leeward P= 0.5*P_{air} $(V_{des\theta})^2$ C_{dyn} C_{fig}	Side wall P= 0.5*P_{air} $(V_{des\theta})^2$ C_{dyn} C_{fig}
F1	3	3.0	0.830	31.54	3.0	0.71	3.39	4.08	0.035	0.0579	1.03	2.35	0.968	0.72	-0.45	-0.468	433.3	-589.5	-613.1
F2	6	3.0	0.830	31.54	6.0	0.71	3.39	4.08	0.035	0.0579	1.06	2.35	0.971	0.72	-0.45	-0.468	434.7	-589.5	-613.1
F3	9	3.0	0.830	31.54	9.0	0.72	3.39	4.08	0.035	0.0579	1.09	2.35	0.973	0.72	-0.45	-0.468	436.1	-589.5	-613.1
F4	12	3.0	0.854	32.45	12.0	0.72	3.39	3.96	0.036	0.0594	1.12	2.46	0.979	0.72	-0.45	-0.468	464.5	-589.5	-613.1
F5	15	3.0	0.890	33.82	15.0	0.73	3.39	3.80	0.037	0.0616	1.15	2.62	0.985	0.72	-0.45	-0.468	508.4	-589.5	-613.1
F6	21	6.0	0.946	35.95	21.0	0.74	3.39	3.58	0.039	0.0649	1.21	2.88	0.997	0.72	-0.45	-0.468	582.2	-589.5	-613.1
F7	24.1	3.1	0.964	36.63	24.1	0.74	3.39	3.51	0.039	0.0660	1.24	2.96	1.002	0.72	-0.45	-0.468	608.1	-589.5	-613.1
F8	27.2	3.1	0.983	37.36	27.2	0.74	3.39	3.44	0.040	0.0671	1.27	3.05	1.007	0.72	-0.45	-0.468	636.4	-589.5	-613.1
F9	30.3	3.1	1.001	38.04	30.3	0.75	3.39	3.38	0.040	0.0682	1.30	3.14	1.012	0.72	-0.45	-0.468	663.5	-589.5	-613.1
F10	33.4	3.1	1.013	38.49	33.4	0.75	3.39	3.34	0.040	0.0689	1.33	3.20	1.017	0.72	-0.45	-0.468	683.1	-589.5	-613.1
F11	36.5	3.1	1.026	38.99	36.5	0.76	3.39	3.30	0.041	0.0696	1.36	3.26	1.021	0.72	-0.45	-0.468	704.4	-589.5	-613.1
F12	39.6	3.1	1.038	39.44	39.6	0.76	3.39	3.26	0.041	0.0703	1.39	3.32	1.026	0.72	-0.45	-0.468	724.7	-589.5	-613.1
F13	42.7	3.1	1.048	39.82	42.7	0.76	3.39	3.23	0.041	0.0709	1.42	3.37	1.030	0.72	-0.45	-0.468	742.4	-589.5	-613.1
F14	45.8	3.1	1.057	40.17	45.8	0.77	3.39	3.20	0.041	0.0715	1.45	3.41	1.034	0.72	-0.45	-0.468	758.8	-589.5	-613.1
F15	48.9	3.1	1.066	40.51	48.9	0.77	3.39	3.18	0.042	0.0720	1.48	3.45	1.038	0.72	-0.45	-0.468	775.5	-589.5	-613.1
F16	52.0	3.1	1.074	40.81	52.0	0.78	3.39	3.15	0.042	0.0724	1.51	3.49	1.042	0.72	-0.45	-0.468	790.8	-589.5	-613.1
F17	55.1	3.1	1.080	41.04	55.1	0.78	3.39	3.13	0.042	0.0728	1.54	3.52	1.046	0.72	-0.45	-0.468	803.1	-589.5	-613.1

Wind X-direction α =0° Tower1

														windward	Leeward	Side wall	windward	Leeward	Side wall
Floor	z (m)	Effective	$M_{z,cat}$	$V_{site\beta}$	s	B_{sh}	g_R	N	E_t	S	H_s = 1+(s/h)	g_R^2 * S*E_t	C_{dyn}	C_{fig}	C_{fig}	c_{fig}	P= 0.5*P_{air}	P= 0.5*P_{air}	P= 0.5*P_{air}
F18	58.2	3.1	1.086	41.27	58.2	0.78	3.39	3.12	0.042	0.0731	1.57	3.55	1.050	0.72	-0.45	-0.468	788.5	-589.5	-613.1
F19	61.3	3.1	1.093	41.53	61.3	0.79	3.39	3.10	0.042	0.0735	1.60	3.59	1.054	0.72	-0.45	-0.468	801.6	-589.5	-613.1
F20	64.4	3.1	1.099	41.76	64.4	0.79	3.39	3.08	0.043	0.0739	1.63	3.62	1.057	0.72	-0.45	-0.468	813.3	-589.5	-613.1
F21	67.5	3.1	1.105	41.99	67.5	0.79	3.39	3.06	0.043	0.0742	1.66	3.65	1.061	0.72	-0.45	-0.468	825.0	-589.5	-613.1
F22	70.6	3.1	1.111	42.22	70.6	0.79	3.39	3.05	0.043	0.0746	1.69	3.68	1.065	0.72	-0.45	-0.468	836.8	-589.5	-613.1
F23	73.7	3.1	1.117	42.45	73.7	0.80	3.39	3.03	0.043	0.0749	1.72	3.71	1.068	0.72	-0.45	-0.468	848.7	-589.5	-613.1
F24	76.8	3.1	1.123	42.67	76.8	0.80	3.39	3.01	0.043	0.0752	1.75	3.74	1.072	0.72	-0.45	-0.468	860.7	-589.5	-613.1
F25	79.9	3.1	1.128	42.86	79.9	0.80	3.39	3.00	0.043	0.0755	1.78	3.76	1.075	0.72	-0.45	-0.468	871.1	-589.5	-613.1
F26	83.0	3.1	1.133	43.05	83.0	0.80	3.39	2.99	0.043	0.0758	1.81	3.79	1.078	0.72	-0.45	-0.468	881.5	-589.5	-613.1
F27	86.1	3.1	1.137	43.21	86.1	0.80	3.39	2.98	0.044	0.0760	1.84	3.81	1.081	0.72	-0.45	-0.468	890.2	-589.5	-613.1
F28	89.2	3.1	1.142	43.40	89.2	0.81	3.39	2.96	0.044	0.0763	1.87	3.83	1.085	0.72	-0.45	-0.468	900.7	-589.5	-613.1
F29	92.3	3.1	1.147	43.59	92.3	0.81	3.39	2.95	0.044	0.0766	1.90	3.86	1.088	0.72	-0.45	-0.468	911.2	-589.5	-613.1
F30	95.4	3.1	1.152	43.78	95.4	0.81	3.39	2.94	0.044	0.0769	1.94	3.89	1.091	0.72	-0.45	-0.468	921.8	-589.5	-613.1
F31	102	6.6	1.162	44.16	102.0	0.81	3.39	2.91	0.044	0.0775	2.00	3.94	1.097	0.72	-0.45	-0.468	943.2	-589.5	-613.1

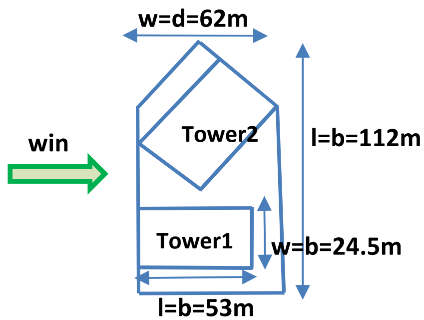

Wind X-direction α =90° Tower1

Floor	*z (m)*	*Effective Height*	$M_{z,cat}$	$V_{site\beta}$	*s*	B_{sh}	g_R	*N*	E_t	*S*	H_s = 1+(s/h)	g_R^2 * $S*E_t$ /£	C_{dyn}	windward C_{fig}	Leeward C_{fig}	Side wall c_{fig}	windward $0.5*P_{air}$ $(V_{des\theta})^2$ $C_{dyn}C_{fig}$	Leeward $0.5*P_{air}$ $(V_{des\theta})^2$ $C_{dyn}C_{fig}$	Side wall $0.5*P_{air}$ $(V_{des\theta})^2$ $C_{dyn}C_{fig}$
F1	3	3.0	0.830	31.54	3.0	0.74	3.39	4.08	0.035	0.0703	1.03	2.86	0.988	0.72	-0.45	-0.468	433.3	-614.9	-639.5
F2	6	3.0	0.830	31.54	6.0	0.75	3.39	4.08	0.035	0.0703	1.06	2.86	0.991	0.72	-0.45	-0.468	434.7	-614.9	-639.5
F3	9	3.0	0.830	31.54	9.0	0.75	3.39	4.08	0.035	0.0703	1.09	2.86	0.994	0.72	-0.45	-0.468	436.1	-614.9	-639.5
F4	12	3.0	0.854	32.452	12.0	0.76	3.39	3.96	0.036	0.0721	1.12	2.99	1.000	0.72	-0.45	-0.468	464.5	-614.9	-639.5
F5	15	3.0	0.890	33.82	15.0	0.76	3.39	3.80	0.037	0.0747	1.15	3.18	1.008	0.72	-0.45	-0.468	508.4	-614.9	-639.5
F6	21	6.0	0.946	35.948	21.0	0.77	3.39	3.58	0.039	0.0786	1.21	3.49	1.022	0.72	-0.45	-0.468	582.2	-614.9	-639.5
F7	24.1	3.1	0.964	36.632	24.1	0.78	3.39	3.51	0.039	0.0799	1.24	3.59	1.028	0.72	-0.45	-0.468	608.1	-614.9	-639.5
F8	27.2	3.1	0.983	37.362	27.2	0.79	3.39	3.44	0.040	0.0812	1.27	3.69	1.034	0.72	-0.45	-0.468	636.4	-614.9	-639.5
F9	30.3	3.1	1.001	38.038	30.3	0.79	3.39	3.38	0.040	0.0825	1.30	3.80	1.040	0.72	-0.45	-0.468	663.5	-614.9	-639.5
F10	33.4	3.1	1.013	38.494	33.4	0.80	3.39	3.34	0.040	0.0833	1.33	3.86	1.045	0.72	-0.45	-0.468	683.1	-614.9	-639.5
F11	36.5	3.1	1.026	38.988	36.5	0.80	3.39	3.30	0.041	0.0842	1.36	3.94	1.051	0.72	-0.45	-0.468	704.4	-614.9	-639.5
F12	39.6	3.1	1.038	39.444	39.6	0.81	3.39	3.26	0.041	0.0850	1.39	4.01	1.056	0.72	-0.45	-0.468	724.7	-614.9	-639.5
F13	42.7	3.1	1.048	39.824	42.7	0.81	3.39	3.23	0.041	0.0857	1.42	4.07	1.061	0.72	-0.45	-0.468	742.4	-614.9	-639.5
F14	45.8	3.1	1.057	40.166	45.8	0.82	3.39	3.20	0.041	0.0863	1.45	4.12	1.067	0.72	-0.45	-0.468	758.8	-614.9	-639.5
F15	48.9	3.1	1.066	40.508	48.9	0.83	3.39	3.18	0.042	0.0869	1.48	4.17	1.072	0.72	-0.45	-0.468	775.5	-614.9	-639.5
F16	52.0	3.1	1.074	40.812	52.0	0.83	3.39	3.15	0.042	0.0874	1.51	4.22	1.077	0.72	-0.45	-0.468	790.8	-614.9	-639.5
F17	55.1	3.1	1.080	41.04	55.1	0.84	3.39	3.13	0.042	0.0878	1.54	4.25	1.081	0.72	-0.45	-0.468	803.1	-614.9	-639.5
F18	58.2	3.1	1.086	41.268	58.2	0.85	3.39	3.12	0.042	0.0882	1.57	4.29	1.086	0.72	-0.45	-0.468	815.6	-614.9	-639.5

Wind X-direction			**α =90°**	**Tower1**										**windward**	**Leeward**	**Side wall**	**windward**	**Leeward**	**Side wall**
Floor	***z (m)***	***Effective Height***	$M_{z,cat}$	$V_{site\beta}$	***s***	B_{sh}	g_R	***N***	E_t	***S***	$H_s = 1+(s/h)$	$g_R^2 * S*E_t /£$	C_{dyn}	C_{fig}	C_{fig}	c_{fig}	$P= 0.5*P_{air} (V_{des\theta})^2 C_{dyn} C_{fig}$	$P= 0.5*P_{air} (V_{des\theta})^2 C_{dyn} C_{fig}$	$P= 0.5*P_{air} (V_{des\theta})^2 C_{dyn} C_{fig}$
F19	61.3	3.1	1.093	41.534	61.3	0.85	3.39	3.10	0.042	0.0887	1.60	4.33	1.091	0.72	-0.45	-0.468	829.8	-614.9	-639.5
F20	64.4	3.1	1.099	41.762	64.4	0.86	3.39	3.08	0.043	0.0891	1.63	4.36	1.095	0.72	-0.45	-0.468	842.4	-614.9	-639.5
F21	67.5	3.1	1.105	41.99	67.5	0.86	3.39	3.06	0.043	0.0895	1.66	4.40	1.100	0.72	-0.45	-0.468	855.2	-614.9	-639.5
F22	70.6	3.1	1.111	42.218	70.6	0.87	3.39	3.05	0.043	0.0899	1.69	4.43	1.104	0.72	-0.45	-0.468	868.1	-614.9	-639.5
F23	73.7	3.1	1.128	42.864	73.7	0.87	3.39	3.00	0.043	0.0910	1.72	4.54	1.111	0.72	-0.45	-0.468	881.1	-614.9	-639.5
F24	76.8	3.1	1.133	43.054	76.8	0.88	3.39	2.99	0.043	0.0913	1.75	4.57	1.115	0.72	-0.45	-0.468	894.2	-614.9	-639.5
F25	79.9	3.1	1.137	43.206	79.9	0.88	3.39	2.98	0.044	0.0916	1.78	4.59	1.119	0.72	-0.45	-0.468	905.6	-614.9	-639.5
F26	83.0	3.1	1.142	43.396	83.0	0.89	3.39	2.96	0.044	0.0919	1.81	4.62	1.123	0.72	-0.45	-0.468	917.1	-614.9	-639.5
F27	86.1	3.1	1.147	43.586	86.1	0.89	3.39	2.95	0.044	0.0923	1.84	4.65	1.128	0.72	-0.45	-0.468	926.7	-614.9	-639.5
F28	89.2	3.1	1.152	43.776	89.2	0.89	3.39	2.94	0.044	0.0926	1.87	4.68	1.131	0.72	-0.45	-0.468	938.2	-614.9	-639.5
F29	92.3	3.1	1.162	44.156	92.3	0.90	3.39	2.91	0.044	0.0932	1.90	4.74	1.136	0.72	-0.45	-0.468	949.6	-614.9	-639.5
F30	95.4	3.1	1.162	44.156	95.4	0.90	3.39	2.91	0.044	0.0932	1.94	4.74	1.139	0.72	-0.45	-0.468	961.0	-614.9	-639.5
F31	102.0	6.6	1.162	44.156	102.0	0.90	3.39	2.91	0.044	0.0932	2.00	4.74	1.144	0.72	-0.45	-0.468	983.9	-614.9	-639.5

Appendix D:

Advanced parameters used for numerical modelling

D.1 Parameters used for the Numerical Modelling

Generally, numerical simulation (RANS approach) ends up with having stable, time dependent solution.

D.1.1 Iterative method

Similar to most of the commercially available software, Abaqus uses the iterative process to solve the governing equations. Therefore, all the basic equations are transformed in to the algebraic equations. At the first stage, initial value for each flow variable is assumed. Then the iteration process has continued by recalculating those variable until the algebraic equations are resolved up to user defined error. In general, termination criteria is based on the variables of the algebraic equations and those are forced to become zero at the end. Then the variables after first iteration should be compared with initial value and calculate the dropping amount of initial error. Generally, 0.001 is used as termination criteria for industrial applications, which is much higher value. However, it is essential to set the limit to a much lower criterion in order to endorse the turbulent models. Reduction of the residuals should be at least fifth orders of its magnitude Therefore, linear iteration convergence limit is set to very lower criteria such as 10^{-5} in this case study. In addition, the convergence is checked after every 2 *s* and the flow variables are recorded. If the flow variables are constant, the solution of the interested region should be considered as the converged. Under relaxation factor is set as 1.If solution indicates the bad convergence or no convergence, relaxation factor can be reduced in order to get the converged solution.

D.1.2 CFD

A flow step is defined with all the aforementioned boundary conditions and other features. Analysis has been carried out for S-A turbulent model as described in previous section. In order to maintain the convergence and the accuracy of the solution, Courant Friedrichs–Lewy (CFL) is fixed for maximum value. 0.45. The total time are adjusted based on trial and error process & there is no hard and fast rule for it. Therefore, the total time is set in to 40*s* and which is fair enough to converge & get the stable solution. Minimum increment (0.001s) is specified in order to prevent the huge time consuming for simulation. A number of other conditions are set in the CFD solver as shown in Table D.1 to make this simulation run properly. Those important settings, which affect to the simulation, are listed in below table.

Table D.1 Parameters used for the simulation -ABAQUS/CFD

CFD Basic Settings	
Analysis Type	Turbulent Flow
Total Time Step	40 *s*
Increment Adjustment	30 000
Initial increment size	0.001
Divergence Tolerance	1 E-10
Under-Relaxation Factor	1
Solver (Momentum ,Pressure, Transport Equations)	
Iteration limit	500
Convergence Checking	2
Linear convergence Limit	1 E-05

D.1.3 Selection of FE solver

Few more conditions are set for the FEA (standard- explicit) solver to run properly. A dynamic, implicit step is defined relating to all previously mentioned boundary conditions and other features. Implicit method is capable for solving the governing equations at the nodes by iterative process. Dynamic condition is required to evaluate the building motion. The initial time step is set to start at 0.001 in order to prevent the huge time consuming for simulation. Parameters used for the simulation are given in below Table D.2.

Table D.2 Parameters used for the simulation -ABAQUS/Standard

Standard-Explicit Settings	
Analysis Type	Dynamic Implicit
Total Time Step	40 *s*
Maximum number of	30 000
Initial increment size	0.001
Solution technique	Full Newton

D.2 Co- Execution Parameters

The co-execution is described as the carry out the co-simulation of two analysis jobs. ABAQUS/CFD analysis job and ABAQUS/Standard & Explicit analysis job are created independently for this case study. Then the jobs are performed in synchronizing each other (as shown in Figure D.1) using the same parameters defined in early chapters. Specified job parameters such as total time period, maximum number of increment, initial increment size etc. should be similar in both CFD job and the Standard & Explicit job in order to synchronize with each other well. In addition, following parameters are specified to run the simulation properly.

Memory

95% of the memory is allocated for the analysis in order to fulfill the high computational demand as shown in Figure D.2 (a).

Parallelization

The technique of parallelization process is be either domain level or loop level. Among those two option, domain level is selected for this case study. In this technique, model is broken into several topological domains and then each domain is assigned in to a processor. Therefore, parallel execution can be processed by setting the number of processors and this can be helped to reduce the computational time immensely. However, it is a difficult task to decide the exact number of processes which leads parallelize the simulation properly. Because, there are some factors which is caused to limit the parallelization such as the degrees of freedom (DOF). Less number of DOF leads to relatively bigger overhead for parallelization process. Conversely, large number of processors leads to greater parallelization time when assembling the results at the intersecting points of two different domains run in different cores. Therefore, number of processes is set by following the rule of thumb, which means that at least 5000 DOF should have per each core. Hence, setting the number of processors should be a trial and error process.

In addition, the analysis run time can be reduced with the help of the "dynamic load balancing" option. Therefore, optimal performance can be seen in most problems when the number of domains are set as two to four times the number of processors.

By considering all the aforementioned facts, the number of processors are set as 6 and the number of domains are set as two times the number of process for this simulation process. With all the techniques, analysis time for single simulation is an average of 1.5 days in this case study. Settings of parallelization are shown in Figure D.1.

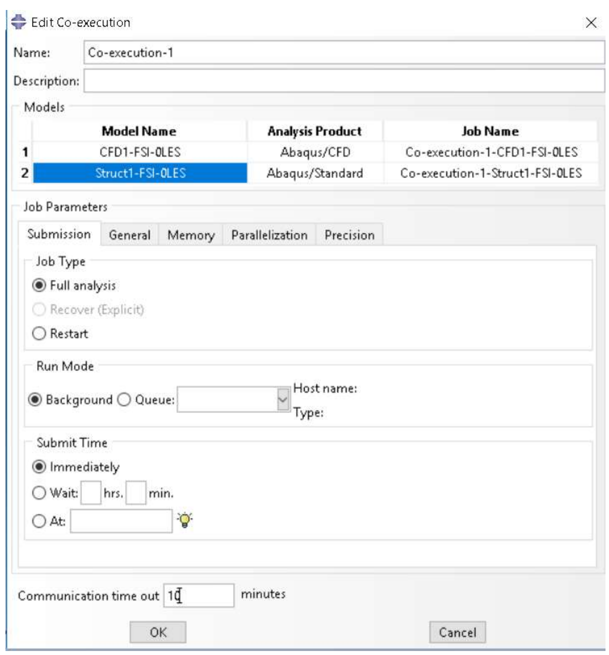

Figure D.1 Co- execution settings. ABAQUS/CFD & ABAQUS/Standard –Explicit

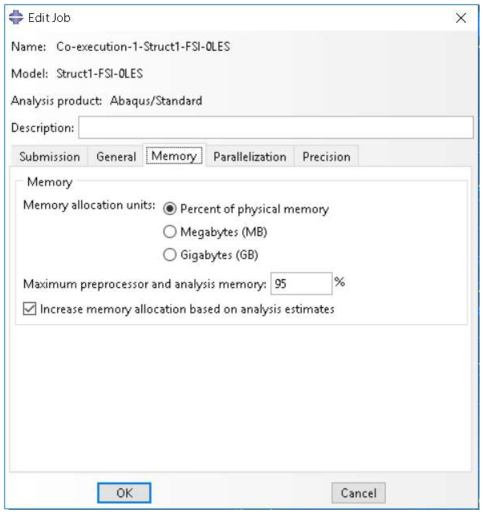

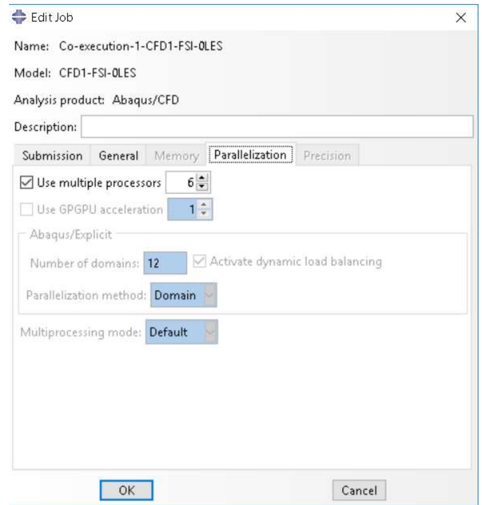

(a) (b)

FigureD.2 (a) Settings for memory (b) settings for parallelization

<u>Precision</u>

Single precision is set as per the accuracy of the results in order to reduce the analysis time

D.3 Minimum Time step selection during analysis

Stable time step for ABAQUS/CFD and ABAQUS/Standard & Explicit is calculated independently for this case**.** Accordingly, minimum time step Δt is selected as minimum of those two in order to get the steady solution.

The stable time step for "structure" part is calculated based on element density, size and stiffness as shown in following expression.

$$\Delta t_{structure} = \frac{L_{min}}{C_d} \quad (1)$$

where

L_{min} = smallest element dimension in the FEA mesh

c_d = dilatational wave speed- can be calculated as expression 2

$$C_d = \sqrt{\frac{(\lambda+2\alpha\,)}{\rho}} \tag{2}$$

λ and α are Lame constants for structure material.

The maximum time step for "fluid" part is calculated based on the velocity gradient and the grid size as shown in following expression

$$\Delta t_{fluid} = [\min(\frac{h_{mk}}{V_{mk}})]_{fluid-stucture\ interface} \tag{3}$$

where,

h_{mk} = distance between m-th and k-th cells

V_{mk} = velocity of the fluid between those cells.

Cells m and k are cells that lie near the fluid-structure interface.

Since, both are answerable to transfer the disturbance between the nodes, the minimum time step for simulation is selected as minimum between those two.

$$\Delta t = \min\ (\Delta t_{structure}, \Delta t_{fluid})$$

In order to avoid the analysis run time, it is important to identify the elements, which are having very much lower stable time increment than specified value. Therefore, the quality of the mesh is verified by "verify mesh" tool. If some elements are caused to limit the time increment, it is required modify them if possible. Minimum time steps calculated in CFD and Standard analysis are shown in Figure D.3 (a) and (b).

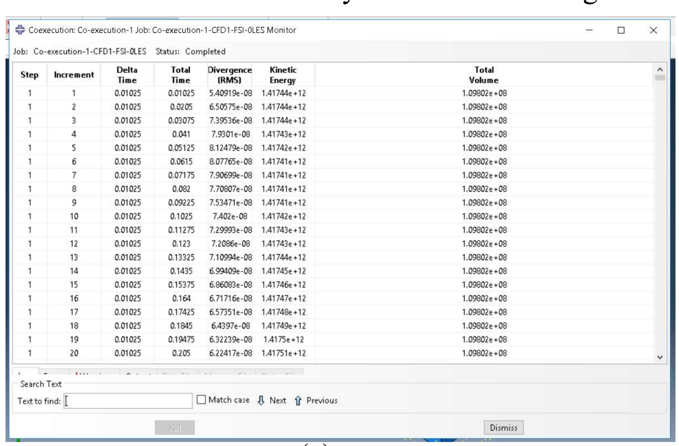

Step	Increment	Delta Time	Total Time	Divergence (RMS)	Kinetic Energy	Total Volume
1	1	0.01025	0.01025	5.40919e-08	1.41744e+12	1.09802e+08
1	2	0.01025	0.0205	6.50575e-08	1.41744e+12	1.09802e+08
1	3	0.01025	0.03075	7.39536e-08	1.41744e+12	1.09802e+08
1	4	0.01025	0.041	7.9301e-08	1.41743e+12	1.09802e+08
1	5	0.01025	0.05125	8.12479e-08	1.41742e+12	1.09802e+08
1	6	0.01025	0.0615	8.07765e-08	1.41741e+12	1.09802e+08
1	7	0.01025	0.07175	7.90699e-08	1.41741e+12	1.09802e+08
1	8	0.01025	0.082	7.70807e-08	1.41741e+12	1.09802e+08
1	9	0.01025	0.09225	7.53471e-08	1.41741e+12	1.09802e+08
1	10	0.01025	0.1025	7.402e-08	1.41742e+12	1.09802e+08
1	11	0.01025	0.11275	7.29993e-08	1.41743e+12	1.09802e+08
1	12	0.01025	0.123	7.2086e-08	1.41743e+12	1.09802e+08
1	13	0.01025	0.13325	7.10994e-08	1.41744e+12	1.09802e+08
1	14	0.01025	0.1435	6.99409e-08	1.41745e+12	1.09802e+08
1	15	0.01025	0.15375	6.86083e-08	1.41746e+12	1.09802e+08
1	16	0.01025	0.164	6.71716e-08	1.41747e+12	1.09802e+08
1	17	0.01025	0.17425	6.57351e-08	1.41748e+12	1.09802e+08
1	18	0.01025	0.1845	6.4397e-08	1.41749e+12	1.09802e+08
1	19	0.01025	0.19475	6.32239e-08	1.4175e+12	1.09802e+08
1	20	0.01025	0.205	6.22417e-08	1.41751e+12	1.09802e+08

(a)

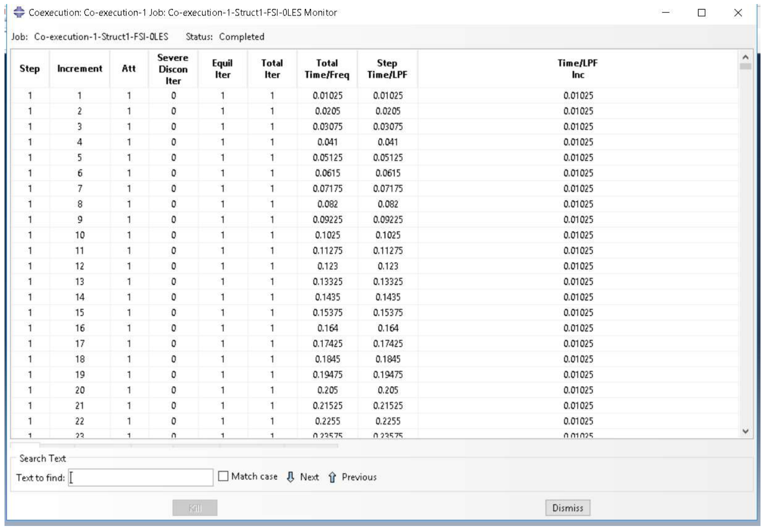

Coexecution: Co-execution-1 Job: Co-execution-1-Struct1-FSI-0LES Monitor

Job: Co-execution-1-Struct1-FSI-0LES Status: Completed

Step	Increment	Att	Severe Discon Iter	Equil Iter	Total Iter	Total Time/Freq	Step Time/LPF	Time/LPF Inc
1	1	1	0	1	1	0.01025	0.01025	0.01025
1	2	1	0	1	1	0.0205	0.0205	0.01025
1	3	1	0	1	1	0.03075	0.03075	0.01025
1	4	1	0	1	1	0.041	0.041	0.01025
1	5	1	0	1	1	0.05125	0.05125	0.01025
1	6	1	0	1	1	0.0615	0.0615	0.01025
1	7	1	0	1	1	0.07175	0.07175	0.01025
1	8	1	0	1	1	0.082	0.082	0.01025
1	9	1	0	1	1	0.09225	0.09225	0.01025
1	10	1	0	1	1	0.1025	0.1025	0.01025
1	11	1	0	1	1	0.11275	0.11275	0.01025
1	12	1	0	1	1	0.123	0.123	0.01025
1	13	1	0	1	1	0.13325	0.13325	0.01025
1	14	1	0	1	1	0.1435	0.1435	0.01025
1	15	1	0	1	1	0.15375	0.15375	0.01025
1	16	1	0	1	1	0.164	0.164	0.01025
1	17	1	0	1	1	0.17425	0.17425	0.01025
1	18	1	0	1	1	0.1845	0.1845	0.01025
1	19	1	0	1	1	0.19475	0.19475	0.01025
1	20	1	0	1	1	0.205	0.205	0.01025
1	21	1	0	1	1	0.21525	0.21525	0.01025
1	22	1	0	1	1	0.2255	0.2255	0.01025
1	23	1	0	1	1	0.23575	0.23575	0.01025

Search Text
Text to find: Match case Next Previous
Kill Dismiss

(b)

Figure D.3 (a) Minimum time step –CFD (b) Minimum time step – FE solver

D.4 Field Output Request

Field output is set to every x=1 unit time to get the output variables as shown in Figure D.4.

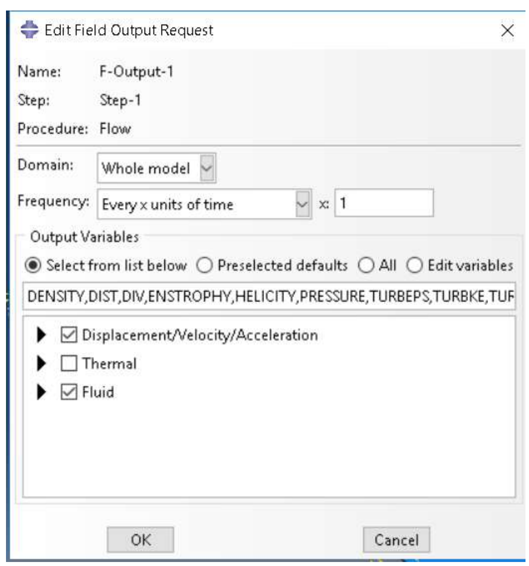

Figure D.4 Field output request –ABAQUS/CAE